

Supporting Information for

Organogold oligomers: exploiting iClick and aurophilic cluster formation to prepare solution stable Au₄ repeating units.

Xi Yang, Shanshan Wang, Ion Ghiviriga, Khalil A. Abboud and Adam S. Veige *

University of Florida, Department of Chemistry, Center for Catalysis, P.O. Box 117200, Gainesville, FL, 32611.

Table of Contents

1. GENERAL CONSIDERATIONS	S3
2. SYNTHESIS.....	S4
Synthesis of 1.....	S4
Synthesis of 2.....	S5
Synthesis of 4.....	S6
Synthesis of 5.....	S6
Synthesis of 7.....	S7
Synthesis of 8.....	S8
PPhMe ₂ AuN ₃	S8
3. NMR SPECTRA	S10
NMR spectra of 1	S10
NMR spectra of 2	S13
NMR spectra of 5	S19
NMR spectra of 7	S21
NMR spectra of 8	S26
NMR spectra of PPhMe ₂ AuN ₃	S29

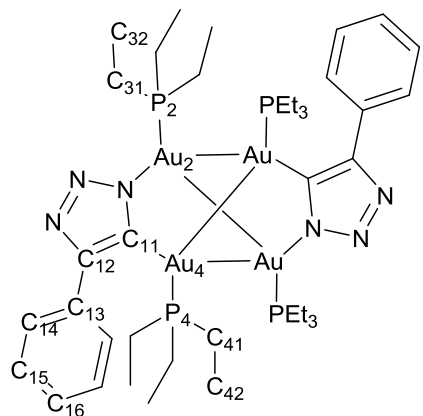
4. DIFFUSION ORDER SPECTROSCOPY (DOSY) NMR ANALYSIS	S31
¹ H DOSY NMR Analysis of 1 and 2	S32
¹ H DOSY NMR Analysis of 8.....	S33
5. VARIABLE TEMPERATURE (VT) NMR STUDIES OF COMPLEXES 1 AND 2	S37
The VT NMR study of complex 1 in DMSO-d ₆	S37
The VT NMR study of complex 2 in DMSO-d ₆	S38
6. INFRARED SPECTRUM (IR) AND POWDER X-RAY DIFFRACTION (PXRD).....	S39
7. X-RAY STRUCTURE DETERMINATION.....	S40
X-ray experiment details of 1.....	S40
X-ray experiment details of 2.....	S52
X-ray experiment details of 4.....	S63
8. PHOTOPHYSICAL STUDY OF COMPLEX 1 AND 8	S73
Absorption and emission spectra of complex 1.....	S73
Absorption and emission spectra of complex 9.....	S74
Absorption and emission spectra of oligomeric 8.	S75
9. REFERENCE	S77

1. General Considerations

Unless specified otherwise, all manipulations were performed under an inert atmosphere using standard Schlenk or glove-box techniques. Pentane, methylene chloride, diethyl ether, and tetrahydrofuran were degassed by sparging with high purity argon, and were dried using a GlassContour drying column. Methanol was dried over anhydrous copper(II)sulfate, distilled and stored over 4 Å molecular sieves; benzene-*d*₆ (Cambridge Isotopes) was dried over sodium benzophenone ketyl, distilled, and stored over 4 Å molecular sieves; chloroform-*d* (Cambridge Isotopes) and methylene chloride-*d*₂ (Cambridge Isotopes) were dried over calcium hydride, distilled, and stored over 4 Å molecular sieves; dimethylsulfoxide-*d*₆ (Cambridge Isotopes) was used as received. ¹H, ¹³C{¹H}, and ³¹P{¹H} NMR spectra were acquired on a Varian Mercury Broad Band 300 MHz, a Varian Mercury 300 MHz, or an Inova 500 MHz spectrometer. 2D NMR spectra were obtained on an Inova 500 MHz spectrometer. Chemical shifts are reported in δ (ppm). For ¹H and ¹³C{¹H} NMR spectra, the residual solvent peak was used as an internal reference, while ³¹P{¹H} spectra were referenced to an 85% phosphoric acid external standard (0 ppm). Elemental analyses were performed at Complete Analysis Laboratory Inc., Parsippany, New Jersey. The following materials were purchased and used as received: Thallium Acetylacetonate ([Tl(acac)]) (Sigma-Aldrich), chloro(triethylphosphine)gold(I) (PEt₃AuCl) (Sigma-Aldrich), chloro(dimethylphenylphosphine)gold(I) (PPhMe₂AuCl) (Sigma-Aldrich), azidotrimethylsilane (TMSN₃) (Acros), 1,4-diethynylbenzene (1,4-HC≡C-C₆H₄) (Sigma-Aldrich). The following were prepared by literature methods: PEt₃AuN₃,¹ PPh₃AuN₃,² PEt₃AuC≡CC₆H₅,³ PPhMe₂AuC≡CC₆H₅,⁴ 2,7-diethynyl-9,9-dihexyl-9*H*-fluorene,⁵ 1,4-PPh₃AuC≡C-C₆H₄(3).⁶

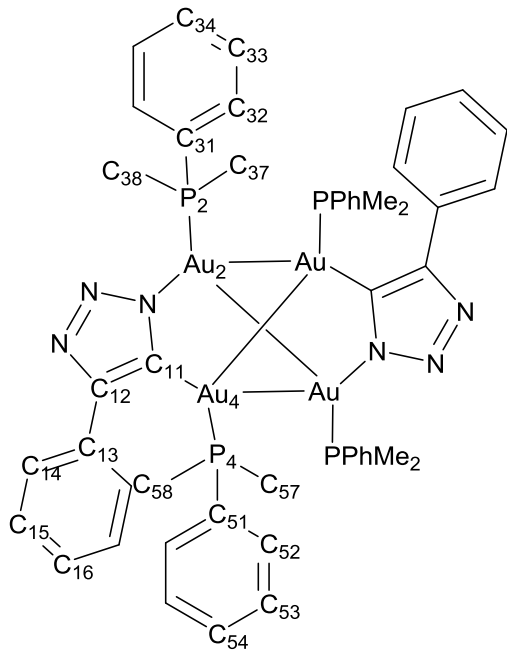
2. Synthesis

Synthesis of 1



PEt₃AuC≡CC₆H₅ (42 mg, 0.1 mmol) and PEt₃AuN₃ (36 mg, 0.1 mmol) were dissolved in 0.7 ml C₆D₆ at room temperature. After 72 h a white crystalline powder deposited from the reaction medium. The white precipitate was collected, washed with cold toluene and pentane and then all volatiles were removed in vacuo to give the product (yield: 64 mg, 83%). ¹H NMR (500 MHz, CDCl₃, 25 °C, δ (ppm)): 8.45 (d, ³J_{HH} = 6.8 Hz, 4H, HC₁₄), 7.27 (dd, ³J_{HH} = 7.4 Hz, 4H, HC₁₅), 7.13 (dd, ³J_{HH} = 7.4 Hz, 2H, HC₁₆), 1.49 (dq, ³J_{HH} = 7.8 Hz, ²J_{HP} = 7.8 Hz, 6H, HC₃₁), 1.47 (dq, ³J_{HH} = 7.8 Hz, ²J_{HP} = 7.8 Hz, 6H, HC₄₁), 1.08 (dt, ³J_{HH} = 7.3 Hz, ³J_{HP} = 3.4 Hz, 9H, HC₄₂), 1.05 (dt, ³J_{HH} = 7.3 Hz, ³J_{HP} = 3.4 Hz, 9H, HC₃₂). ¹³C{¹H} NMR Shifts (500 MHz, CDCl₃, 25 °C, δ (ppm)): 152.7 (C₁₃), 137.0 (C₁₂), 127.7 (C₁₅), 126.6 (C₁₄), 125.1 (C₁₆), 17.3 (C₄₂), 16.5 (C₃₂), 8.5 (C₃₁, C₄₁). ³¹P{¹H} NMR (121.4 MHz, CDCl₃, 25 °C, δ (ppm)) δ (ppm): 31.96 (s, P₄), 20.64 (s, P₂). Anal. Calcd. (%) for C₄₀H₇₀Au₄N₆P₄: C, 31.06; H, 4.56; N, 5.43. Found: C, 31.13; H, 4.70; N, 5.58.

Synthesis of 2



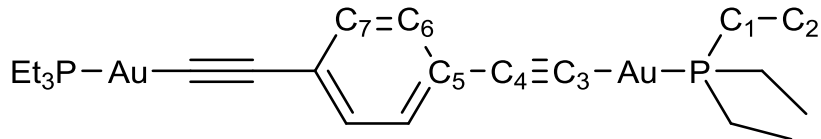
$\text{PPhMe}_2\text{AuC}\equiv\text{CC}_6\text{H}_5$ (21.8 mg, 0.05 mmol) and $\text{PPhMe}_2\text{AuN}_3$ (18.9 mg, 0.05 mmol) were dissolved in 2 ml of toluene at room temperature and stirred for 24 h. During the reaction an off-white crystalline powder deposited. The precipitate was collected and washed with cold toluene and pentane followed by removal of all volatiles in vacuo to give the product (yield: 33.5 mg, 82%). ^1H NMR (500 MHz, CDCl_3 , 25 °C, δ (ppm)): 8.32 (d, $^3J_{\text{HH}} = 7.2$ Hz, 4H, HC_{14}), 7.59 (dd, $^3J_{\text{HH}} = 7.6$ Hz, $^3J_{\text{HP}} = 12.4$ Hz, 4H, HC_{32}), 7.48 (dd, $^3J_{\text{HH}} = 6.9$ Hz, $^3J_{\text{HP}} = 10.3$ Hz, 4H, HC_{52}), 7.43 (t, $^3J_{\text{HH}} = 7.3$ Hz, 2H, HC_{54}), 7.40 (t, $^3J_{\text{HH}} = 7.6$ Hz, 2H, HC_{34}), 7.36 (t, $^3J_{\text{HH}} = 8.1$ Hz, 4H, HC_{53}), 7.32 (t, $^3J_{\text{HH}} = 8.1$ Hz, 4H, HC_{33}), 7.27 (t, $^3J_{\text{HH}} = 7.2$ Hz, 4H, HC_{15}), 7.21 (d, $^3J_{\text{HH}} = 7.0$ Hz, 2H, HC_{16}), 1.47 (d, $^2J_{\text{HP}} = 10.7$ Hz, 3H, HC_{37}), 1.37(d, $^2J_{\text{HP}} = 10.7$ Hz, 3H, HC_{38}), 1.31 (d, $^2J_{\text{HP}} = 10.7$ Hz, 3H, HC_{58}), 1.28 (d, $^2J_{\text{HP}} = 10.7$ Hz, 3H, HC_{57}). $^{13}\text{C}\{\text{H}\}$ NMR Shifts (500 MHz, CDCl_3 , 25 °C, δ (ppm)): 152.6 (C₁₂), 136.9 (C₁₃), 135.0 (C₅₁), 132.9 (C₃₁), 131.1 (C₃₂, C₅₂), 130.8 (C₃₄), 130.3 (C₅₄), 128.8 (C₃₃), 128.7 (C₅₃), 127.9 (C₁₅), 126.5 (C₁₄), 125.3 (C₁₆), 14.8 (C₅₈), 14.6

(C₃₇, C₅₇), 13.8 (C₃₈). ³¹P{¹H} NMR (121.4 MHz, CDCl₃, 25 °C, δ (ppm)): 11.79 (s, P₄), -1.50 (s, P₂). Anal. Calcd. (%) for C₄₈H₅₄Au₄N₆P₄: C, 35.44; H, 3.35; N, 5.17. Found: C, 35.56; H, 3.39; N, 5.11.

Synthesis of 4

Compound **3** (20.8 mg, 0.02 mmol) and PPh₃AuN₃ (20.1 mg, 0.04 mmol) were suspended in 1 ml of CHCl₃. After 2 h, the reaction mixture became a beige colored solution. The resultant solution was filtered into a small test tube. After 48 h, crystals deposited in the test tube. The crystals were collected, washed first with 2 ml of cold CHCl₃ and then 5 ml of pentane. After washing all volatiles were removed in vacuo to give the product (yield: 27.8 mg, 68%). Anal. Calcd. (%) for C₈₂H₆₄Au₄N₆P₄: C, 48.16; H, 3.15; N, 4.11. Found: C, 48.07; H, 3.07; N, 4.08.

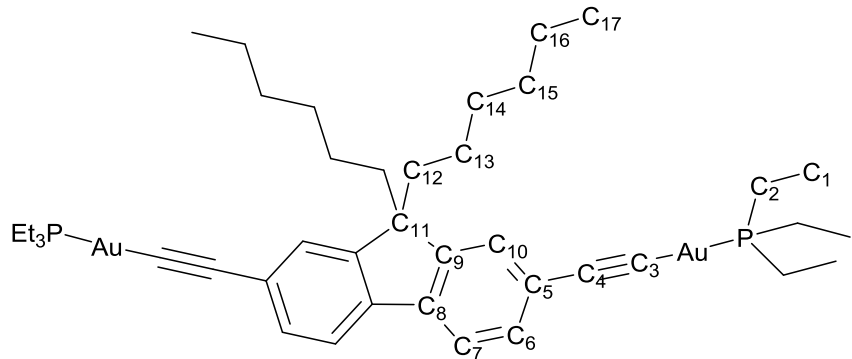
Synthesis of 5



In a vial with a stir bar, 1 ml of THF was added into a mixture of PEt₃AuCl (200 mg, 0.57 mmol) and 1,4-HC≡C-C₆H₄ (30.6 mg, 0.30 mmol). To the THF solution, a methanol (20 ml) solution of NaOH (228 mg, 5.7 mmol) was added. The mixture was stirred at room temperature for 12 h. A light yellow powder precipitates and was collected by filtration. The powder was re-dissolved in 5 ml of toluene and filtered through a Celite® plug. The filtrate was concentrated to 0.5 ml and 10 ml of pentane was added to induce precipitation. The product was collected by filtration as a yellow powder. (yield: 190 mg, 89%). ¹H NMR (500 MHz, CDCl₃, 25 °C, δ (ppm)): 7.30 (s, 4H, HC₆, HC₇), 1.77 (dq, ³J_{HH} = 7.7 Hz, ²J_{HP} = 9.5 Hz, 12H, HC₁), 1.17 (dt, ³J_{HH} = 7.7 Hz, ²J_{HP} =

18.0 Hz, 18H, HC_2). $^{13}\text{C}\{\text{H}\}$ NMR Shifts (500 MHz, CDCl_3 , 25 °C, δ (ppm)): 131.9 (C_5), 123.2 (C_6 , C_7), 104.1 (C_4), 17.9 (C_1), 8.9 (C_2). $^{31}\text{P}\{\text{H}\}$ NMR (121.4 MHz, CDCl_3 , 25 °C, δ (ppm)): 37.91 (s). Anal. Calcd. (%) for $\text{C}_{22}\text{H}_{34}\text{Au}_2\text{P}_2$: C, 35.03; H, 4.54. Found: C, 35.08; H, 4.48.

Synthesis of 7



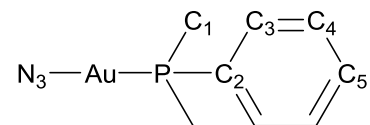
In a vial with a stir bar, 2 ml of THF was added into a mixture of PEt_3AuCl (200 mg, 0.57 mmol) and 2,7-diethynyl-9,9-dihexyl-9*H*-fluorene (115 mg, 0.30 mmol). To the THF solution, a methanol (20 ml) solution of NaOH (228 mg, 5.7 mmol) was added under stirring. The heterogenous mixture was stirred at room temperature for 12 h. Then, the supernatant was removed by decanting. The dark yellow residue was extracted with 5 ml of toluene and filtered through a plug of Celite®. The filtrate was concentrated to 0.5 ml and 10 ml of pentane was added to induce precipitation. The product was collected by filtration as a light yellow powder (yield: 180 mg, 62.5%). ^1H NMR (500 MHz, C_6D_6 , 25 °C, δ (ppm)): 7.81 (d, $^4J_{\text{HH}} = 1.0$ Hz, 2H, HC_{10}), 7.73 (dd, $^4J_{\text{HH}} = 1.1$ Hz, $^3J_{\text{HH}} = 8.0$ Hz, 2H, HC_6), 7.33 (d, $^3J_{\text{HH}} = 8.0$ Hz, 2H, HC_7), 1.85 (m, 4H, HC_{12}), 1.05 (tq, $^3J_{\text{HH}} = 7.6$ Hz, 4H, HC_{16}), 1.00 (dq, $^3J_{\text{HH}} = 7.6$ Hz, $^3J_{\text{HP}} = 10.8$ Hz, 12H, HC_2), 0.94 (tt, $^3J_{\text{HH}} = 7.7$ Hz, 4H, HC_{14}), 0.84 (tt, $^3J_{\text{HH}} = 7.2$ Hz, 4H, HC_{15}), 0.79 (m, 4H, HC_{13}), 0.74 (t, $^3J_{\text{HH}} = 7.3$ Hz, 6H, HC_{17}), 0.66 (dt, $^3J_{\text{HH}} = 7.7$ Hz, $^3J_{\text{HP}} = 17.9$ Hz, 18H, HC_1). $^{13}\text{C}\{\text{H}\}$ NMR Shifts (500 MHz, C_6D_6 , 25 °C, δ (ppm)): 150.8 (C_9), 139.4 (C_8), 131.2 (C_6), 126.6 (C_{10}),

125.5 (C₅), 119.5 (C₇), 104.0 (C₄), 54.8 (C₁₁), 40.5 (C₁₂), 31.4 (C₁₅), 29.9 (C₁₄), 23.9 (C₁₃), 22.8 (C₁₆), 17.4 (C₂), 14.0 (C₁₇), 8.5 (C₁). ³¹P{¹H} NMR (121.4 MHz, C₆D₆, 25 °C, δ (ppm)): 37.59 (s). Anal. Calcd. (%) for C₄₁H₆₂Au₂P₂: C, 48.72; H, 6.18. Found: C, 48.50; H, 6.36.

Synthesis of 8

A 1 ml C₆D₆ solution of **7** (40 mg, 0.398 mmol) and PEt₃AuN₃ (28.6 mg, 0.800 mmol) was added into a sealable NMR tube. The reaction medium was heated at 37 °C for 48 h. The solvent was removed in vacuo and the resulting golden residue was sonicated for 5 min in 5 ml of toluene. After sonication, the toluene supernatant was removed by decanting. The residue was re-dissolved into 2 ml of dichloromethane. The solution was filtered through a plug of Celite® and the solvent was removed in vacuo to provide the product (Yield: 56 mg, 81.5%). ¹H NMR (500 MHz, CDCl₃, 25 °C, δ (ppm)): 8.66 (d, ³J_{HH} = 7.8 Hz), 8.27(s), 7.50 (d, ³J_{HH} = 7.8 Hz), 2.09 (m), 1.91 (m), 1.51 (bs), 1.22-0.94 (m), 0.72-0.67 (m). ¹³C{¹H} NMR Shifts (500 MHz, CDCl₃, 25 °C, δ (ppm)): 153.43, 150.82, 138.92, 135.47, 125.20, 120.79, 117.70, 55.35, 41.09, 31.98, 22.78, 17.30, 17.06, 16.68, 16.40, 14.03, 8.43. ³¹P{¹H} NMR (121.4 MHz, CDCl₃, 25 °C, δ (ppm)): 31.28 (s), 20.32 (s). Due to the significant broadness and overlapping signals, some resonances were not able to be assigned. Anal. Calcd. (%) for C₅₃H₉₂Au₄N₆P₄: C, 36.90; H, 5.38; N, 4.87. Found: C, 37.03; H, 5.26; N, 5.02.

PPhMe₂AuN₃



In a 100 ml round bottom flask, [Tl(acac)] (173 mg, 0.57 mmol) was suspended in a toluene (20 ml) solution of PPhMe₂AuCl (200 mg, 0.54 mmol). The suspension was stirred at room temperature for 6 h. Then, the mixture was filtered through a plug of Celite®. To the filtrate TMSN₃ (0.14 ml, 122.6 mg, 1.07 mmol) and methanol (1 ml) were added. The reaction mixture was stirred for another 12 h followed by filtered through a plug of Celite®. The filtrate was concentrated to 1 ml and 15 ml of pentane was added to precipitate the product as an off-white power (yield: 180mg, 88%). ¹H NMR (500 MHz, CDCl₃, 25 °C, δ (ppm)): 7.72-7.68 (m, 2H, HC₃), 7.56-7.49 (m, 3H, HC₄, HC₅), 1.87 (d, ²J_{HP} = 10.7 Hz, 6H, HC₁). ¹³C{¹H} NMR Shifts (500 MHz, CDCl₃, 25 °C, δ (ppm)): 132.9 (C₅), 131.77 (C₃), 131.22 (C₂), 129.38 (C₄), 11.59 (C₁). ³¹P{¹H} NMR (121.4 MHz, CDCl₃, 25 °C, δ (ppm)): 1.11 (bs). Anal. Calcd. (%) for C₈H₁₁AuN₃P: C, 25.48; H, 2.94; N, 11.14. Found: C, 25.67; H, 3.28; N, 10.93.

3. NMR Spectra

NMR spectra of 1

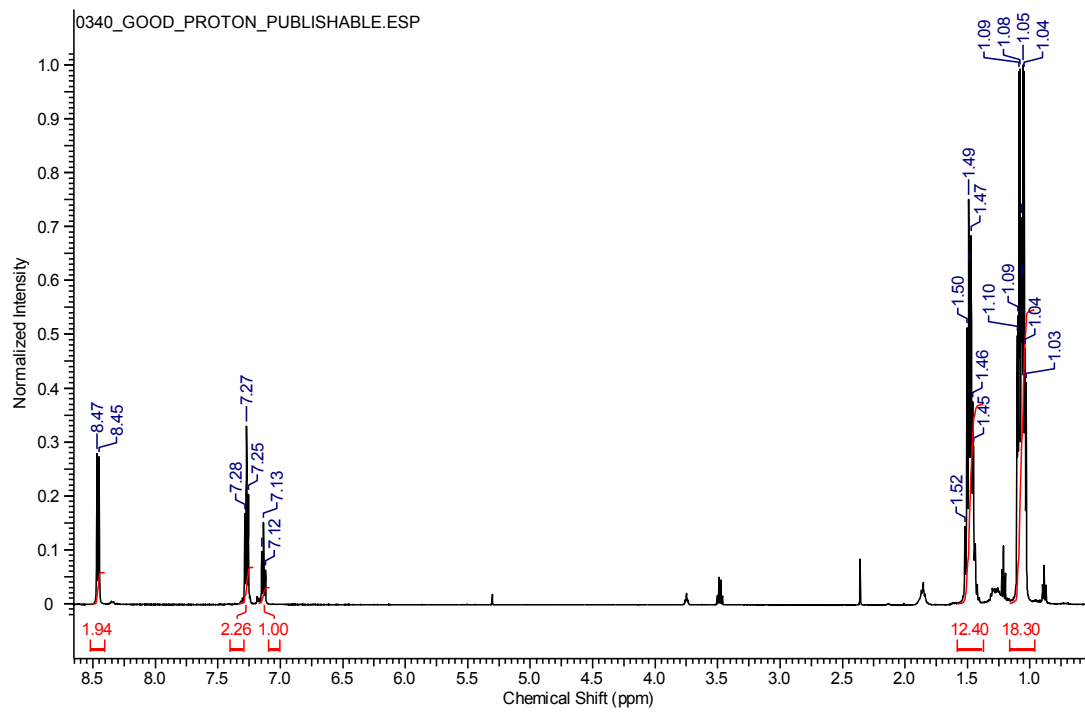


Figure S1. ^1H NMR spectrum of **1** (500 MHz, CDCl_3), integration levels are set for $\frac{1}{2}$ of the complex.

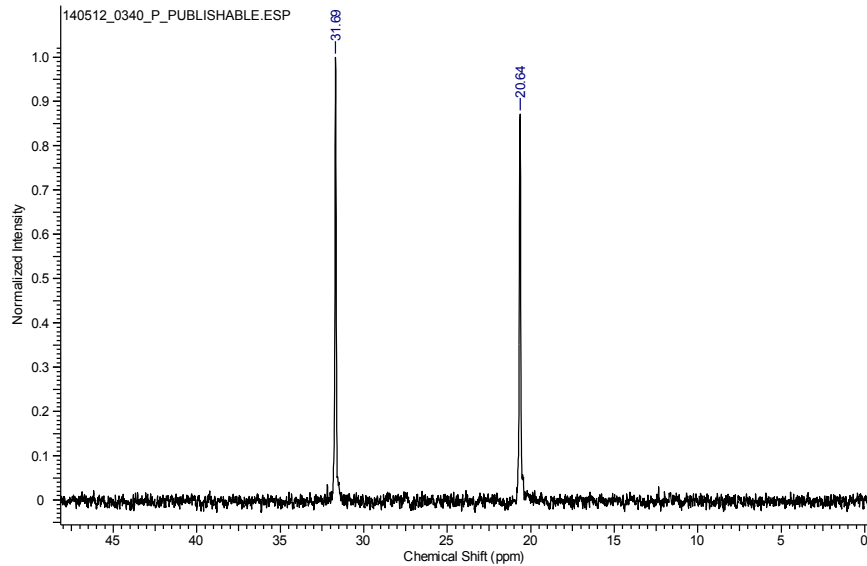


Figure S2. $^{31}\text{P}\{\text{H}\}$ NMR spectrum of **1** (121 MHz, CDCl_3).

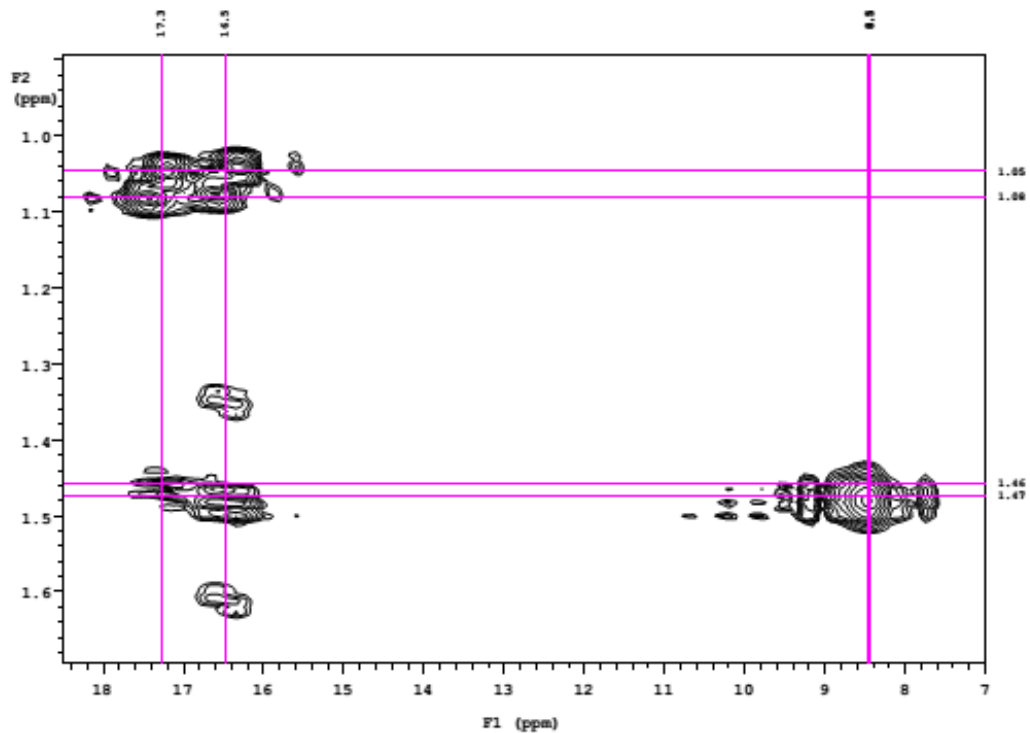


Figure S3. ^1H - ^{13}C gHMBC spectrum of **1** (500 MHz, CDCl_3) (expanded region F2: 1.0-1.6 ppm).

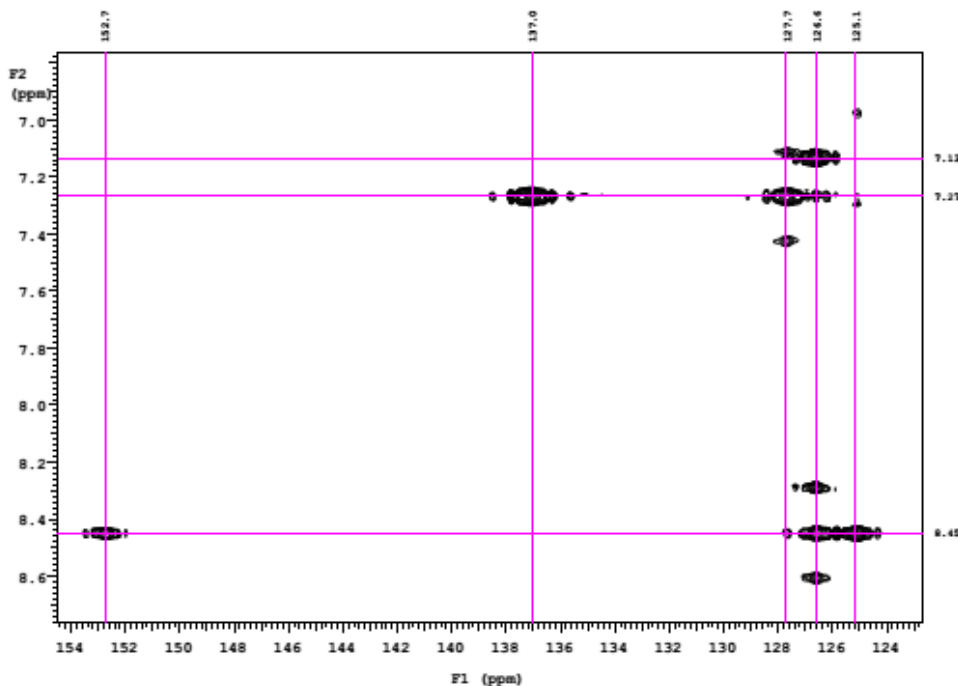


Figure S4. ^1H - ^{13}C gHMBC spectrum of **1** (500 MHz, CDCl_3) (expanded region F2: 7.0-8.6 ppm).

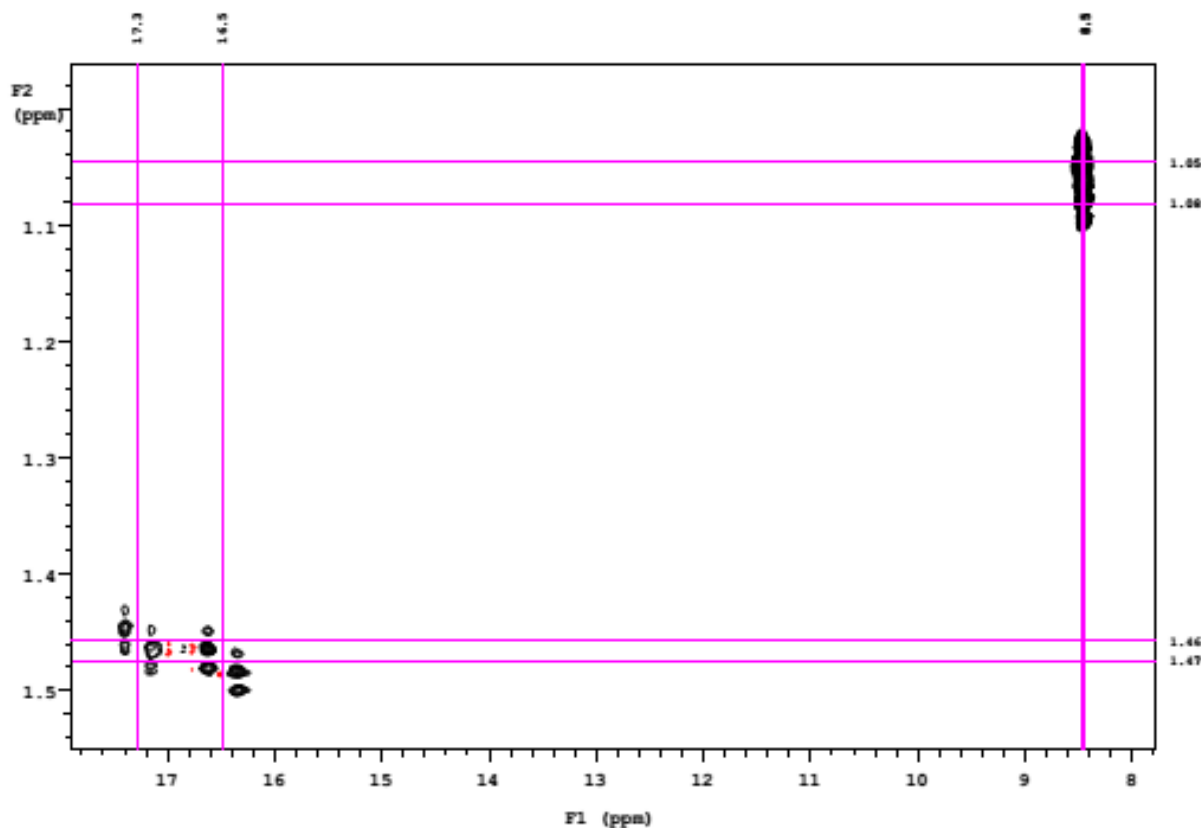


Figure S5. ^1H - ^{13}C gHMBC spectrum of **1** (500 MHz, CDCl_3) (expanded region F2: 7.0-8.6 ppm).

NMR spectra of 2

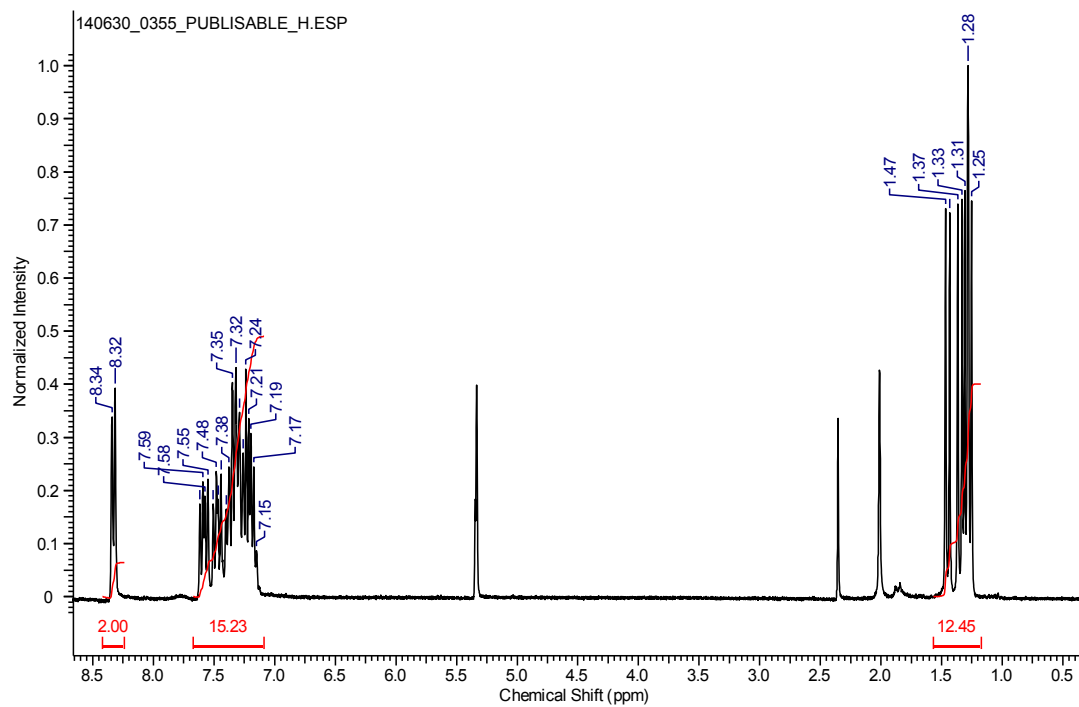


Figure S6. ^1H NMR spectrum of **2** (500 MHz, CDCl_3), integration levels are set for $\frac{1}{2}$ of the complex.

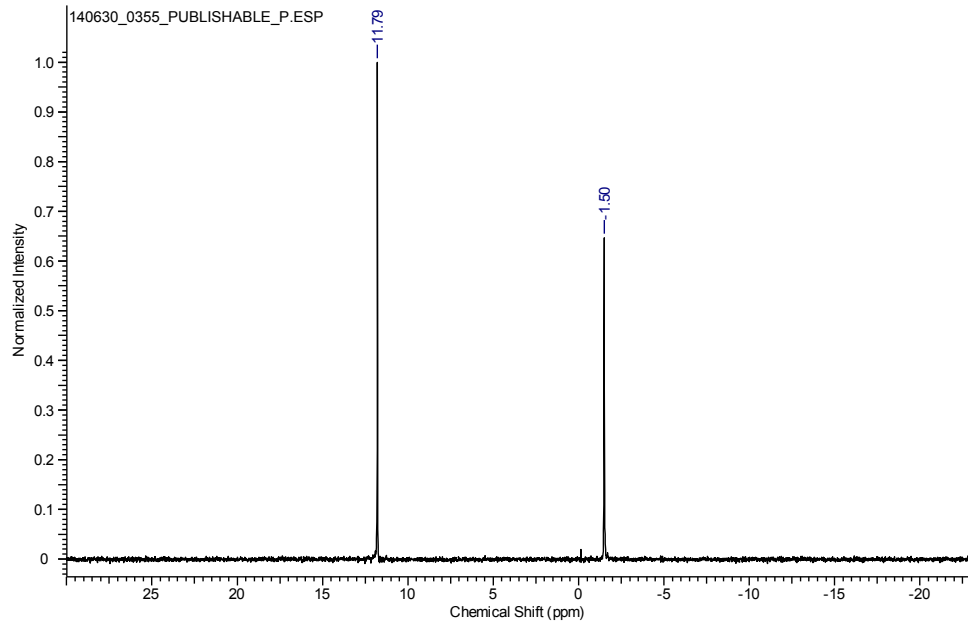


Figure S7. $^{31}\text{P}\{\text{H}\}$ NMR spectrum **2** (121 MHz, CDCl_3).

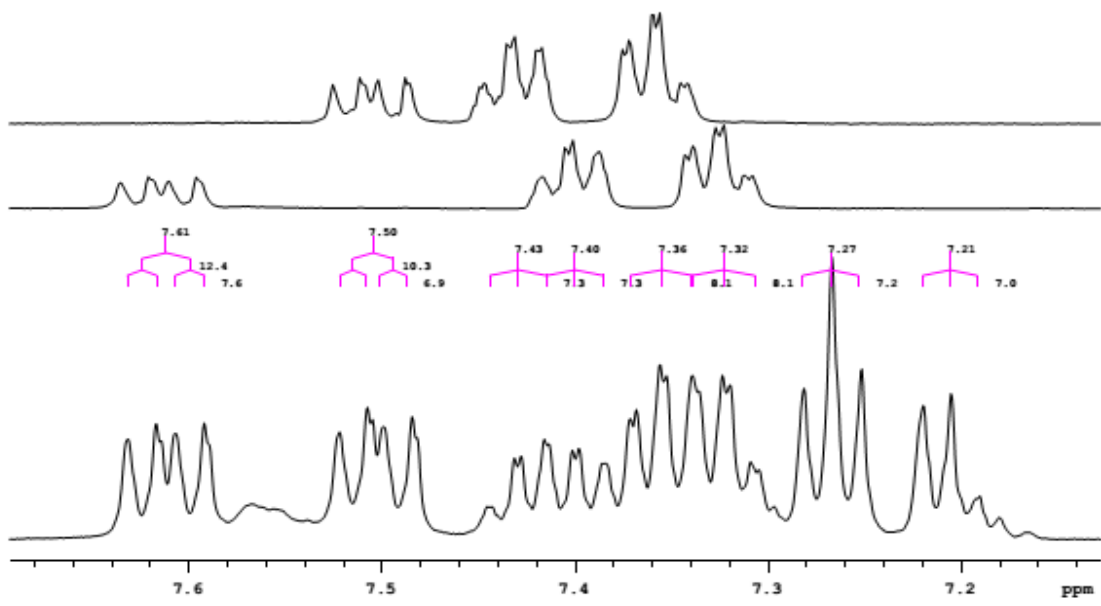


Figure S8. ¹H NMR spectrum of **2**, expansion of aromatic region (bottom) and TOCSY 1D spectra with selective excitation at 7.61 ppm (middle) and 7.50 ppm (top).

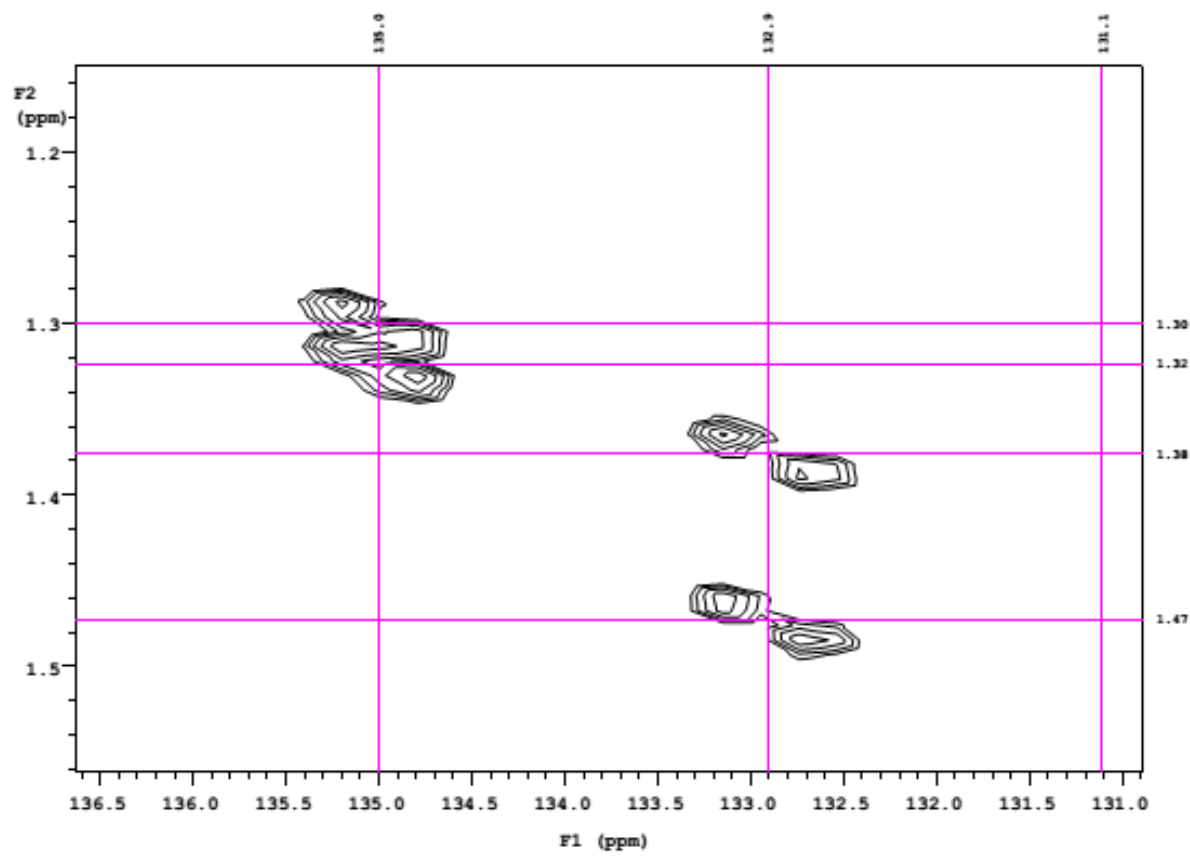


Figure S9. ¹H-¹³C gHMBC spectrum of **2** (500 MHz, CDCl₃) (expanded region F2: 1.1-1.6 ppm).

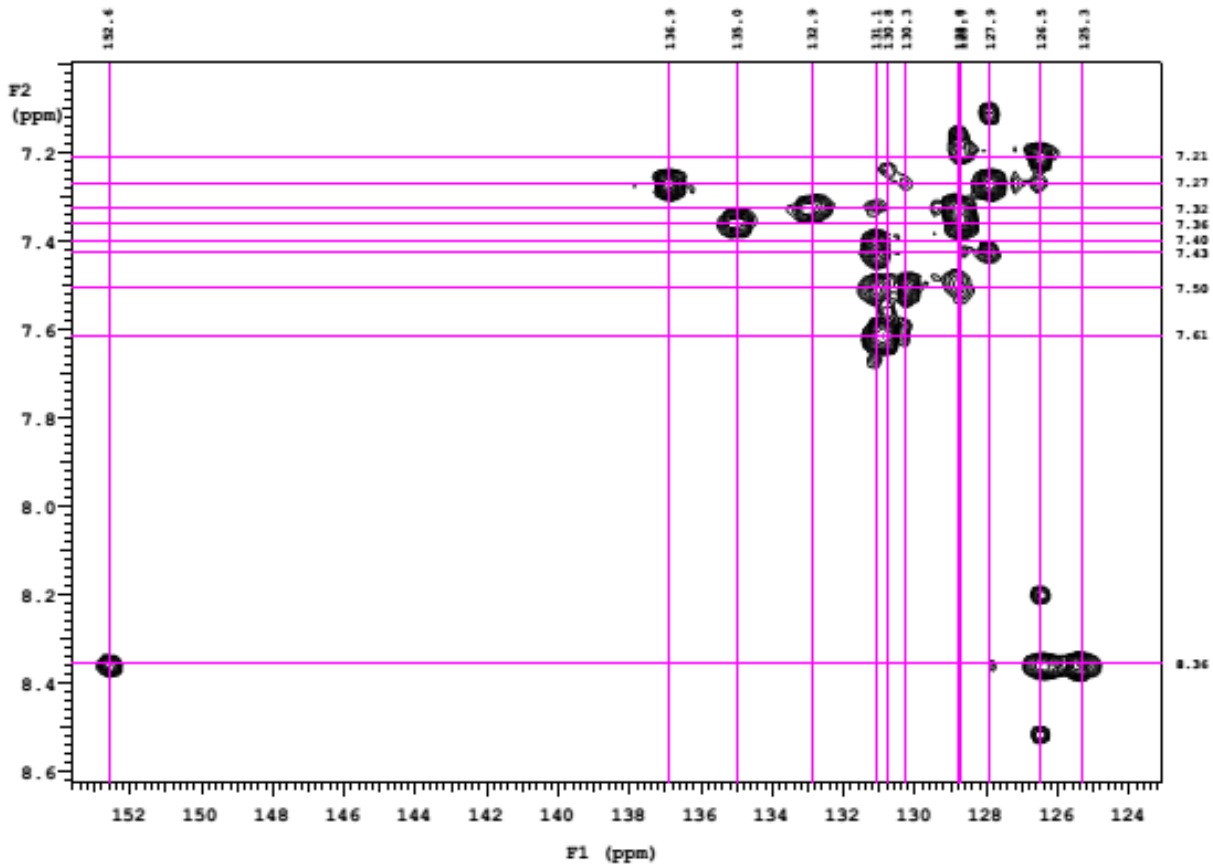


Figure S10. ^1H - ^{13}C gHMBC spectrum of **2** (500 MHz, CDCl_3) (expanded region F2: 7.1-8.6 ppm).

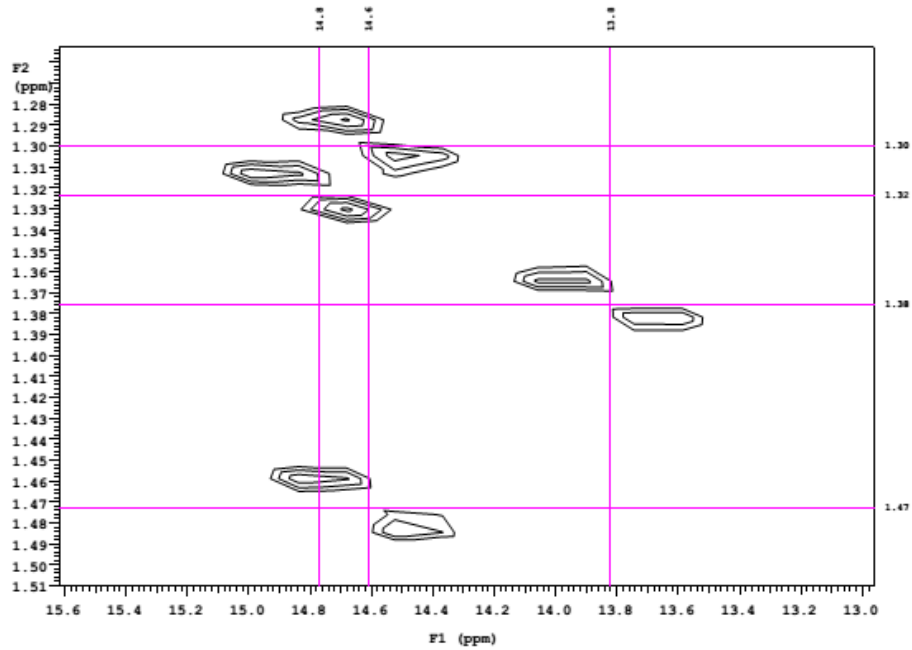


Figure S11. ^1H - ^{13}C gHSQC spectrum of **2** (500 MHz, CDCl_3) (expanded region F2: 1.2-1.6 ppm).

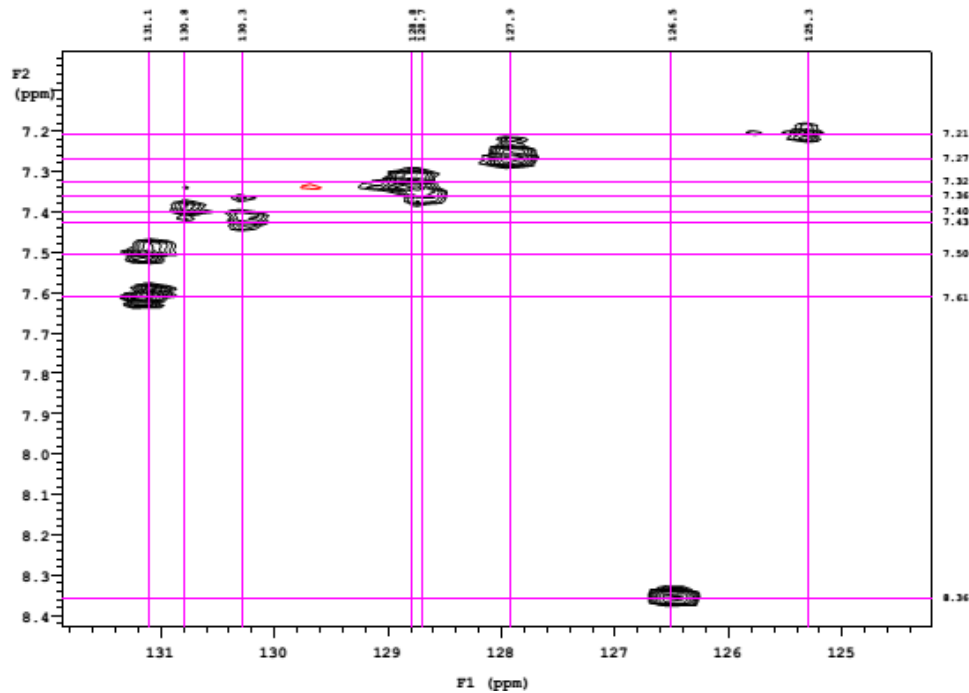


Figure S12. ^1H - ^{13}C gHSQC spectrum of **2** (500 MHz, CDCl_3) (expanded region F2: 7.1-8.4 ppm).

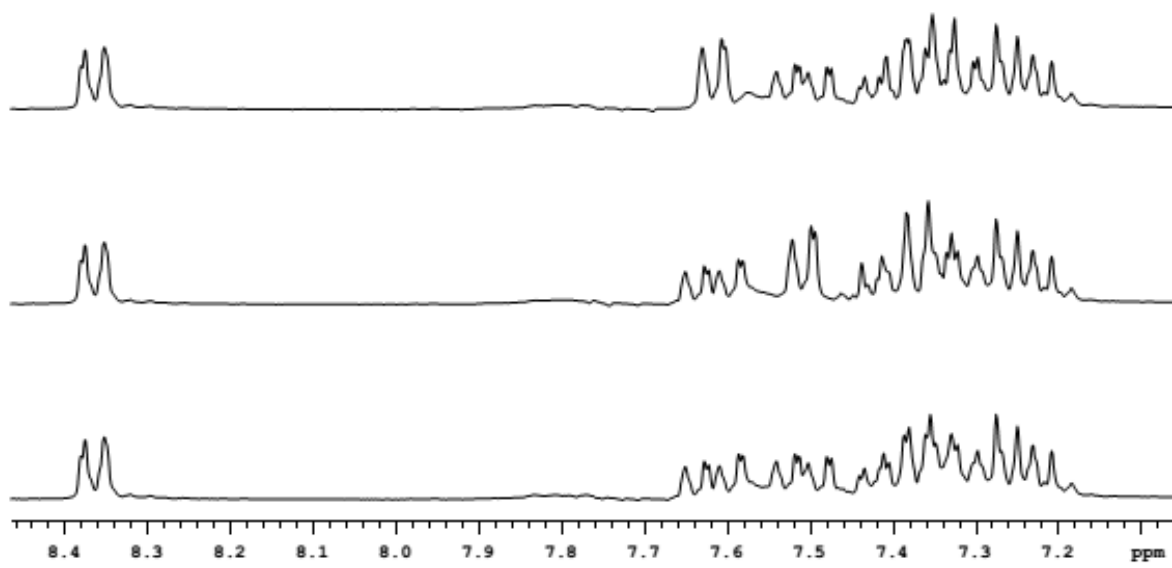


Figure S13. ^1H NMR spectrum of **2**, expansion of the aromatic region (bottom) and proton spectra with selective ^{31}P decoupling at 11.79 ppm (middle) and -1.50 ppm (top).

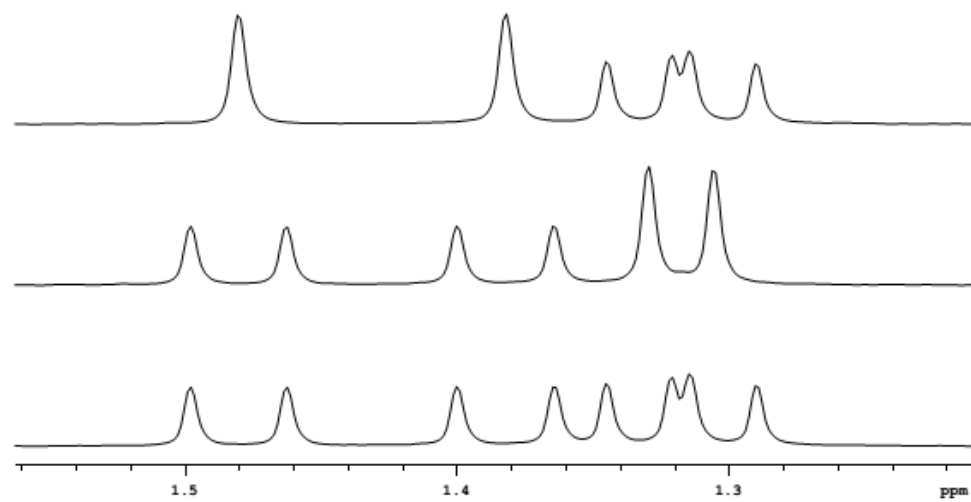


Figure S14. ^1H NMR spectrum of **2**, expansion of the aliphatic region (bottom) and proton spectra with selective ^{31}P decoupling at 11.79 ppm (middle) and -1.50 ppm (top).

NMR spectra of 5

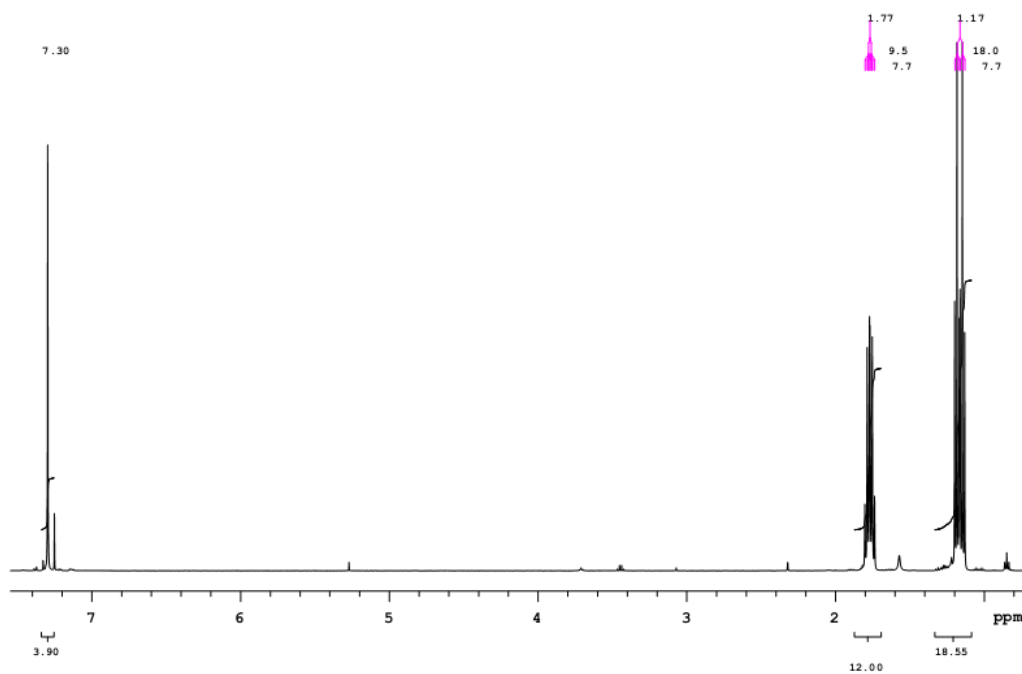


Figure S15. ^1H NMR spectrum of **5** (500 MHz, CDCl_3).

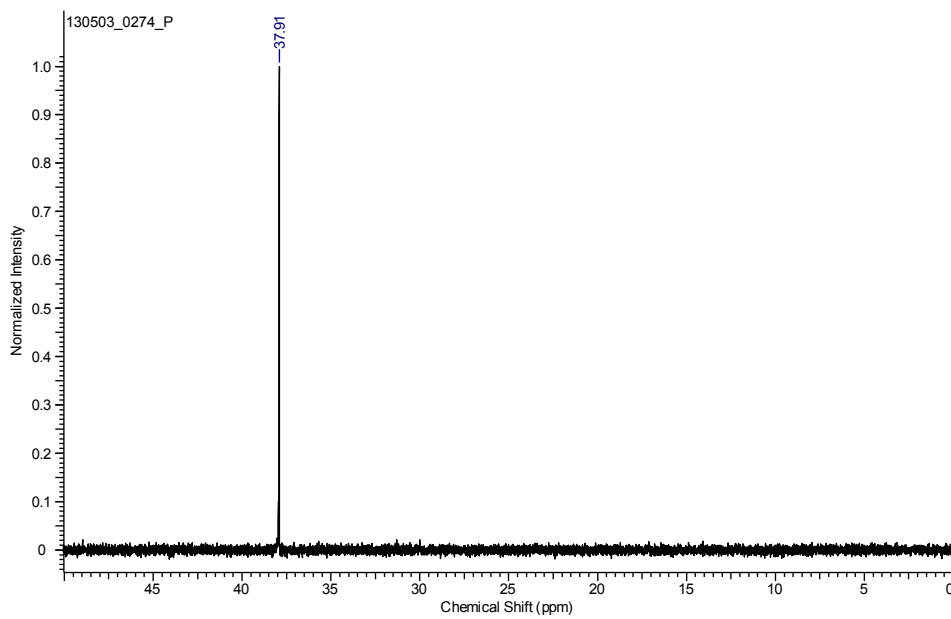


Figure S16. $^{31}\text{P}\{\text{H}\}$ NMR spectrum of **5** (121 MHz, CDCl_3).

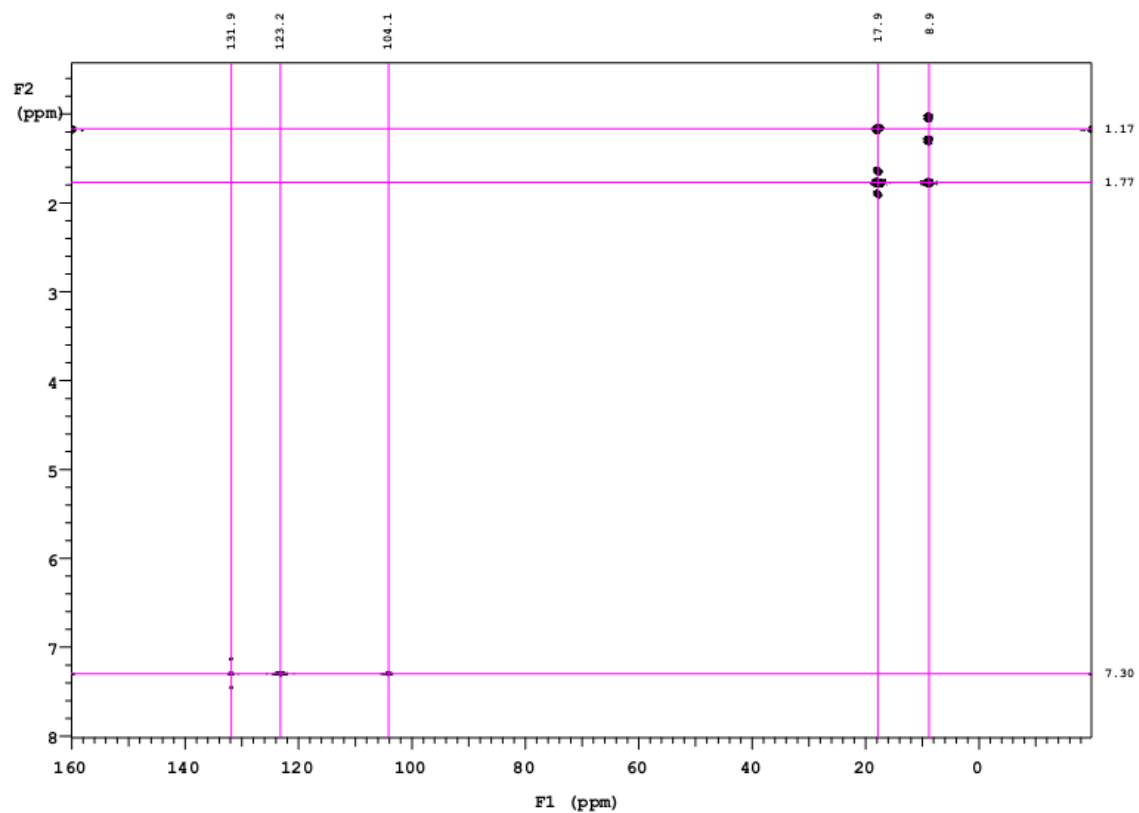


Figure S17. ^1H - ^{13}C gHMBC spectrum of **5** (500 MHz, CDCl_3).

NMR spectra of 7

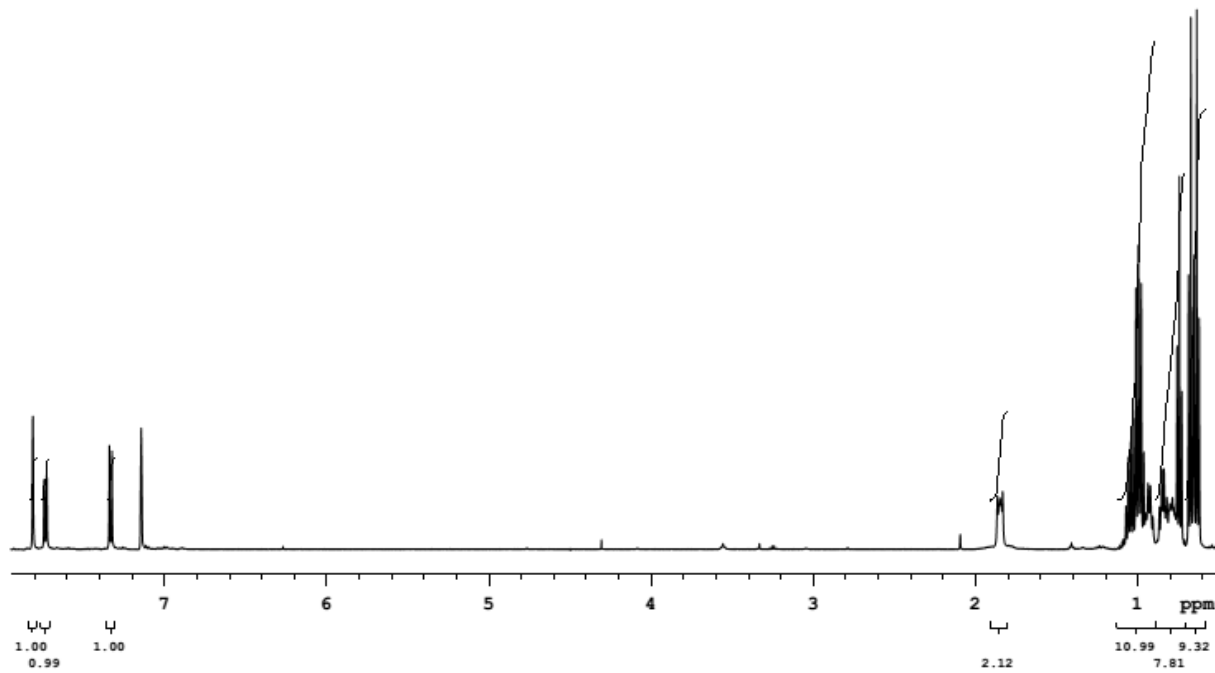


Figure S18. ¹H NMR spectrum of 7 (500 MHz, C₆D₆).

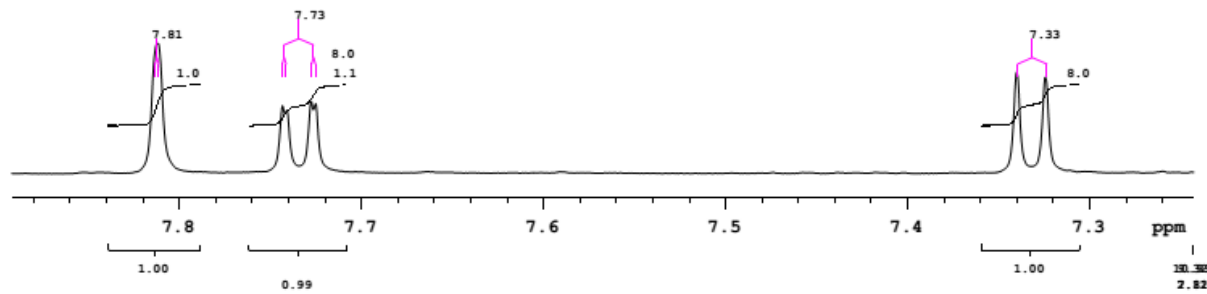


Figure S19. ¹H NMR spectrum of 7 (500 MHz, C₆D₆) (expanded region: 7.3-7.9 ppm).

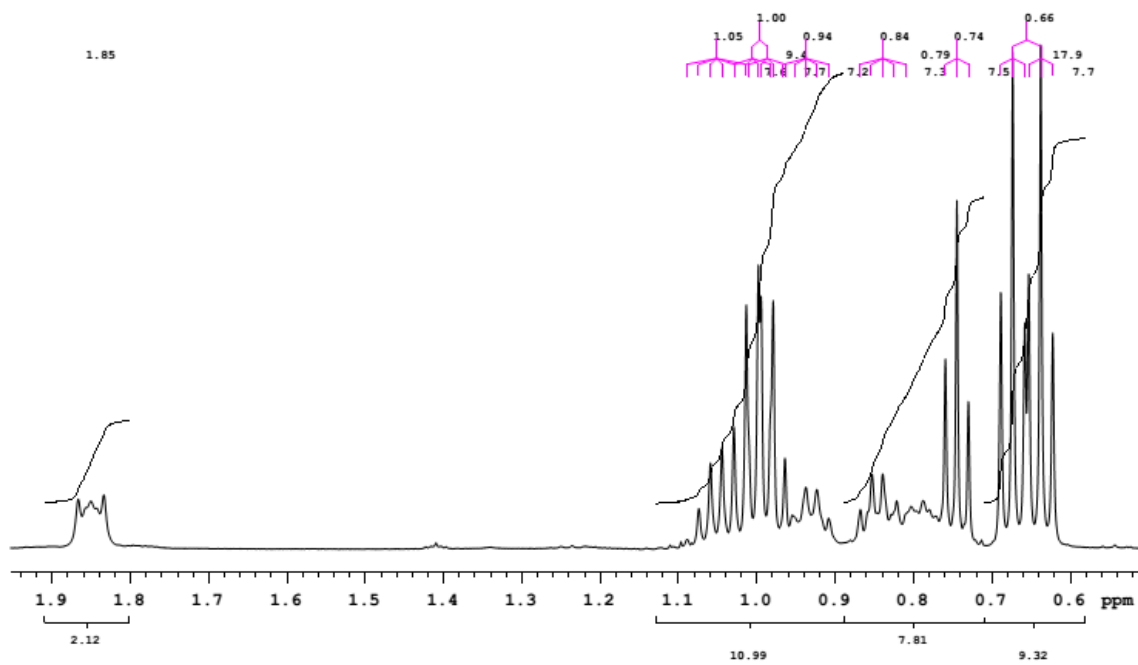


Figure S20. ^1H NMR spectrum of **7** (500 MHz, C_6D_6) (expanded region: 0.5-2.0 ppm).

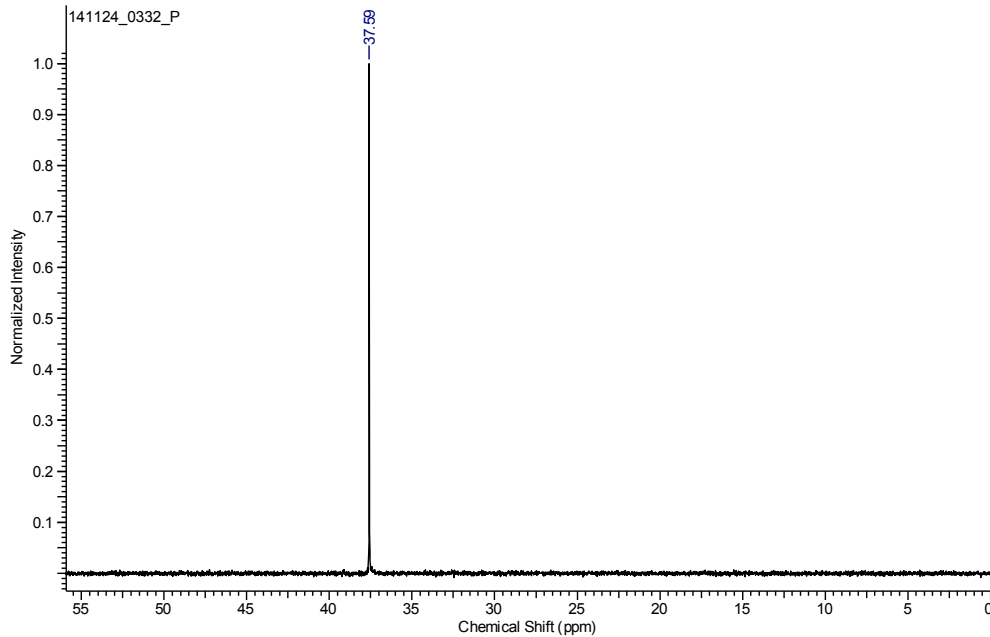


Figure S21. $^{31}\text{P}\{\text{H}\}$ NMR spectrum of **7** (121 MHz, C_6D_6).

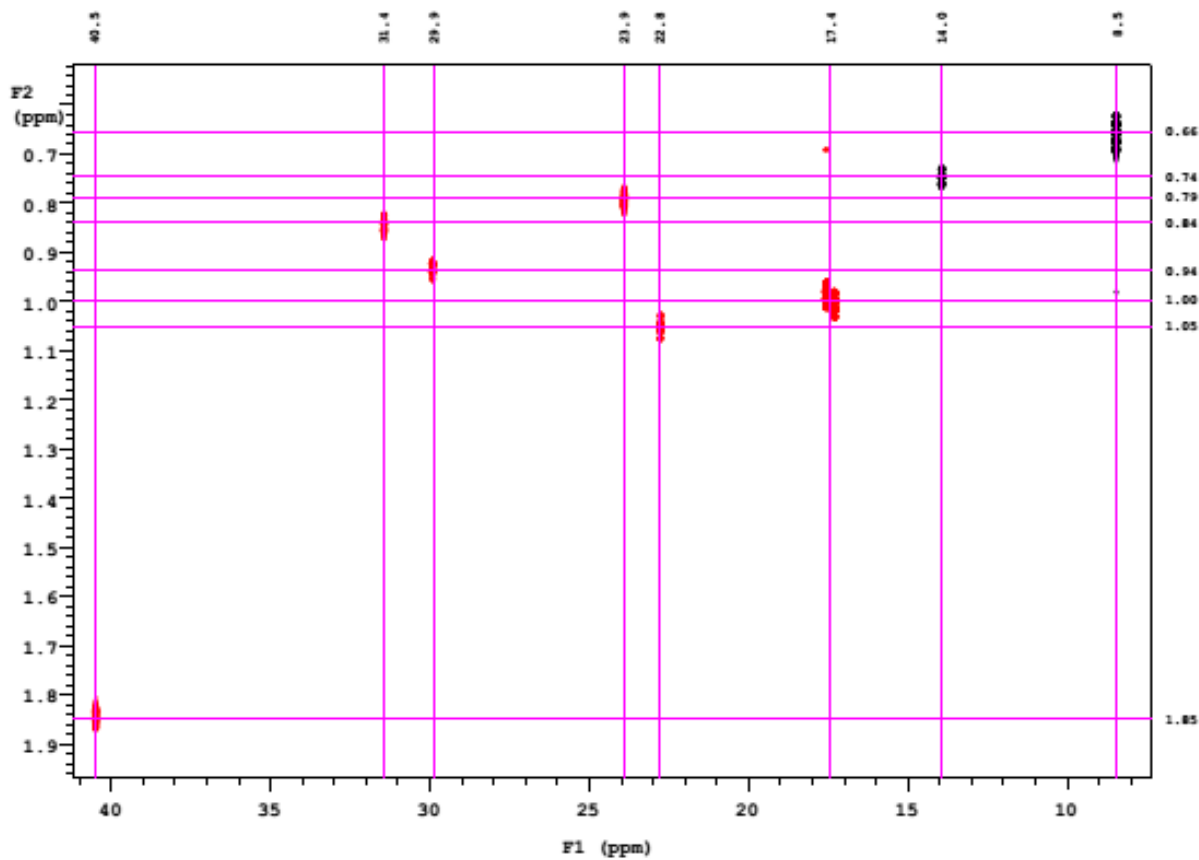


Figure S22. ¹H-¹³C gHSQC spectrum of **7** (500 MHz, C₆D₆) (expanded region F1: 10-40 ppm; F2: 0.5-2.0 ppm).

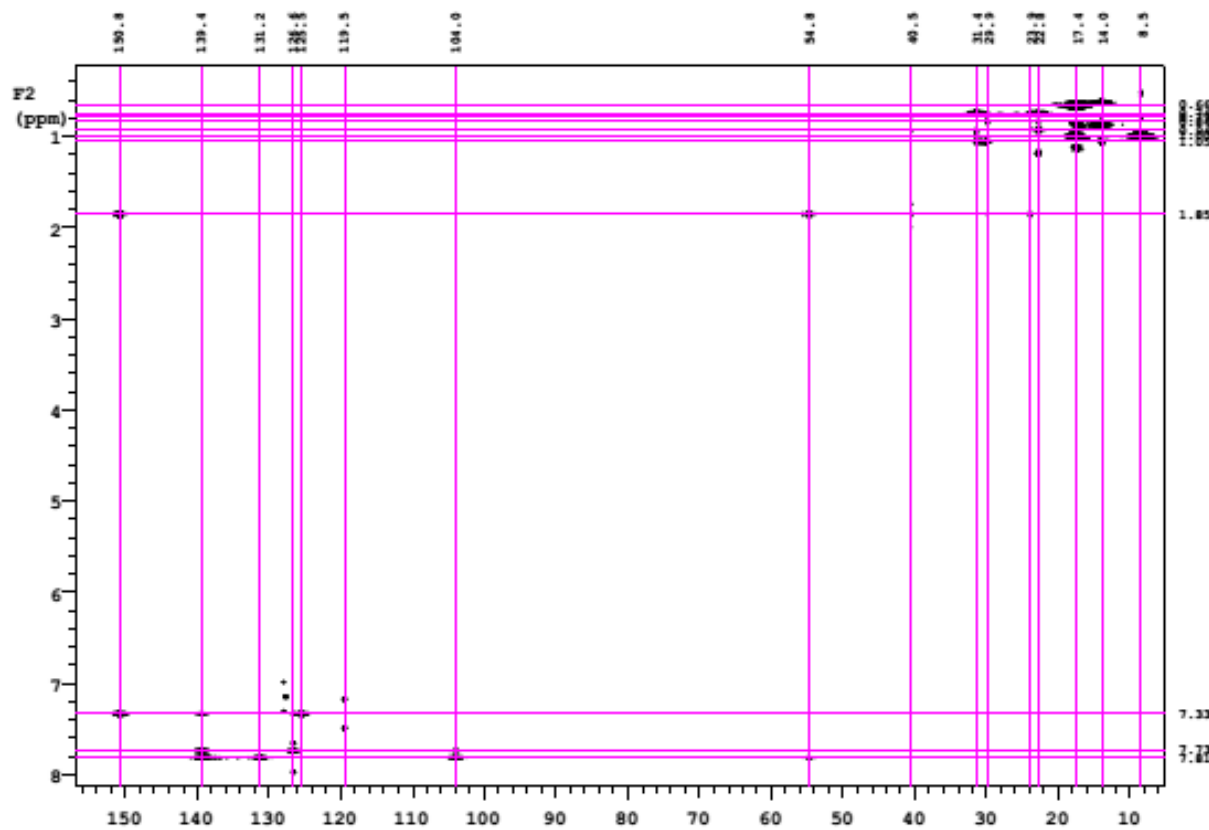


Figure S23. ^1H - ^{13}C gHMBC spectrum of **7** (500 MHz, C_6D_6).

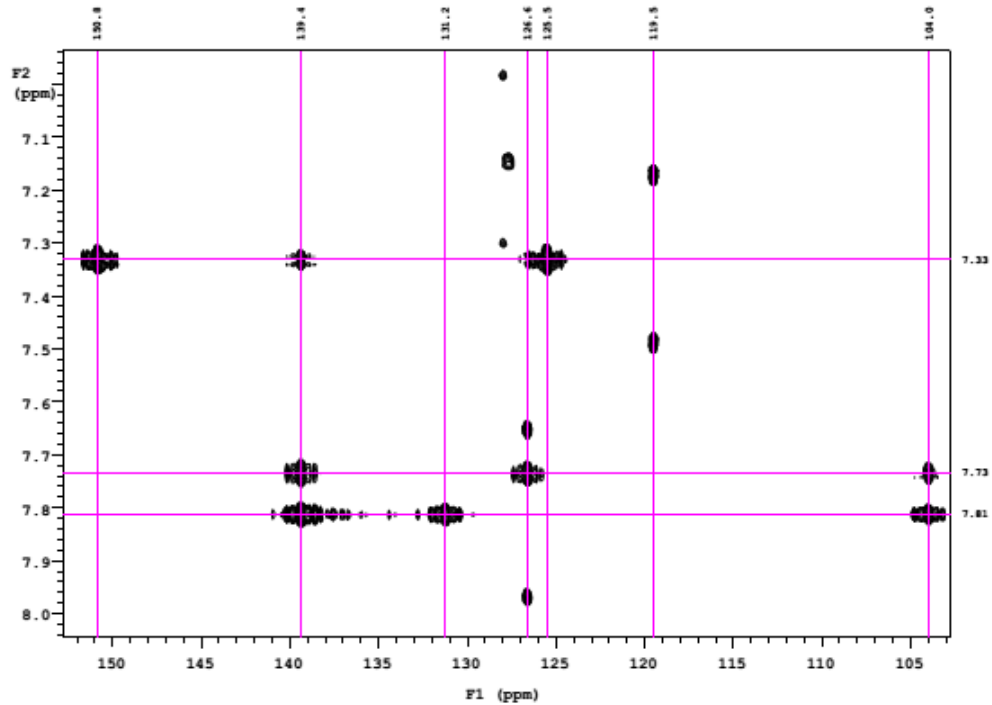


Figure S24. ^1H - ^{13}C gHMBC spectrum of **7** (500 MHz, C_6D_6) (expanded region F1: 105- 150 ppm; F2: 7.0-8.0 ppm).

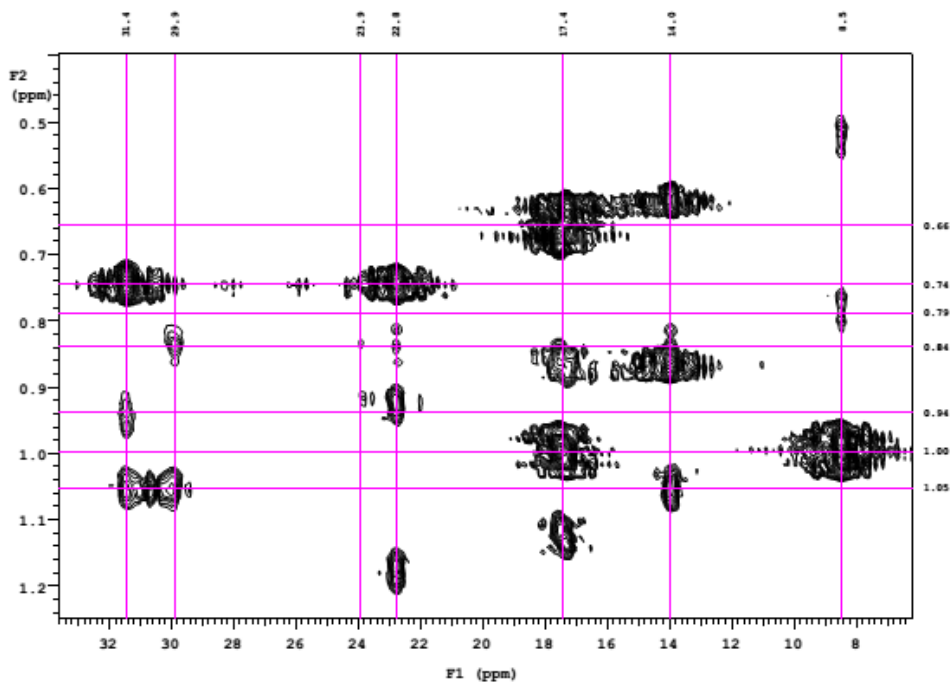


Figure S25. ^1H - ^{13}C gHMBC spectrum of **7** (500 MHz, C_6D_6) (expanded region F1: 7-33 ppm; F2: 0.4-1.2 ppm).

NMR spectra of 8

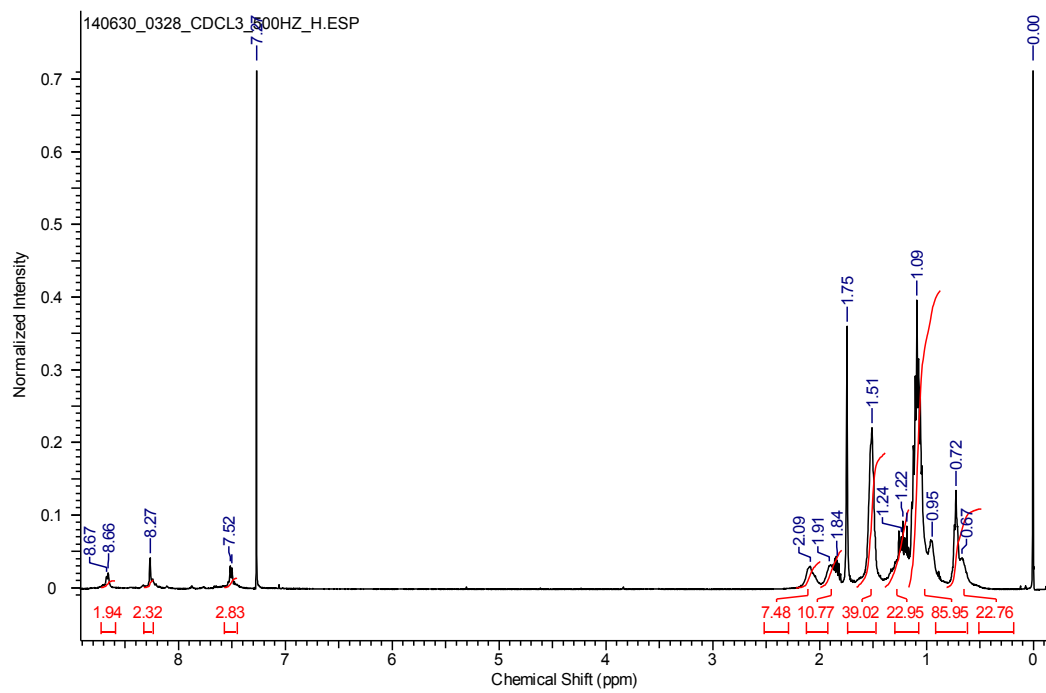


Figure S26. ^1H NMR spectrum of **8** (500 MHz, CDCl_3).

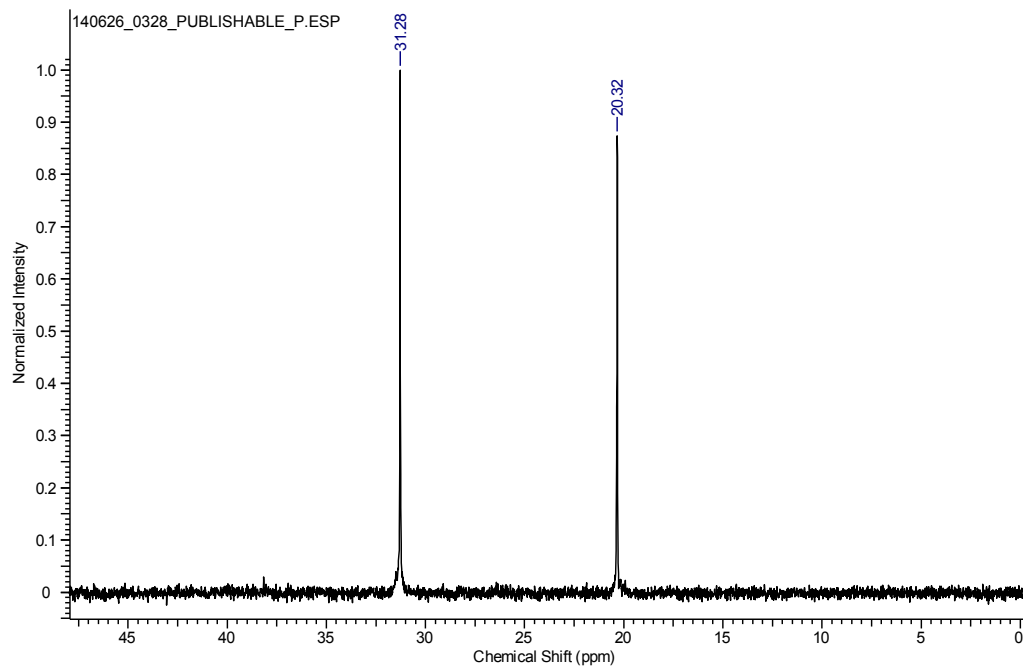


Figure S27. $^{31}\text{P}\{^1\text{H}\}$ NMR spectrum of **8** (121MHz, CDCl_3).

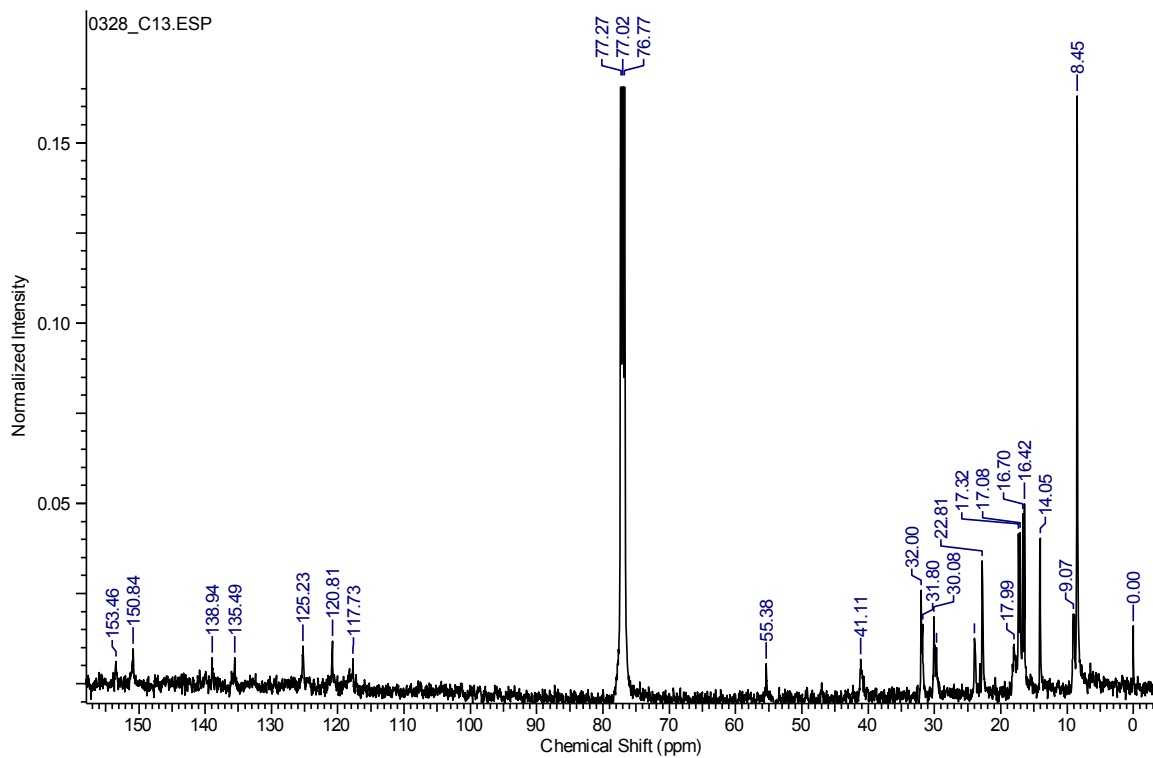


Figure S28. ^{13}C NMR spectrum of **8** (126 MHz, CDCl_3).

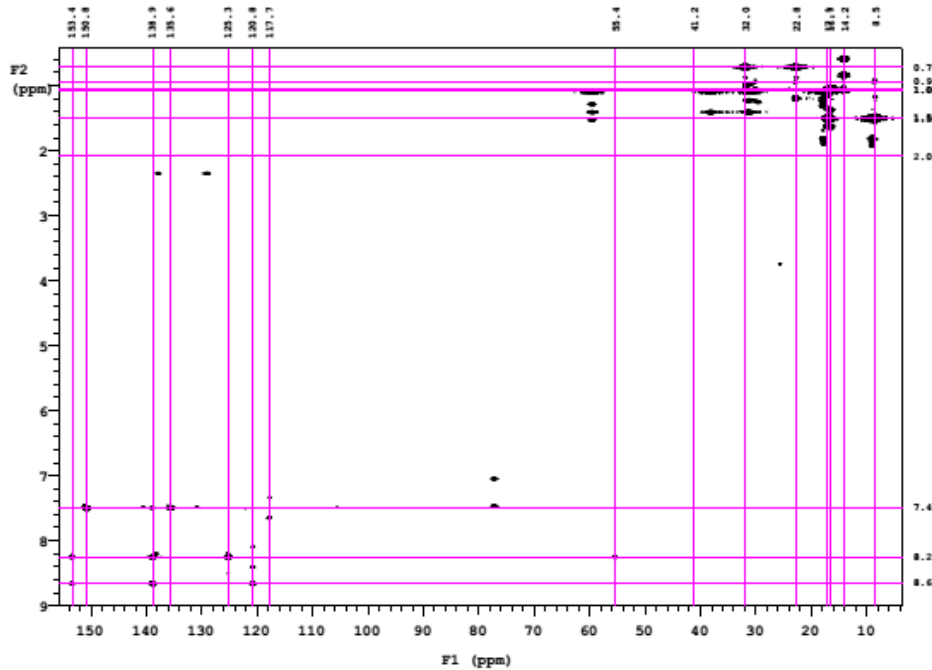


Figure S29. ^1H - ^{13}C gHMBC spectrum of **8** (500 MHz, CDCl_3).

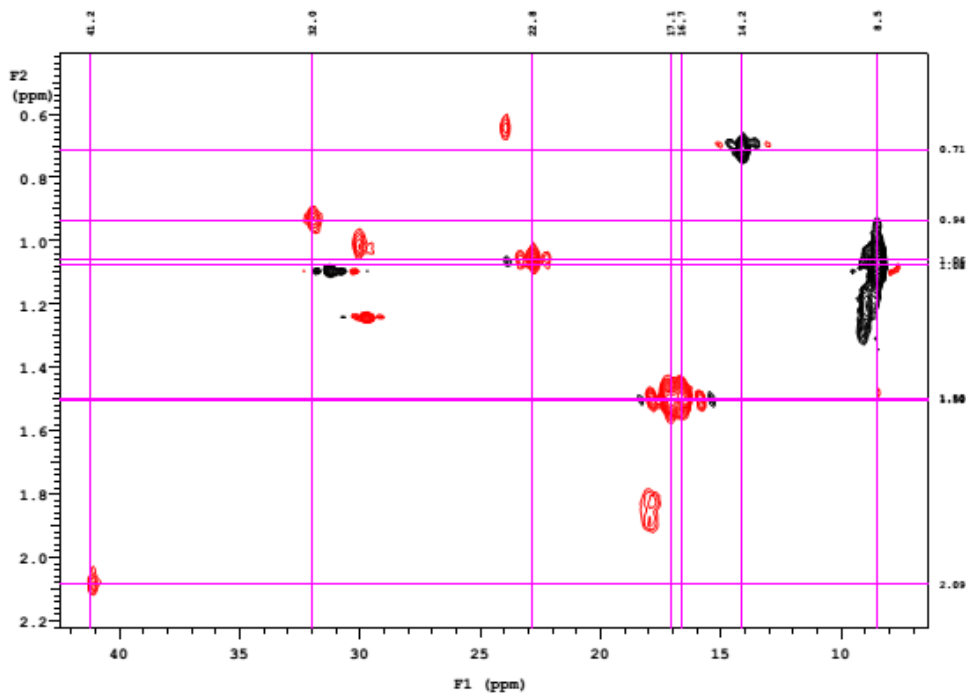


Figure S30. ^1H - ^{13}C gHSQC spectrum of **8** (500 MHz, CDCl_3) (expanded region F2: 0.5-2.2 ppm).

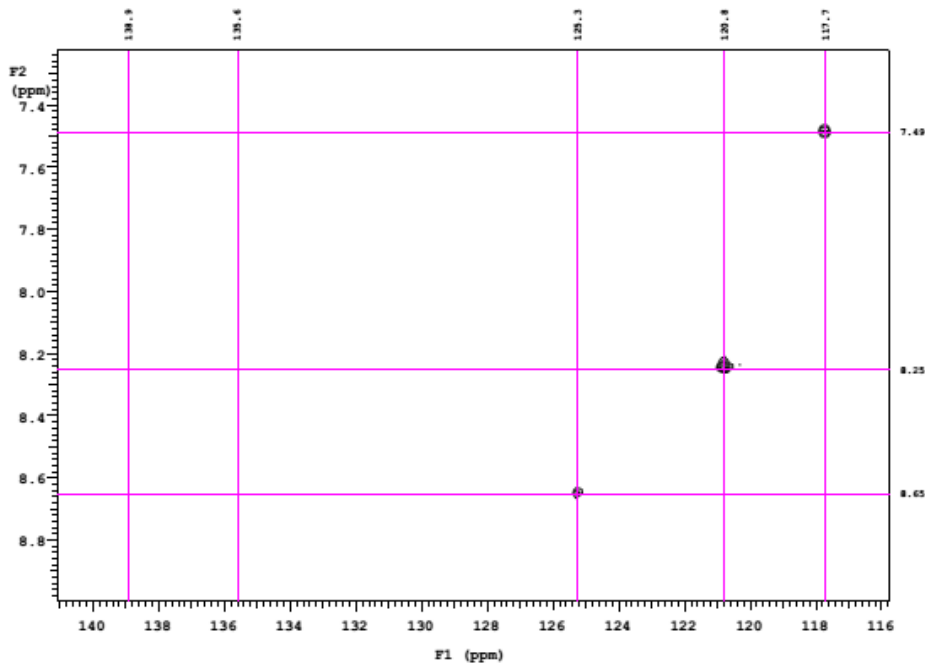


Figure S31. ^1H - ^{13}C gHSQC spectrum of **8** (500 MHz, CDCl_3) (expanded region F2: 7.3-8.9 ppm).

NMR spectra of PPhMe₂AuN₃

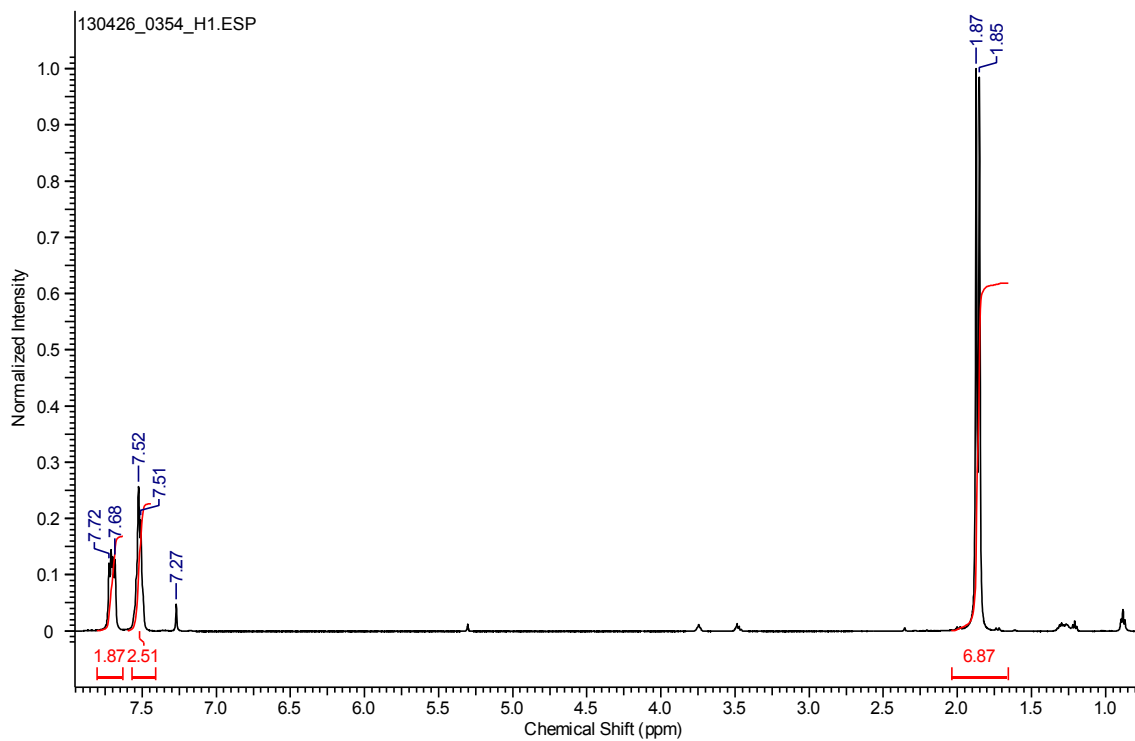


Figure S32. ¹H NMR spectrum of PPhMe₂AuN₃ (500MHz, CDCl₃).

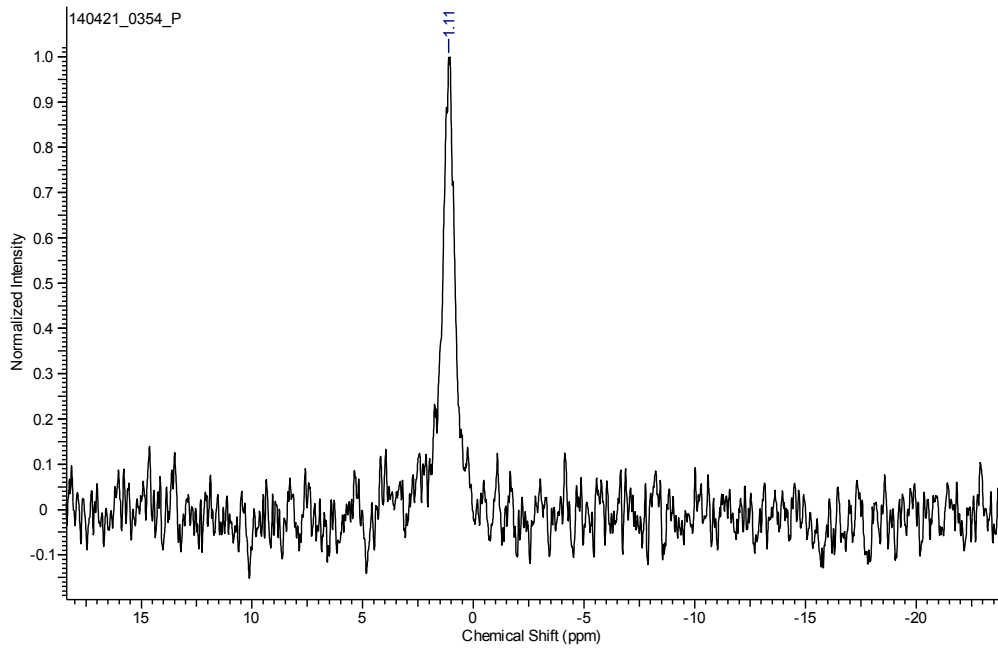


Figure S33. ³¹P{¹H} NMR spectrum of PPhMe₂AuN₃ (121 MHz, CDCl₃).

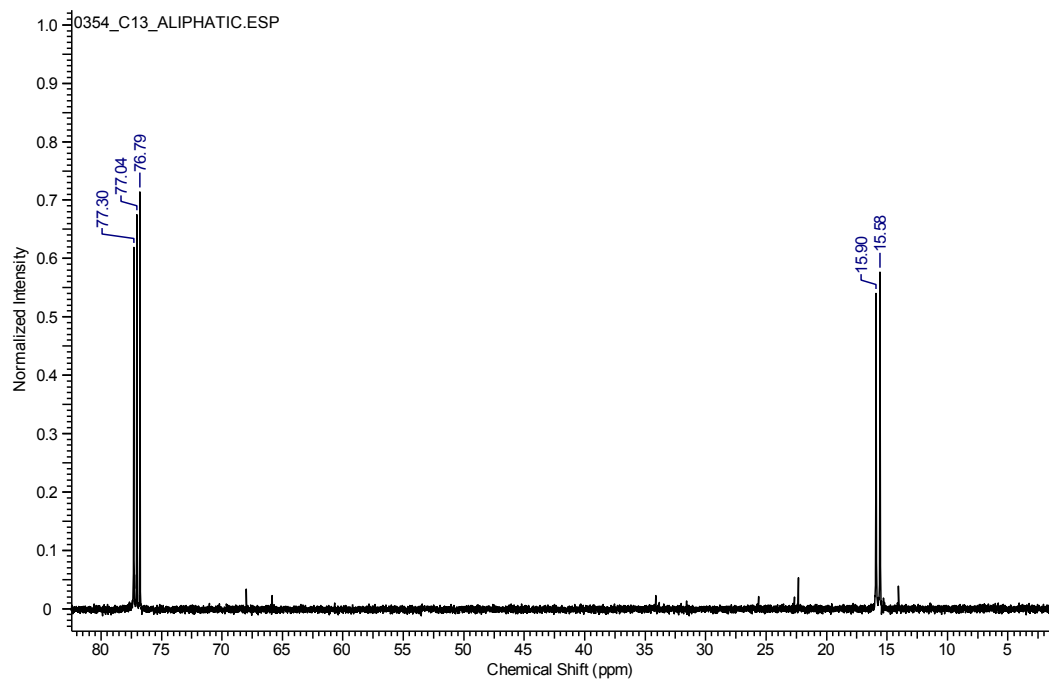


Figure S34. $^{13}\text{C}\{^1\text{H}\}$ NMR spectrum of $\text{PPhMe}_2\text{AuN}_3$ (expanded region: 5-80 ppm) (126 MHz, CDCl_3).

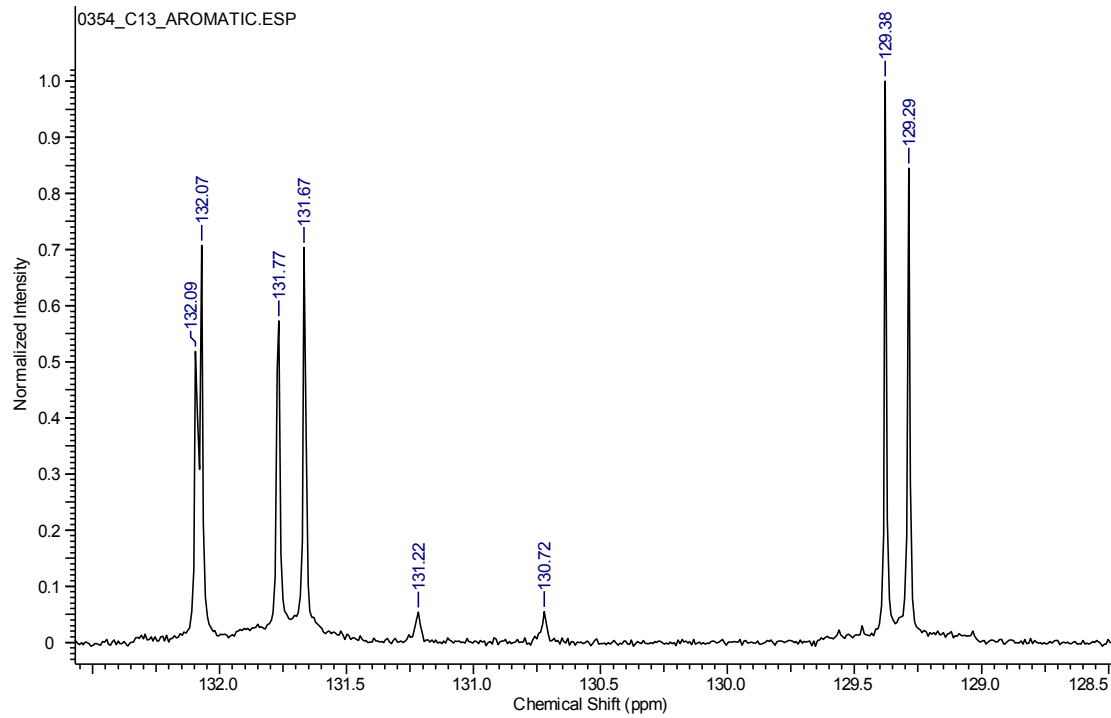


Figure S35. $^{13}\text{C}\{^1\text{H}\}$ NMR spectrum of $\text{PPhMe}_2\text{AuN}_3$ (expanded region: 128.5-133.0 ppm) (126 MHz, CDCl_3).

4. Diffusion Order Spectroscopy (DOSY) NMR Analysis

The diffusion coefficients were measured on an Inova NMR spectrometer, operating at 500 MHz for proton, equipped with a 5 mm indirect detection probe with z-axis gradients. The maximum gradient field was 60 Gauss/cm. The experiment was a bipolar pulse pair stimulated echo with convection compensation with a gradient time of 2 ms and a diffusion time of 100 ms. The gradient power was arrayed in 15 steps, from 1 to 60 Gauss/cm. The temperatures were kept at 25 °C and no spinning was applied to NMR samples. The samples were studied in CDCl₃, C₆D₆ and DMSO-*d*₆. Tetramethylsilane (TMS) was used as an internal standard.

The Stokes-Einstein equation⁷ modified for the size of the diffusion molecule⁸ was used for simulated the pseudo-spherical hydrodynamic radii (r_h):

$$D = \frac{k_B T \left(1 + 0.695 \left(\frac{r_{sl}}{r_H} \right)^{2.234} \right)}{6\pi\eta r_H}$$

D is the diffusion coefficient. k_B is the Boltzmann constant. T is the absolute temperature. r_h is the hydrodynamic radii of the solvents. η is the viscosity of the solution. The η and r_{sl} of the solvents are listed below⁹:

Solvent	r _{sl} (Å)	η (× 10 ⁻⁴ mPa·s)
CDCl ₃	2.65	5.28
C ₆ D ₆	2.68	6.94
DMSO- <i>d</i> ₆	2.72	21.9

The hydrodynamic radii of complexes **1** and **2**, as simulated from the diffusion coefficients (D) were compared to the radii calculated from the single crystal structure studies (ESI section 7).

The volumes of the complexes were derived from their unit cell volume and Z. The complexes were assumed to be spherical.

¹H DOSY NMR Analysis of **1 and **2****

Diffusion coefficients (D) of **1** and **2**, the hydrodynamic radii (r_h) simulated from the diffusion coefficients and the radii (r) calculated from the crystal structure data are listed in the Table S1. These experiments were done in CDCl₃ at 25 °C with a sample concentration of 50 μM.

Table S1. Diffusion coefficients of **1** and **2** and the comparison of the hydrodynamic radii with the radii derived from the crystal structure data.

Complex	D ($\times 10^{-10}$ m ² s ⁻¹)	r_h (Å)	r (Å)
1	6.96 ± 0.03	6.50	6.60
2	6.25 ± 0.03	7.12	6.63

Dissolving complex **1** in DMSO-*d*₆ at 25 °C establishes equilibrium between the Au₄ cluster and the Au₂ intermediate due to the dissociation of **1**. The diffusion coefficients of these two species and their simulated hydrodynamic radii are listed in the Table S2. As the predicted ratio of r_h values between the Au₄ cluster and the Au₂ intermediate is about 1.2.¹⁰ Consistent with the expected value, the ratio of **1** (Au₄) and the dissociated complex Au₂ is 1.21. This experiment was performed in DMSO-*d*₆ at 25 °C with the sample's concentration as 5 μM.

Table S2. Diffusion coefficients and simulated hydrodynamic radii of the Au₄ cluster and Au₂ intermediate of complex **1**.

Complex	D ($\times 10^{-10}$ m ² s ⁻¹)	r_h (Å)
1 (Au ₄ cluster)	2.06 ± 0.07	5.53
1 (Au ₂ intermediate)	2.65 ± 0.12	4.58

¹H DOSY NMR Analysis of 8

The diffusion coefficient (D) of **8** measured in CDCl₃, the simulated hydrodynamic radius r_h, and the diameter of **8** measured by dynamic light scattering (DLS) in CH₂Cl₂, are listed in Table S3. The experiments were performed at 25 °C with concentration as 5 μM and 0.5 μM for the ¹H DOSY NMR and DLS experiments, respectively.

Table S3. The diffusion coefficient in CDCl₃ and DLS in CH₂Cl₂ of complex **8**.

Complex	D ($\times 10^{-10}$ m ² s ⁻¹)	r _h (Å)	DLS (Å)
8	1.70 ± 0.02	24.4	16.0

A variable concentration ¹H DOSY NMR experiment of complex **8** was performed in C₆D₆ at 25 °C with a concentration range from 5 to 50 μM. The diffusion coefficients of TMS in samples of 10 μM and 30 μM were statistically the same within the experimental errors indicating that the decrease in the diffusion coefficient with the concentration is due to an increase in the degree of oligomerization. All the data are listed in the Table S4 (nm = “not measured”). A plot of the diffusion coefficients vs concentration is depicted in Figure S36 and the red dash line represents the diffusion coefficient changing trend.

Table S4. Variable concentration ¹H DOSY NMR experiments of complex **8**.

Concentration (μM)	5	10	20	30	50
D of 8 ($\times 10^{-10}$ m ² s ⁻¹)	1.39 ± 0.10	1.06 ± 0.06	0.93 ± 0.05	0.54 ± 0.04	0.35 ± 0.01
D of TMS ($\times 10^{-10}$ m ² s ⁻¹)	nm	21.25 ± 0.32	nm	20.78 ± 0.64	nm

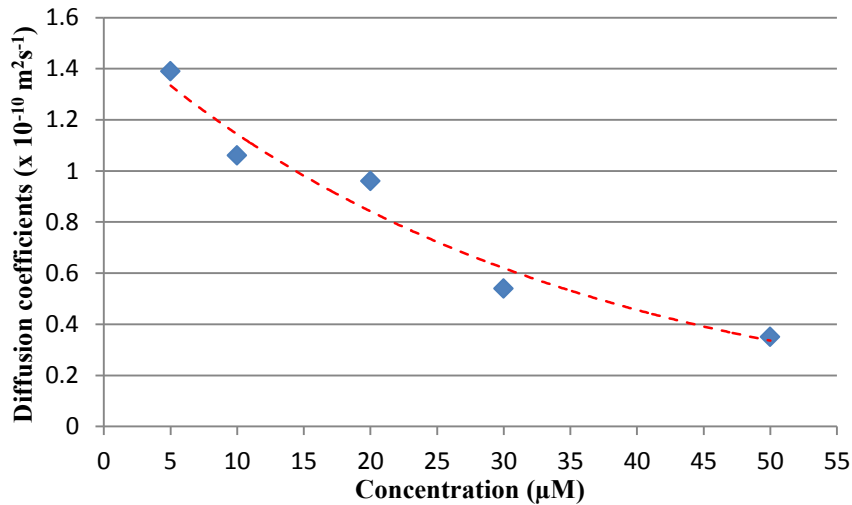


Figure S36. Plot of the diffusion coefficients of complex **8** vs concentration.

A variable temperature (25 to 65 °C) ^1H DOSY NMR experiment was performed on a sample of **8** with a concentration of 30 μM in C_6D_6 . The diffusion coefficient at each temperature was normalized to 25 °C by multiplying it with the ratio of the diffusion coefficients of TMS at 25 °C vs current temperature. The normalized diffusion coefficients in the last row of the Table S5 demonstrate that the dissociation of **8** begins at temperatures higher than *ca.* 50 °C in C_6D_6 .

Table S5. Variable temperature ^1H DOSY NMR experiment of **8**.

Temperature (°C)	25	35	45	55	65
D of 8 ($\times 10^{-10} \text{ m}^2 \text{s}^{-1}$)	0.54 ± 0.02	0.61 ± 0.03	0.74 ± 0.03	0.96 ± 0.04	1.26 ± 0.05
D of TMS ($\times 10^{-10} \text{ m}^2 \text{s}^{-1}$)	20.78 ± 0.64	24.38 ± 0.52	28.78 ± 0.77	33.23 ± 1.10	37.29 ± 1.26
normalized D of 8 ($\times 10^{-10} \text{ m}^2 \text{s}^{-1}$)	0.54 ± 0.02	0.52 ± 0.03	0.54 ± 0.03	0.6 ± 0.04	0.7 ± 0.04

Titrating **8** with one equiv. of **1** in C_6D_6 at 50 °C gave a series of complexes, as determined by ^{31}P NMR spectroscopy (Scheme S1, Figure S37). The ^1H DOSY NMR analysis of the mixture reveals that there are three major species present in solution with diffusion coefficients listed in

the Table S6. The diffusion coefficients confirmed that the higher order **8** was broken into smaller capped complexes ($m = 1, 2$ or 3 etc.), in which complex **1** is the capping reagent.

Scheme S1. Treating **8** with **1** in C_6D_6 gave a series of small capped gold-oligomers.

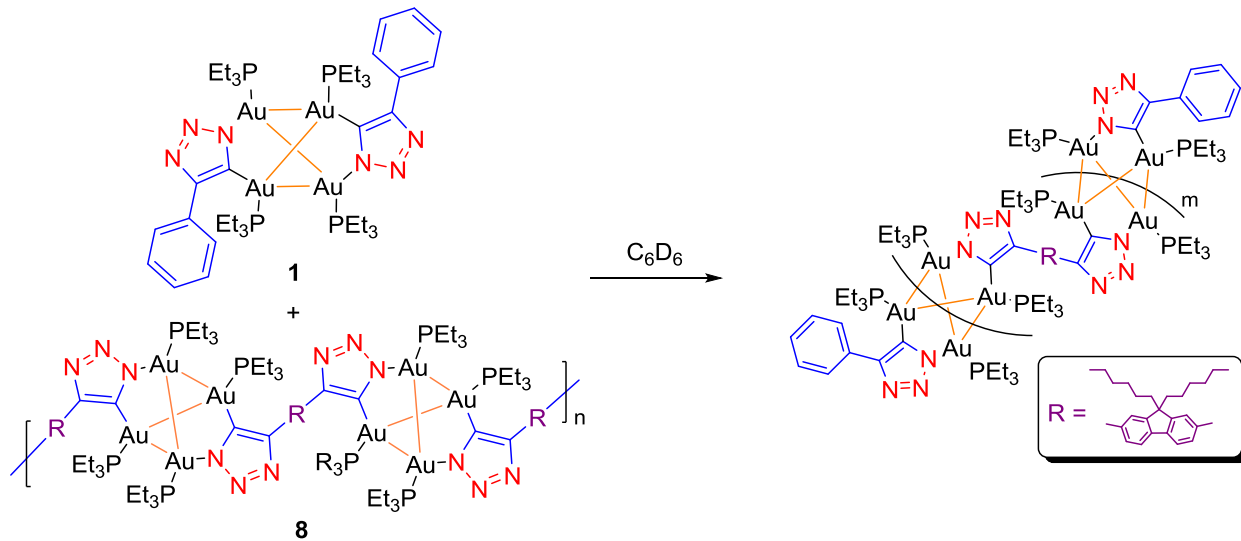


Table S6. Diffusion coefficients of small capped complexes.

Species	Diffusion coefficient ($\times 10^{-10} \text{ m}^2\text{s}^{-1}$)
1	4.17 ± 0.12
2	3.84 ± 0.09
3	3.73 ± 0.09
4	3.11 ± 0.11

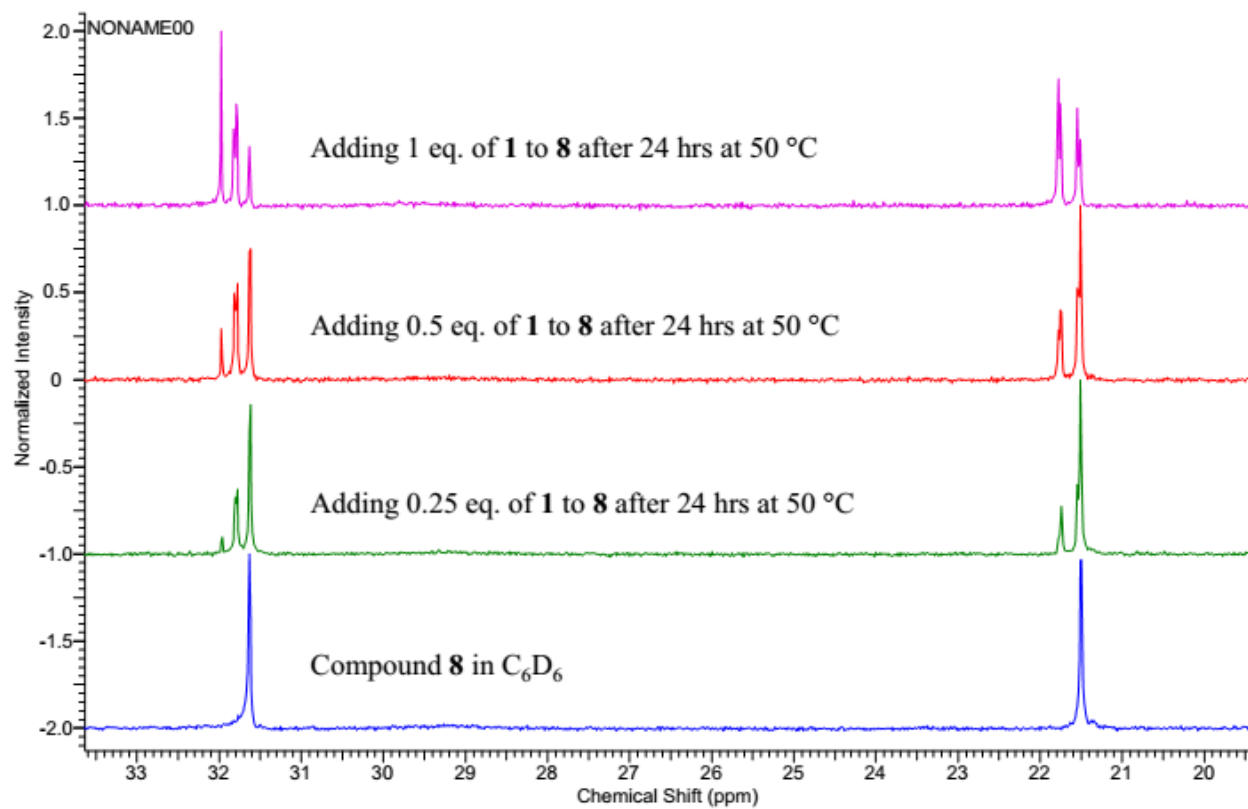


Figure S37. $^{31}P\{^1H\}$ NMR spectra for the titration **1** to **8** in C_6D_6 at 50 °C.

5. Variable temperature (VT) NMR studies of complexes 1 and 2

The VT NMR study of complex 1 in DMSO-*d*₆

The ratios of Au₄ cluster **1** vs the dissociated Au₂ species at different temperatures were determined by NMR integration of the resonances at 8.33 ppm (Au₄ clusters) vs 8.18 ppm (Au₂ intermediates) in the ¹H NMR spectra. All the data for the Van't Hoff plot ($\ln K_{eq}$ vs $1/T$) was derived and are listed in the Table S7. The enthalpy (ΔH) was determined from the slope of the plot while the entropy (ΔS) was determined as the intercept (Figure 2(b)). The full spectra are shown in Figure S38.

Table S7. Data for the Van't Hoff plot of the dissociation process of **1** in DMSO-*d*₆.

temp	Au ₂ /Au ₄ ratio	K _{eq}	lnK _{eq}	1/T
30	1.94	1.91	0.65	0.0033
40	3.21	3.96	1.38	0.00319
50	5.11	7.35	1.99	0.00309
60	8.96	14.65	2.68	0.003
70	14.74	26.29	3.27	0.00291

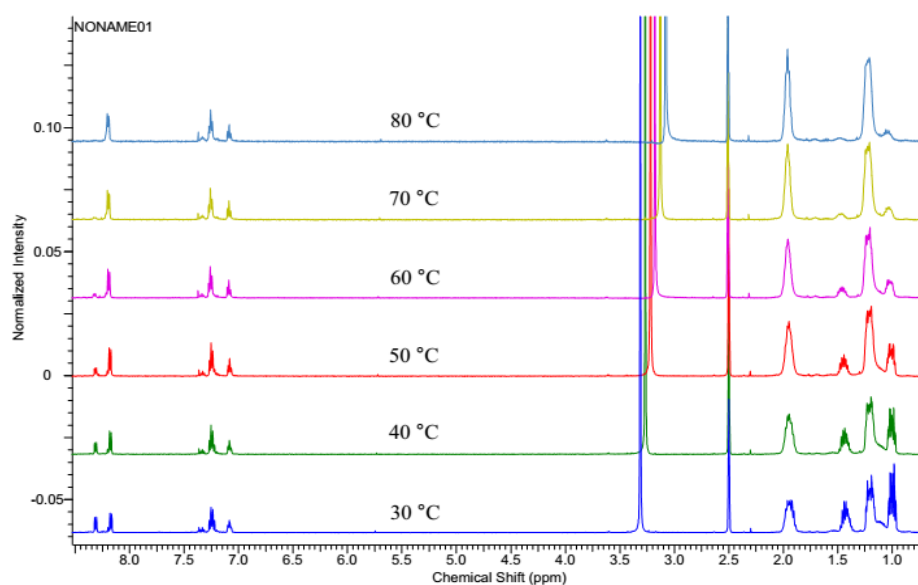


Figure S38. Full spectra of VT NMR analysis of complex **1** in DMSO-*d*₆ (30-80 °C).

The VT NMR study of complex **2** in DMSO-*d*₆

The full spectra of VT analysis of **2** are shown in Figure S39. Due to the broadness of the spectra after 60 °C, the ratio between Au₄ cluster **2** and the dissociated Au₂ intermediate cannot be determined. Therefore, the enthalpy (ΔH) and entropy (ΔS) cannot be determined via Van't Hoff analysis. However, the four doublet resonances at 1.4 ppm are indicative of a Au₄ cluster in solution. It can therefore be inferred that even at 80 °C, significant amounts of the Au₄ cluster **2** remain in the DMSO-*d*₆.

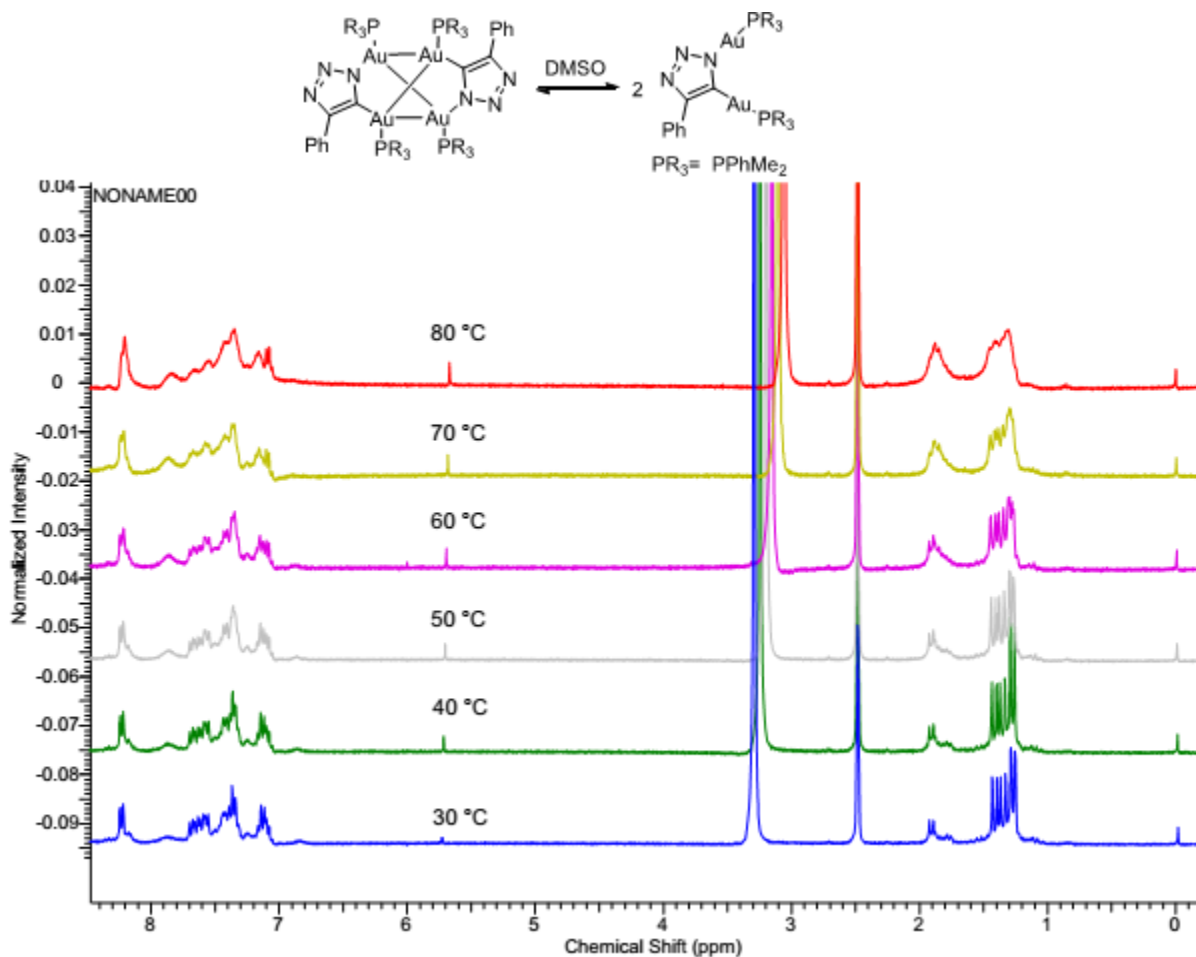


Figure S39. Full spectra of VT analysis of complex **2** in DMSO-*d*₆ (30-80 °C).

6. Infrared spectrum (IR) and Powder X-ray Diffraction (PXRD)

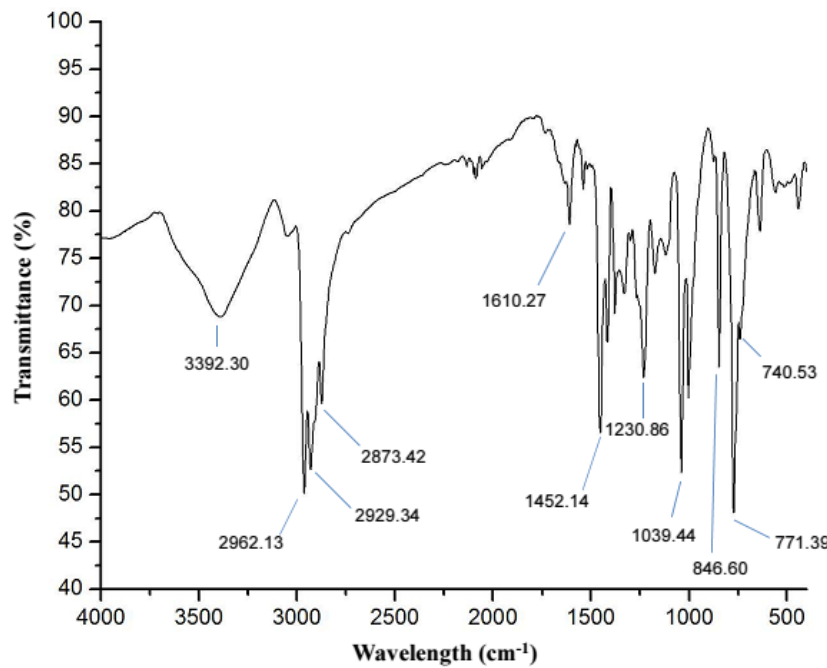


Figure S40. IR spectrum of **6** in solid state.

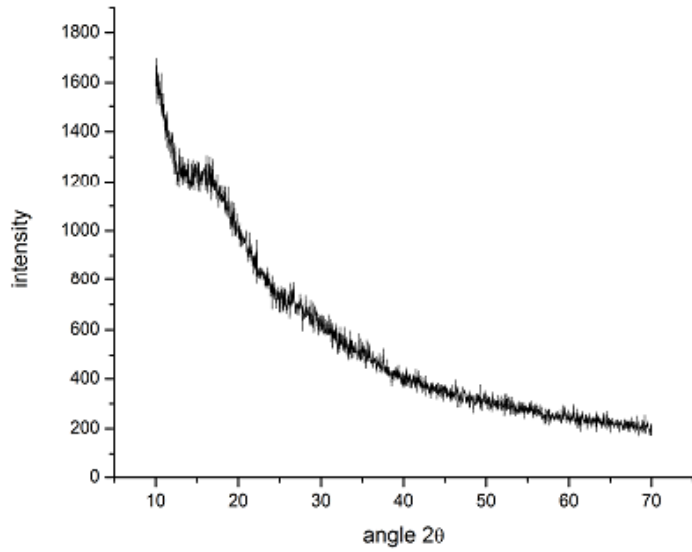


Figure S41. PXRD spectrum of **6**.

7. X-ray structure determination

X-ray experiment details of 1

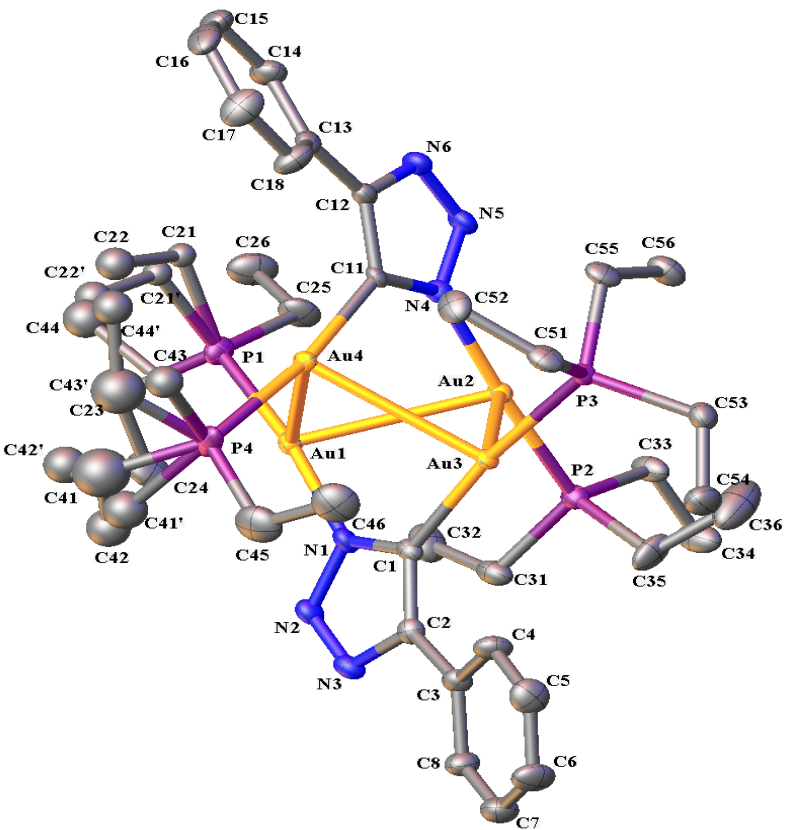


Figure S42. Solid structure (hydrogens are removed for clarity) of **1**.

The single crystals obtained from slow diffusion of pentane into dichloromethane solution of complex **1** are suitable for the single crystal X-ray diffraction experiment. Figure S42 depicts the solid state structure of the complex **1**.

X-Ray Intensity data were collected at 100 K on a Bruker **DUO** diffractometer using MoK α radiation ($\lambda = 0.71073 \text{ \AA}$) and an APEXII CCD area detector.

Raw data frames were read by program SAINT¹ and integrated using 3D profiling algorithms. The resulting data were reduced to produce hkl reflections and their intensities and estimated standard deviations. The data were corrected for Lorentz and polarization effects and numerical absorption corrections were applied based on indexed and measured faces.

The structure was solved and refined in SHELXTL2013,¹¹ using full-matrix least-squares refinement. The non-H atoms were refined with anisotropic thermal parameters and all of the H atoms were calculated in idealized positions and refined riding on their parent atoms. One ethyl group on P1 and two on P4 are disordered and refined in two parts for each. The structure was solved and refined in space group Pna2₁. The structure was checked for the presence of mirror or inversion symmetry but none was found, thus confirming the space group chosen. In the final cycle of refinement, 11069 reflections (of which 10723 are observed with $I > 2\sigma(I)$) were used to refine 483 parameters and the resulting R_1 , wR_2 and S (goodness of fit) were 1.95%, 4.28% and 0.918, respectively. The refinement was carried out by minimizing the wR_2 function using F^2 rather than F values. R_1 is calculated to provide a reference to the conventional R value but its function is not minimized.

SHELXTL6 (2008). Bruker-AXS, Madison, Wisconsin, USA.

Table S8. Crystal data and structure refinement for **1**.

Identification code	xy08
Empirical formula	C40H70Au4N6P4
Formula weight	1546.76
Temperature	100(2) K
Wavelength	0.71073 Å
Crystal system	Orthorhombic

Space group	P n a 2 ₁	
Unit cell dimensions	a = 17.0309(10) Å	α = 90°.
	b = 23.5362(14) Å	β = 90°.
	c = 12.0454(7) Å	γ = 90°.
Volume	4828.3(5) Å ³	
Z	4	
Density (calculated)	2.128 Mg/m ³	
Absorption coefficient	12.283 mm ⁻¹	
F(000)	2912	
Crystal size	0.322 × 0.023 × 0.023 mm ³	
Theta range for data collection	1.476 to 27.500°.	
Index ranges	-22 ≤ h ≤ 21, -29 ≤ k ≤ 30, -15 ≤ l ≤ 15	
Reflections collected	74359	
Independent reflections	11069 [R(int) = 0.0468]	
Completeness to theta = 25.242°	100.00%	
Absorption correction	Analytical	
Max. and min. transmission	0.8264 and 0.3022	
Refinement method	Full-matrix least-squares on F ²	
Data / restraints / parameters	11069 / 1 / 483	
Goodness-of-fit on F ²	0.918	
Final R indices [I > 2sigma(I)]	R1 = 0.0195, wR2 = 0.0428 [10723]	
R indices (all data)	R1 = 0.0227, wR2 = 0.0435	
Absolute structure parameter	-0.016(3)	
Extinction coefficient	n/a	
Largest diff. peak and hole	1.519 and -0.829 e.Å ⁻³	

$$R1 = \sum(|F_O| - |F_C|) / \sum|F_O|$$

$$wR2 = [\sum[w(F_O^2 - F_C^2)^2] / \sum[w(F_O^2)^2]]^{1/2}$$

$$S = [\sum[w(F_O^2 - F_C^2)^2] / (n-p)]^{1/2}$$

$$w = 1/[\sigma^2(F_O^2) + (m*p)^2 + n*p], p = [\max(F_O^2, 0) + 2*F_C^2]/3, m \text{ & } n \text{ are constants.}$$

Table S9. Atomic coordinates ($\times 10^4$) and equivalent isotropic displacement parameters ($\text{\AA}^2 \times 10^3$) for **1**. U(eq) is defined as one third of the trace of the orthogonalized U_{ij} tensor.

	x	y	z	U(eq)
Au(1)	1882(1)	5388(1)	1145(1)	16(1)
Au(2)	3456(1)	4770(1)	1214(1)	15(1)
Au(3)	2743(1)	4412(1)	3506(1)	12(1)
Au(4)	2353(1)	5670(1)	3529(1)	14(1)
P(1)	2172(1)	6186(1)	211(2)	21(1)
P(2)	3237(1)	3951(1)	302(2)	17(1)
P(3)	3824(1)	4409(1)	4644(1)	14(1)
P(4)	1160(1)	5636(1)	4420(2)	30(1)
N(1)	1476(3)	4636(3)	1780(5)	18(1)
N(2)	796(3)	4432(2)	1336(5)	19(1)
N(3)	605(3)	3969(3)	1855(5)	19(1)
N(4)	3751(3)	5520(2)	1959(5)	15(1)
N(5)	4406(3)	5793(3)	1578(5)	22(1)
N(6)	4502(3)	6261(3)	2154(5)	20(1)
C(1)	1720(4)	4294(3)	2623(6)	15(1)
C(2)	1159(4)	3872(3)	2672(6)	18(1)
C(3)	1026(4)	3401(3)	3452(6)	19(1)
C(4)	1386(5)	3389(3)	4496(6)	26(2)
C(5)	1205(5)	2966(4)	5264(7)	32(2)
C(6)	680(5)	2541(4)	4994(7)	32(2)
C(7)	333(5)	2547(3)	3954(7)	31(2)
C(8)	496(4)	2963(3)	3191(6)	24(2)
C(11)	3424(4)	5829(3)	2808(5)	13(1)
C(12)	3918(4)	6300(3)	2925(6)	16(1)
C(13)	3892(4)	6776(3)	3703(6)	18(2)
C(14)	4166(4)	7310(3)	3390(7)	28(2)
C(15)	4155(5)	7759(3)	4123(8)	32(2)
C(16)	3886(5)	7690(3)	5193(7)	33(2)
C(17)	3608(6)	7175(4)	5510(7)	35(2)

C(18)	3604(5)	6717(3)	4770(6)	28(2)
C(21)	2565(11)	6810(5)	935(11)	18(4)
C(22)	2043(14)	7013(7)	1881(12)	32(5)
C(21')	2286(17)	6813(8)	1079(18)	19(5)
C(22')	1680(20)	6933(10)	1918(18)	29(7)
C(23)	1337(5)	6406(3)	-633(7)	28(2)
C(24)	1043(5)	5917(4)	-1348(7)	39(2)
C(25)	2986(5)	6076(4)	-760(7)	31(2)
C(26)	3082(5)	6522(4)	-1659(7)	41(2)
C(31)	2288(4)	3917(3)	-394(6)	25(2)
C(32)	2164(5)	4376(4)	-1249(7)	37(2)
C(33)	3960(4)	3812(3)	-778(6)	26(2)
C(34)	3816(4)	3276(3)	-1462(8)	35(2)
C(35)	3235(5)	3321(3)	1183(8)	33(2)
C(36)	4028(7)	3193(4)	1702(9)	64(4)
C(41)	356(15)	5939(12)	3810(20)	72(8)
C(42)	91(13)	5657(9)	2803(17)	43(5)
C(43)	1223(11)	6085(7)	5697(14)	31(4)
C(44)	1243(13)	6756(9)	5110(19)	44(5)
C(41')	271(12)	5663(9)	3370(19)	44(5)
C(42')	298(11)	6170(8)	2505(16)	41(5)
C(43')	930(15)	6249(10)	5120(20)	63(7)
C(44')	1441(11)	6685(8)	5638(16)	35(4)
C(45)	836(5)	4983(4)	5009(8)	42(2)
C(46)	1369(5)	4745(4)	5892(7)	42(2)
C(51)	3599(4)	4606(3)	6076(7)	25(2)
C(52)	3416(4)	5244(3)	6208(8)	27(2)
C(53)	4218(4)	3694(3)	4806(7)	23(2)
C(54)	3604(5)	3252(4)	5105(8)	33(2)
C(55)	4658(4)	4852(3)	4314(6)	23(2)
C(56)	5132(4)	4637(4)	3299(6)	29(2)

Symmetry transformations used to generate equivalent atoms:

Table S10. Bond lengths [\AA] of **1**.

Bond	Length (\AA)	Bond	Length (\AA)
Au(1)-N(1)	2.048(6)	N(5)-N(6)	1.312(8)
Au(1)-P(1)	2.2450(19)	N(6)-C(12)	1.365(9)
Au(1)-Au(2)	3.0516(4)	C(1)-C(2)	1.38(1)
Au(1)-Au(4)	3.0543(4)	C(2)-C(3)	1.47(1)
Au(2)-N(4)	2.042(6)	C(3)-C(4)	1.399(11)
Au(2)-P(2)	2.2505(19)	C(3)-C(8)	1.407(9)
Au(2)-Au(3)	3.1318(4)	C(4)-C(5)	1.393(11)
Au(3)-C(1)	2.060(7)	C(5)-C(6)	1.381(11)
Au(3)-P(3)	2.2962(17)	C(6)-C(7)	1.385(11)
Au(3)-Au(4)	3.0334(4)	C(7)-C(8)	1.371(11)
Au(4)-C(11)	2.055(6)	C(11)-C(12)	1.398(9)
Au(4)-P(4)	2.300(2)	C(12)-C(13)	1.462(10)
P(1)-C(21)	1.818(19)	C(13)-C(18)	1.383(11)
P(1)-C(23)	1.822(8)	C(13)-C(14)	1.393(10)
P(1)-C(25)	1.833(8)	C(14)-C(15)	1.376(11)
P(1)-C(21')	1.834(13)	C(15)-C(16)	1.378(12)
P(2)-C(33)	1.821(7)	C(16)-C(17)	1.356(12)
P(2)-C(31)	1.822(8)	C(17)-C(18)	1.398(11)
P(2)-C(35)	1.823(8)	C(21)-C(22)	1.522(19)
P(3)-C(55)	1.805(8)	C(21')-C(22')	1.47(3)
P(3)-C(53)	1.822(8)	C(23)-C(24)	1.521(12)
P(3)-C(51)	1.826(8)	C(25)-C(26)	1.518(11)
P(4)-C(41)	1.71(3)	C(31)-C(32)	1.508(11)
P(4)-C(43')	1.72(2)	C(33)-C(34)	1.526(10)
P(4)-C(45)	1.781(10)	C(35)-C(36)	1.519(13)
P(4)-C(43)	1.869(17)	C(41)-C(42)	1.45(3)
P(4)-C(41')	1.97(2)	C(43)-C(44)	1.73(3)
N(1)-C(1)	1.361(9)	C(41')-C(42')	1.58(3)
N(1)-N(2)	1.364(8)	C(43')-C(44')	1.48(3)
N(2)-N(3)	1.299(8)	C(45)-C(46)	1.506(13)
N(3)-C(2)	1.383(9)	C(51)-C(52)	1.542(10)
N(4)-N(5)	1.367(8)	C(53)-C(54)	1.518(11)
N(4)-C(11)	1.373(8)	C(55)-C(56)	1.55(1)

Symmetry transformations used to generate equivalent atoms:

Table S11. Bond Angles [°] of **1**.

Bond	Angle (°)	Bond	Angle (°)
N(1)-Au(1)-P(1)	169.92(17)	C(41')-P(4)-Au(4)	112.2(6)
N(1)-Au(1)-Au(2)	82.77(16)	C(1)-N(1)-N(2)	110.1(6)
P(1)-Au(1)-Au(2)	102.67(5)	C(1)-N(1)-Au(1)	133.4(5)
N(1)-Au(1)-Au(4)	85.73(16)	N(2)-N(1)-Au(1)	116.4(4)
P(1)-Au(1)-Au(4)	103.39(5)	N(3)-N(2)-N(1)	108.6(6)
Au(2)-Au(1)-Au(4)	81.196(9)	N(2)-N(3)-C(2)	108.1(6)
N(4)-Au(2)-P(2)	174.66(17)	N(5)-N(4)-C(11)	109.3(6)
N(4)-Au(2)-Au(1)	79.38(16)	N(5)-N(4)-Au(2)	117.3(4)
P(2)-Au(2)-Au(1)	104.42(5)	C(11)-N(4)-Au(2)	133.4(5)
N(4)-Au(2)-Au(3)	86.57(16)	N(6)-N(5)-N(4)	108.7(5)
P(2)-Au(2)-Au(3)	97.78(5)	N(5)-N(6)-C(12)	108.9(6)
Au(1)-Au(2)-Au(3)	79.118(9)	N(1)-C(1)-C(2)	104.3(6)
C(1)-Au(3)-P(3)	170.5(2)	N(1)-C(1)-Au(3)	124.3(5)
C(1)-Au(3)-Au(4)	87.22(19)	C(2)-C(1)-Au(3)	131.3(5)
P(3)-Au(3)-Au(4)	99.95(5)	C(1)-C(2)-N(3)	108.8(6)
C(1)-Au(3)-Au(2)	84.79(19)	C(1)-C(2)-C(3)	132.6(7)
P(3)-Au(3)-Au(2)	102.46(5)	N(3)-C(2)-C(3)	118.3(6)
Au(4)-Au(3)-Au(2)	80.237(9)	C(4)-C(3)-C(8)	117.8(7)
C(11)-Au(4)-P(4)	171.1(2)	C(4)-C(3)-C(2)	121.5(6)
C(11)-Au(4)-Au(3)	88.88(19)	C(8)-C(3)-C(2)	120.6(7)
P(4)-Au(4)-Au(3)	99.44(5)	C(5)-C(4)-C(3)	121.0(7)
C(11)-Au(4)-Au(1)	82.84(18)	C(6)-C(5)-C(4)	120.3(8)
P(4)-Au(4)-Au(1)	101.49(7)	C(5)-C(6)-C(7)	118.8(7)
Au(3)-Au(4)-Au(1)	80.624(9)	C(8)-C(7)-C(6)	121.9(8)
C(21')-P(1)-C(23)	100.1(8)	C(7)-C(8)-C(3)	120.2(7)
C(21')-P(1)-C(25)	113.6(10)	N(4)-C(11)-C(12)	104.6(6)
C(23)-P(1)-C(25)	106.0(4)	N(4)-C(11)-Au(4)	125.3(5)
C(23)-P(1)-C(21)	108.9(5)	C(12)-C(11)-Au(4)	129.5(5)
C(25)-P(1)-C(21)	98.1(7)	N(6)-C(12)-C(11)	108.5(6)
C(21')-P(1)-Au(1)	114.5(7)	N(6)-C(12)-C(13)	120.6(6)
C(23)-P(1)-Au(1)	110.2(3)	C(11)-C(12)-C(13)	130.9(6)
C(25)-P(1)-Au(1)	111.5(3)	C(18)-C(13)-C(14)	117.5(7)
C(21)-P(1)-Au(1)	120.8(4)	C(18)-C(13)-C(12)	121.9(6)
C(33)-P(2)-C(31)	105.3(4)	C(14)-C(13)-C(12)	120.6(7)
C(33)-P(2)-C(35)	105.7(4)	C(15)-C(14)-C(13)	121.0(8)
C(31)-P(2)-C(35)	103.4(4)	C(14)-C(15)-C(16)	120.9(8)
C(33)-P(2)-Au(2)	112.9(3)	C(17)-C(16)-C(15)	119.0(8)
C(31)-P(2)-Au(2)	114.2(3)	C(16)-C(17)-C(18)	120.7(8)

C(35)-P(2)-Au(2)	114.4(3)	C(13)-C(18)-C(17)	120.9(7)
C(55)-P(3)-C(53)	105.5(3)	C(22)-C(21)-P(1)	113.2(10)
C(55)-P(3)-C(51)	103.1(3)	C(22')-C(21')-P(1)	118.4(15)
C(53)-P(3)-C(51)	102.1(4)	C(24)-C(23)-P(1)	111.0(5)
C(55)-P(3)-Au(3)	119.8(2)	C(26)-C(25)-P(1)	116.0(6)
C(53)-P(3)-Au(3)	111.2(2)	C(32)-C(31)-P(2)	114.0(6)
C(51)-P(3)-Au(3)	113.2(2)	C(34)-C(33)-P(2)	115.1(5)
C(41)-P(4)-C(45)	106.5(10)	C(36)-C(35)-P(2)	113.5(7)
C(43')-P(4)-C(45)	117.3(9)	C(42)-C(41)-P(4)	115(2)
C(41)-P(4)-C(43)	99.6(11)	C(44)-C(43)-P(4)	100.4(12)
C(45)-P(4)-C(43)	100.3(6)	C(42')-C(41')-P(4)	115.1(14)
C(43')-P(4)-C(41')	96.5(11)	C(44')-C(43')-P(4)	130.8(18)
C(45)-P(4)-C(41')	92.6(7)	C(46)-C(45)-P(4)	114.5(7)
C(41)-P(4)-Au(4)	119.4(9)	C(52)-C(51)-P(3)	112.8(6)
C(43')-P(4)-Au(4)	113.7(8)	C(54)-C(53)-P(3)	113.9(5)
C(45)-P(4)-Au(4)	119.3(3)	C(56)-C(55)-P(3)	113.3(5)
C(43)-P(4)-Au(4)	108.3(6)		

Symmetry transformations used to generate equivalent atoms:

Table S12. Anisotropic displacement parameters ($\text{\AA}^2 \times 10^3$) for **1**. The anisotropic displacement factor exponent takes the form: $-2\pi^2 [h^2 a^{*2} U^{11} + \dots + 2 h k a^{*} b^{*} U^{12}]$.

	U11	U22	U33	U23	U13	U12
Au(1)	15(1)	17(1)	14(1)	1(1)	-1(1)	3(1)
Au(2)	13(1)	17(1)	14(1)	-3(1)	1(1)	0(1)
Au(3)	10(1)	14(1)	12(1)	0(1)	-2(1)	0(1)
Au(4)	12(1)	15(1)	15(1)	-1(1)	4(1)	0(1)
P(1)	26(1)	19(1)	17(1)	3(1)	-4(1)	2(1)
P(2)	17(1)	19(1)	16(1)	-4(1)	1(1)	1(1)
P(3)	13(1)	16(1)	13(1)	0(1)	-2(1)	1(1)
P(4)	22(1)	22(1)	46(1)	2(1)	20(1)	3(1)
N(1)	11(3)	23(3)	19(3)	1(2)	-1(2)	2(2)
N(2)	15(3)	24(3)	19(3)	1(3)	-3(2)	1(2)
N(3)	14(3)	26(3)	18(3)	-3(3)	0(2)	-2(3)
N(4)	15(3)	20(3)	11(3)	-2(2)	0(2)	0(2)
N(5)	12(3)	27(3)	26(3)	-2(3)	2(2)	0(3)

N(6)	14(3)	22(3)	24(3)	-1(3)	4(2)	-2(2)
C(1)	13(3)	19(4)	12(3)	-4(3)	0(2)	1(3)
C(2)	18(4)	20(4)	14(3)	-1(3)	2(3)	2(3)
C(3)	17(3)	20(3)	21(3)	1(3)	3(3)	-2(3)
C(4)	26(4)	25(4)	27(4)	4(3)	2(3)	-9(3)
C(5)	36(5)	36(5)	25(4)	8(4)	-2(4)	1(4)
C(6)	36(5)	28(5)	34(5)	12(4)	-3(4)	-10(4)
C(7)	26(4)	27(4)	40(5)	1(4)	-1(4)	-6(3)
C(8)	25(4)	21(4)	27(4)	-1(3)	-3(3)	-4(3)
C(11)	8(3)	18(3)	15(3)	0(3)	-1(2)	2(3)
C(12)	13(3)	17(4)	19(3)	3(3)	0(3)	0(3)
C(13)	15(3)	19(3)	21(4)	-1(3)	-5(3)	2(3)
C(14)	24(4)	26(4)	34(5)	0(4)	6(4)	-6(3)
C(15)	28(4)	17(4)	49(6)	-4(4)	6(4)	-2(3)
C(16)	36(5)	22(4)	42(5)	-16(4)	-12(4)	5(4)
C(17)	55(6)	31(5)	20(4)	-3(3)	4(4)	2(4)
C(18)	44(5)	17(4)	23(4)	-1(3)	0(3)	-3(3)
C(23)	28(4)	31(5)	26(4)	9(4)	-6(3)	10(4)
C(24)	34(5)	52(5)	30(5)	6(4)	-13(4)	0(4)
C(25)	25(4)	38(5)	31(4)	13(4)	6(3)	-8(4)
C(26)	46(5)	43(5)	34(5)	13(4)	-2(4)	-14(4)
C(31)	18(4)	31(4)	26(4)	-8(3)	2(3)	-4(3)
C(32)	33(5)	47(5)	29(5)	-4(4)	-10(4)	8(4)
C(33)	19(4)	33(4)	26(4)	-13(3)	7(3)	-4(3)
C(34)	28(4)	42(5)	36(4)	-19(4)	8(4)	-6(3)
C(35)	57(5)	18(4)	25(4)	6(4)	-9(5)	5(3)
C(36)	98(10)	38(6)	57(7)	-10(5)	-43(7)	17(6)
C(45)	33(5)	54(6)	39(5)	-5(5)	15(4)	-4(5)
C(46)	42(5)	52(6)	31(5)	8(4)	9(4)	-3(4)
C(51)	20(3)	36(4)	18(4)	-4(4)	-6(3)	-3(3)
C(52)	30(4)	31(4)	22(3)	-12(4)	0(4)	6(3)
C(53)	19(4)	25(4)	26(4)	-2(3)	-3(3)	3(3)

C(54)	31(5)	26(5)	42(5)	8(4)	-2(4)	-3(4)
C(55)	17(4)	32(4)	20(4)	0(3)	-7(3)	-4(3)
C(56)	19(4)	40(5)	27(4)	2(3)	3(3)	-2(3)

Table S13. Hydrogen coordinates ($\times 10^4$) and isotropic displacement parameters ($\text{\AA}^2 \times 10^3$) for **1**.

	x	y	z	U(eq)
H(4A)	1758	3673	4684	31
H(5A)	1444	2970	5976	39
H(6A)	559	2249	5512	39
H(7A)	-28	2255	3764	37
H(8A)	250	2954	2483	29
H(14A)	4363	7366	2660	34
H(15A)	4336	8121	3887	38
H(16A)	3895	7998	5702	40
H(17A)	3414	7125	6243	42
H(18A)	3401	6361	5004	34
H(21A)	3090	6716	1235	22
H(21B)	2630	7123	394	22
H(22A)	2287	7341	2244	48
H(22B)	1976	6706	2421	48
H(22C)	1529	7123	1585	48
H(21C)	2796	6781	1468	23
H(21D)	2322	7147	582	23
H(22D)	1820	7280	2325	43
H(22E)	1646	6614	2438	43
H(22F)	1172	6986	1551	43
H(23A)	908	6538	-143	34
H(23B)	1494	6726	-1115	34
H(24A)	595	6045	-1792	58
H(24B)	881	5602	-870	58

H(24C)	1465	5790	-1842	58
H(25A)	3480	6057	-328	38
H(25B)	2914	5702	-1122	38
H(26A)	3534	6425	-2126	61
H(26B)	3168	6894	-1316	61
H(26C)	2607	6535	-2117	61
H(31A)	2237	3542	-760	30
H(31B)	1868	3945	172	30
H(32A)	1646	4329	-1592	55
H(32B)	2571	4348	-1822	55
H(32C)	2194	4749	-891	55
H(33A)	3973	4142	-1288	31
H(33B)	4484	3782	-427	31
H(34A)	4234	3234	-2015	53
H(34B)	3308	3306	-1839	53
H(34C)	3814	2944	-970	53
H(35A)	2844	3374	1782	40
H(35B)	3069	2990	734	40
H(36A)	3988	2852	2165	96
H(36B)	4193	3516	2161	96
H(36C)	4417	3130	1115	96
H(41A)	-81	5943	4348	86
H(41B)	482	6339	3623	86
H(42A)	-371	5854	2510	65
H(42B)	-47	5262	2975	65
H(42C)	511	5663	2248	65
H(43A)	759	6033	6182	37
H(43B)	1707	6006	6125	37
H(44A)	1286	7042	5698	66
H(44B)	758	6819	4688	66
H(44C)	1695	6787	4611	66
H(41C)	256	5300	2955	53

H(41D)	-222	5692	3801	53
H(42D)	-164	6150	2020	61
H(42E)	775	6140	2055	61
H(42F)	298	6533	2903	61
H(43C)	593	6465	4601	75
H(43D)	578	6124	5729	75
H(44D)	1115	6970	6011	52
H(44E)	1758	6869	5063	52
H(44F)	1788	6503	6182	52
H(45A)	308	5041	5333	50
H(45B)	785	4699	4407	50
H(46A)	1153	4385	6166	62
H(46B)	1408	5016	6507	62
H(46C)	1892	4679	5578	62
H(51A)	3142	4382	6333	30
H(51B)	4052	4507	6553	30
H(52A)	3299	5326	6988	41
H(52B)	2961	5343	5749	41
H(52C)	3871	5468	5972	41
H(53A)	4475	3580	4104	28
H(53B)	4625	3700	5393	28
H(54A)	3855	2880	5177	50
H(54B)	3204	3237	4520	50
H(54C)	3356	3355	5811	50
H(55A)	4471	5242	4161	28
H(55B)	5010	4868	4967	28
H(56A)	5572	4896	3157	43
H(56B)	4790	4624	2646	43
H(56C)	5335	4255	3453	43

X-ray experiment details of 2

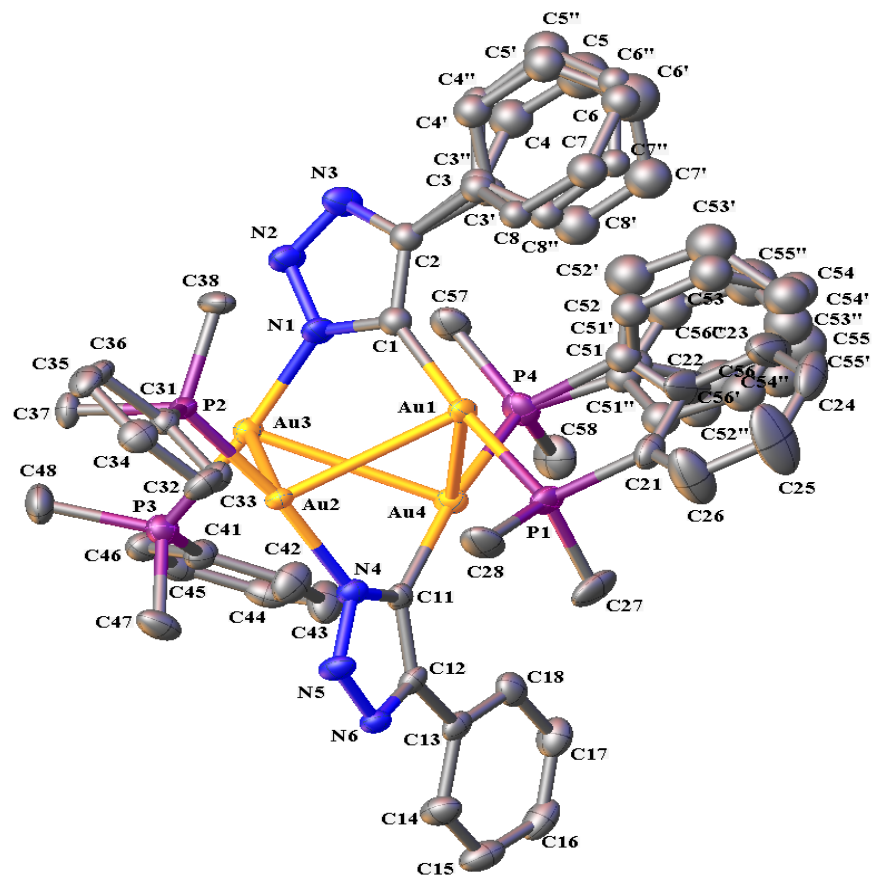


Figure S43. Solid structure (hydrogens are removed for clarity) of **2**.

The single crystals obtained from slow diffusion of pentane into dichloromethane solution of complex **2** are suitable for the single crystal X-ray diffraction experiment. Figure S43 depicts the solid state structure of the complex **2**.

X-Ray Intensity data were collected at 100 K on a Bruker **DUO** diffractometer using MoK α radiation ($\lambda = 0.71073 \text{ \AA}$) and an APEXII CCD area detector.

Raw data frames were read by program SAINT¹ and integrated using 3D profiling algorithms. The resulting data were reduced to produce hkl reflections and their intensities and estimated

standard deviations. The data were corrected for Lorentz and polarization effects and numerical absorption corrections were applied based on indexed and measured faces.

The structure was solved and refined in SHELXTL2013,¹¹ using full-matrix least-squares refinement. The non-H atoms were refined with anisotropic thermal parameters and all of the H atoms were calculated in idealized positions and refined riding on their parent atoms. There are two disordered phenyl rings on C1 and P4 and each was refined in three parts. All disordered parts were constrained to maintain ideal hexagons using commands “AFIX 66”. The pivot atoms of each group of disordered parts had their displacement parameters restrained to remain equivalent throughout the refinement. In the final cycle of refinement, 11179 reflections (of which 9946 are observed with $I > 2\sigma(I)$) were used to refine 523 parameters and the resulting R1, wR2 and S (goodness of fit) were 3.39%, 8.60% and 1.163, respectively. The refinement was carried out by minimizing the wR2 function using F2 rather than F values. R1 is calculated to provide a reference to the conventional R value but its function is not minimized.

SHELXTL6 (2008). Bruker-AXS, Madison, Wisconsin, USA.

Table S14. Crystal data and structure refinement for **2**.

Identification code	xy09	
Empirical formula	C48H54Au4N6P4	
Formula weight	1626.71	
Temperature	100(2) K	
Wavelength	0.71073 Å	
Crystal system	Monoclinic	
Space group	P 2 ₁ /c	
Unit cell dimensions	a = 17.4114(12) Å	α= 90°
	b = 16.8969(12) Å	β= 99.4513(14)°
	c = 16.7970(12) Å	γ = 90°
Volume	4874.6(6) Å ³	

Z	4
Density (calculated)	2.217 Mg/m ³
Absorption coefficient	12.173 mm ⁻¹
F(000)	3040
Crystal size	0.162 × 0.156 × 0.113 mm ³
Theta range for data collection	1.186 to 27.499°.
Index ranges	-22≤h≤22, -21≤k≤21, -21≤l≤21
Reflections collected	71946
Independent reflections	11179 [R(int) = 0.0260]
Completeness to theta = 25.242°	100.00%
Absorption correction	Analytical
Refinement method	Full-matrix least-squares on F2
Data / restraints / parameters	11179 / 2 / 523
Goodness-of-fit on F2	1.163
Final R indices [I>2sigma(I)]	R1 = 0.0339, wR2 = 0.0860 [9946]
R indices (all data)	R1 = 0.0405, wR2 = 0.0918
Extinction coefficient	n/a
Largest diff. peak and hole	4.440 and -1.943 e.Å ⁻³

$$R_1 = \sum(|F_O| - |F_C|) / \sum|F_O|$$

$$wR2 = [\sum[w(F_O^2 - F_C^2)^2] / \sum[w(F_O^2)^2]]^{1/2}$$

$$S = [\sum[w(F_O^2 - F_C^2)^2] / (n-p)]^{1/2}$$

$$w = 1/[\sigma^2(F_O^2) + (m*p)^2 + n*p], p = [\max(F_O^2, 0) + 2*F_C^2]/3, m \text{ & } n \text{ are constants.}$$

Table S15. Atomic coordinates ($\times 10^4$) and equivalent isotropic displacement parameters ($\text{\AA}^2 \times 10^3$) for **2**. U(eq) is defined as one third of the trace of the orthogonalized U_{ij} tensor.

	X	Y	Z	U(eq)
Au1	1594(1)	6100(1)	7419(1)	22(1)
Au2	3142(1)	6930(1)	7402(1)	19(1)
Au3	3655(1)	5640(1)	8683(1)	23(1)
Au4	2631(1)	4654(1)	7325(1)	24(1)
P1	1146(1)	6338(1)	6079(1)	28(1)
P2	3199(1)	7905(1)	8326(1)	22(1)
P3	4864(1)	5386(1)	8460(1)	27(1)
P4	2043(1)	3767(1)	8058(1)	32(1)
N1	2603(4)	5824(4)	9049(4)	26(1)
N2	2598(4)	5788(5)	9857(4)	30(2)

N3	1872(4)	5881(5)	9976(4)	30(2)
N4	3234(4)	6088(4)	6537(4)	22(1)
N5	3562(4)	6327(4)	5886(4)	26(1)
N6	3710(4)	5685(4)	5476(4)	21(1)
C1	1872(5)	5945(5)	8633(5)	25(2)
C2	1429(5)	6003(5)	9254(5)	25(2)
C3	577(6)	6165(9)	9187(9)	26(2)
C4	171(9)	5795(10)	9730(10)	45(6)
C5	-633(9)	5876(11)	9646(12)	65(8)
C6	-1031(6)	6326(11)	9018(11)	34(6)
C7	-626(7)	6696(11)	8474(8)	37(5)
C8	178(7)	6615(10)	8559(8)	23(4)
C3'	558(10)	6006(15)	9157(13)	26(2)
C4'	249(12)	6327(14)	9798(12)	33(7)
C5'	-553(13)	6374(16)	9759(14)	39(8)
C6'	-1046(9)	6100(18)	9079(16)	69(17)
C7'	-737(12)	5779(18)	8439(13)	51(10)
C8'	65(13)	5732(16)	8478(11)	47(9)
C3"	564(9)	6126(15)	9242(13)	26(2)
C4"	274(12)	6049(16)	9962(11)	25(7)
C5"	-521(13)	6115(18)	9965(12)	45(10)
C6"	-1027(9)	6259(15)	9250(14)	24(7)
C7"	-737(11)	6336(16)	8530(11)	23(7)
C8"	58(12)	6269(17)	8526(11)	27(7)
C11	3177(4)	5292(4)	6546(4)	20(1)
C12	3496(4)	5043(5)	5871(4)	22(2)
C13	3626(4)	4250(5)	5558(4)	24(2)
C14	4122(6)	4169(6)	4968(5)	34(2)
C15	4245(6)	3453(6)	4644(5)	39(2)
C16	3887(6)	2772(6)	4891(6)	38(2)
C17	3423(5)	2837(5)	5480(6)	36(2)
C18	3295(5)	3584(5)	5825(5)	31(2)
C21	84(5)	6362(6)	5881(5)	33(2)
C22	-315(6)	5950(9)	6377(6)	61(4)
C23	-1119(6)	5892(10)	6241(7)	66(4)
C24	-1537(6)	6295(7)	5605(7)	52(3)
C25	-1156(7)	6719(10)	5107(10)	86(5)
C26	-345(7)	6784(9)	5255(9)	70(4)
C27	1387(6)	5617(7)	5357(5)	46(3)
C28	1475(6)	7263(6)	5712(6)	41(2)
C31	3008(4)	8896(4)	7912(5)	22(2)

C32	2743(5)	9013(5)	7094(5)	29(2)
C33	2575(5)	9771(5)	6795(5)	33(2)
C34	2675(5)	10409(6)	7316(5)	34(2)
C35	2943(5)	10301(5)	8128(5)	32(2)
C36	3112(5)	9546(5)	8428(5)	27(2)
C37	4150(4)	7956(5)	8955(5)	27(2)
C38	2540(5)	7817(5)	9051(5)	31(2)
C41	5061(5)	4342(5)	8458(5)	29(2)
C42	4596(6)	3880(6)	7884(6)	40(2)
C43	4721(5)	3073(6)	7860(7)	42(2)
C44	5309(5)	2725(6)	8413(6)	35(2)
C45	5772(5)	3180(6)	8973(5)	37(2)
C46	5653(5)	3985(6)	9002(5)	31(2)
C47	5124(5)	5743(6)	7529(6)	39(2)
C48	5618(5)	5813(6)	9213(6)	41(2)
C51	953(6)	3678(9)	7810(10)	29(3)
C52	522(8)	4309(7)	8034(9)	34(5)
C53	-287(8)	4278(8)	7888(10)	42(5)
C54	-665(6)	3616(10)	7519(11)	42(6)
C55	-233(9)	2986(9)	7295(11)	63(8)
C56	575(9)	3017(8)	7441(11)	60(7)
C51'	940(9)	3869(14)	7860(12)	29(3)
C52'	471(13)	4120(15)	8405(10)	54(9)
C53'	-333(12)	4129(16)	8181(13)	57(10)
C54'	-669(9)	3887(16)	7412(15)	48(9)
C55'	-200(12)	3635(15)	6866(11)	46(8)
C56'	604(11)	3626(14)	7090(11)	44(8)
C51"	1073(13)	3736(18)	7747(17)	29(3)
C52"	772(14)	4105(16)	7023(15)	33(9)
C54"	-27(15)	4121(18)	6760(15)	44(10)
C53"	-526(12)	3770(20)	7220(20)	54(13)
C55"	-226(17)	3400(20)	7945(19)	66(15)
C56"	573(18)	3382(19)	8208(15)	51(12)
C57	2264(5)	3855(6)	9149(5)	36(2)
C58	2350(6)	2764(6)	7870(7)	46(2)

Table S16. Bond lengths [Å] of **2**.

Bond	Length (Å)	Bond	Length (Å)
Au1-C1	2.033(8)	N5-N6	1.333(9)
Au1-P1	2.293(2)	N6-C12	1.357(10)

Au1-Au2	3.0420(4)	C1-C2	1.400(11)
Au1-Au4	3.0562(5)	C2-C3	1.496(13)
Au2-N4	2.059(6)	C2-C3'	1.498(18)
Au2-P2	2.2539(19)	C2-C3"	1.518(17)
Au2-Au3	3.0882(4)	C11-C12	1.407(10)
Au3-N1	2.049(7)	C12-C13	1.470(11)
Au3-P3	2.240(2)	C13-C18	1.374(12)
Au3-Au4	3.1336(4)	C13-C14	1.425(12)
Au4-C11	2.046(7)	C14-C15	1.356(13)
Au4-P4	2.286(2)	C15-C16	1.403(15)
P1-C28	1.809(10)	C16-C17	1.379(14)
P1-C27	1.816(10)	C17-C18	1.421(13)
P1-C21	1.826(9)	C21-C22	1.361(16)
P2-C38	1.813(8)	C21-C26	1.382(14)
P2-C37	1.814(8)	C22-C23	1.384(14)
P2-C31	1.823(8)	C23-C24	1.371(17)
P3-C41	1.798(9)	C24-C25	1.353(19)
P3-C47	1.802(9)	C25-C26	1.398(16)
P3-C48	1.815(9)	C31-C32	1.389(11)
P4-C51"	1.69(2)	C31-C36	1.394(11)
P4-C57	1.815(9)	C32-C33	1.390(12)
P4-C58	1.821(11)	C33-C34	1.380(12)
P4-C51	1.882(11)	C34-C35	1.378(12)
P4-C51'	1.902(16)	C35-C36	1.385(12)
N1-N2	1.361(9)	C41-C42	1.392(12)
N1-C1	1.363(10)	C41-C46	1.397(11)
N2-N3	1.32(1)	C42-C43	1.383(14)
N3-C2	1.341(10)	C43-C44	1.394(13)
N4-C11	1.348(10)	C44-C45	1.369(14)
N4-N5	1.376(9)	C45-C46	1.378(14)

Symmetry transformations used to generate equivalent atoms:

Table S17. Bond angles [°] of **2**.

Bond	Angle (°)	Bond	Angle (°)
C1-Au1-P1	173.2(2)	N6-N5-N4	108.2(6)
C1-Au1-Au2	90.2(2)	N5-N6-C12	107.8(6)
P1-Au1-Au2	93.99(6)	N1-C1-C2	102.1(7)
C1-Au1-Au4	84.5(2)	N1-C1-Au1	125.6(6)
P1-Au1-Au4	101.42(6)	C2-C1-Au1	132.1(6)

Au2-Au1-Au4	80.579(11)	N3-C2-C1	111.0(7)
N4-Au2-P2	172.43(19)	N3-C2-C3	120.8(9)
N4-Au2-Au1	81.94(18)	C1-C2-C3	128.1(9)
P2-Au2-Au1	105.63(5)	N3-C2-C3'	121.4(11)
N4-Au2-Au3	87.55(17)	C1-C2-C3'	126.2(11)
P2-Au2-Au3	93.52(5)	N3-C2-C3"	117.1(10)
Au1-Au2-Au3	79.842(11)	C1-C2-C3"	131.8(11)
N1-Au3-P3	171.99(18)	C4-C3-C2	118.2(10)
N1-Au3-Au2	86.09(18)	C8-C3-C2	121.5(10)
P3-Au3-Au2	101.02(6)	C4'-C3'-C2	115.5(14)
N1-Au3-Au4	82.49(19)	C8'-C3'-C2	124.5(14)
P3-Au3-Au4	102.40(6)	C4"-C3"-C2	118.4(14)
Au2-Au3-Au4	78.659(11)	C8"-C3"-C2	121.5(14)
C11-Au4-P4	170.5(2)	N4-C11-C12	104.5(6)
C11-Au4-Au1	87.3(2)	N4-C11-Au4	125.1(6)
P4-Au4-Au1	100.14(6)	C12-C11-Au4	130.1(6)
C11-Au4-Au3	85.2(2)	N6-C12-C11	109.4(7)
P4-Au4-Au3	102.02(6)	N6-C12-C13	118.9(7)
Au1-Au4-Au3	78.916(11)	C11-C12-C13	131.7(7)
C28-P1-C27	103.4(5)	C18-C13-C14	118.9(8)
C28-P1-C21	106.6(5)	C18-C13-C12	122.2(7)
C27-P1-C21	103.4(4)	C14-C13-C12	118.9(8)
C28-P1-Au1	114.2(3)	C15-C14-C13	121.2(9)
C27-P1-Au1	117.4(3)	C14-C15-C16	120.4(9)
C21-P1-Au1	110.8(3)	C17-C16-C15	119.2(8)
C38-P2-C37	103.3(4)	C16-C17-C18	120.9(9)
C38-P2-C31	103.6(4)	C13-C18-C17	119.4(8)
C37-P2-C31	105.7(4)	C22-C21-C26	117.6(9)
C38-P2-Au2	116.2(3)	C22-C21-P1	118.7(7)
C37-P2-Au2	111.6(3)	C26-C21-P1	123.7(8)
C31-P2-Au2	115.1(3)	C21-C22-C23	122.6(11)
C41-P3-C47	104.6(5)	C24-C23-C22	119.1(13)
C41-P3-C48	106.0(4)	C25-C24-C23	119.5(10)
C47-P3-C48	102.5(5)	C24-C25-C26	121.0(11)
C41-P3-Au3	111.9(3)	C21-C26-C25	119.8(12)
C47-P3-Au3	117.2(3)	C32-C31-C36	119.4(7)
C48-P3-Au3	113.5(3)	C32-C31-P2	121.2(6)
C51"-P4-C57	110.5(10)	C36-C31-P2	119.3(6)
C51"-P4-C58	103.0(11)	C31-C32-C33	120.3(8)
C57-P4-C58	103.4(5)	C34-C33-C32	119.5(8)
C57-P4-C51	105.6(6)	C35-C34-C33	120.7(9)

C58-P4-C51	101.6(6)	C34-C35-C36	119.9(8)
C57-P4-C51'	102.1(7)	C35-C36-C31	120.0(7)
C58-P4-C51'	111.8(8)	C42-C41-C46	119.6(8)
C51"-P4-Au4	111.6(10)	C42-C41-P3	117.5(6)
C57-P4-Au4	116.8(3)	C46-C41-P3	122.9(7)
C58-P4-Au4	110.3(4)	C43-C42-C41	119.8(9)
C51-P4-Au4	117.2(5)	C42-C43-C44	119.9(9)
C51'-P4-Au4	112.0(7)	C45-C44-C43	120.5(9)
N2-N1-C1	111.1(6)	C44-C45-C46	120.2(8)
N2-N1-Au3	116.5(5)	C45-C46-C41	120.2(8)
C1-N1-Au3	132.4(5)	C52-C51-P4	116.7(9)
N3-N2-N1	108.0(6)	C56-C51-P4	123.3(9)
N2-N3-C2	107.7(7)	C52'-C51'-P4	126.7(12)
C11-N4-N5	110.1(6)	C56'-C51'-P4	113.2(12)
C11-N4-Au2	131.8(5)	C52"-C51"-P4	118.1(16)
N5-N4-Au2	116.7(5)	C56"-C51"-P4	121.9(16)

Symmetry transformations used to generate equivalent atoms:

Table S18. Anisotropic displacement parameters ($\text{\AA}^2 \times 10^3$) for **2**. The anisotropic displacement factor exponent takes the form: $-2\pi^2 [h^2 a^*{}^2 U^{11} + \dots + 2 h k a^* b^* U^{12}]$.

	U11	U22	U33	U23	U13	U12
Au1	18(1)	33(1)	15(1)	2(1)	1(1)	0(1)
Au2	21(1)	24(1)	14(1)	-2(1)	4(1)	-2(1)
Au3	19(1)	30(1)	19(1)	2(1)	1(1)	1(1)
Au4	29(1)	24(1)	20(1)	3(1)	7(1)	-2(1)
P1	26(1)	40(1)	16(1)	1(1)	-1(1)	2(1)
P2	20(1)	29(1)	16(1)	-5(1)	4(1)	-2(1)
P3	22(1)	33(1)	26(1)	2(1)	2(1)	2(1)
P4	32(1)	32(1)	32(1)	10(1)	6(1)	-4(1)
N1	25(3)	36(4)	15(3)	4(3)	2(2)	0(3)
N2	29(4)	43(4)	18(3)	2(3)	3(3)	3(3)
N3	26(3)	42(4)	23(3)	10(3)	3(3)	8(3)
N4	24(3)	24(3)	17(3)	1(2)	2(2)	1(3)
N5	37(4)	25(3)	17(3)	1(3)	9(3)	-2(3)
N6	24(3)	24(3)	15(3)	0(2)	4(2)	0(3)
C11	19(3)	25(4)	16(3)	3(3)	-2(3)	-2(3)
C12	25(4)	24(4)	16(3)	-3(3)	-3(3)	1(3)
C13	21(4)	30(4)	18(3)	-3(3)	-5(3)	5(3)

C14	43(5)	36(5)	25(4)	0(4)	9(4)	-1(4)
C15	45(5)	47(6)	25(4)	-7(4)	4(4)	12(4)
C16	44(5)	30(5)	34(5)	-10(4)	-9(4)	9(4)
C17	37(5)	27(4)	41(5)	-5(4)	-2(4)	1(4)
C18	20(4)	41(5)	31(4)	3(4)	-2(3)	-1(3)
C21	25(4)	40(5)	29(4)	-8(4)	-7(3)	4(4)
C22	23(5)	131(12)	25(5)	1(6)	-6(4)	13(6)
C23	31(5)	130(13)	39(6)	-11(7)	6(4)	-2(7)
C24	28(5)	57(7)	63(7)	-22(6)	-18(5)	11(5)
C25	33(6)	96(11)	117(13)	54(10)	-30(7)	1(7)
C26	42(6)	86(10)	77(9)	41(8)	-6(6)	-13(6)
C27	45(6)	68(7)	20(4)	-13(4)	-11(4)	19(5)
C28	39(5)	60(6)	27(4)	16(4)	9(4)	-5(5)
C31	18(3)	23(4)	24(4)	-3(3)	3(3)	0(3)
C32	29(4)	32(4)	25(4)	-6(3)	2(3)	-4(3)
C33	41(5)	38(5)	19(4)	-4(3)	-1(3)	3(4)
C34	32(4)	35(5)	35(5)	0(4)	4(4)	8(4)
C35	30(4)	32(4)	32(4)	-15(4)	2(3)	2(3)
C36	28(4)	35(4)	17(3)	-8(3)	-1(3)	1(3)
C37	21(4)	25(4)	31(4)	-3(3)	-6(3)	-3(3)
C38	34(4)	37(5)	25(4)	-5(3)	16(3)	-6(4)
C41	25(4)	36(5)	24(4)	-2(3)	1(3)	4(3)
C42	36(5)	42(5)	37(5)	-1(4)	-9(4)	11(4)
C43	27(4)	42(5)	55(6)	-11(5)	-4(4)	5(4)
C44	36(5)	34(5)	41(5)	5(4)	19(4)	8(4)
C45	25(4)	55(6)	31(4)	8(4)	7(3)	11(4)
C46	27(4)	42(5)	23(4)	1(3)	3(3)	2(4)
C47	28(4)	57(6)	34(5)	15(4)	11(4)	3(4)
C48	25(4)	49(6)	47(6)	-11(5)	-3(4)	-9(4)
C57	34(5)	42(5)	31(4)	13(4)	6(4)	-3(4)
C58	50(6)	30(5)	55(6)	7(4)	4(5)	-6(4)

Table S19. Hydrogen coordinates ($\times 10^4$) and isotropic displacement parameters ($\text{\AA}^2 \times 10^3$) for **2**.

	x	y	z	U(eq)
H4A	444	5488	10159	54
H5A	-910	5624	10017	78
H6A	-1580	6381	8960	41
H7A	-898	7003	8045	44

H8A	455	6867	8188	28
H4'A	586	6514	10262	39
H5'A	-765	6593	10197	46
H6'A	-1595	6132	9053	83
H7'A	-1074	5592	7974	61
H8'A	277	5513	8040	57
H4"A	620	5951	10451	29
H5"A	-719	6063	10457	54
H6"A	-1570	6304	9252	29
H7"A	-1083	6434	8041	28
H8"A	256	6322	8034	33
H14A	4372	4624	4798	41
H15A	4575	3413	4249	47
H16A	3963	2273	4656	45
H17A	3186	2377	5656	43
H18A	2983	3621	6238	38
H22A	-31	5693	6836	73
H23A	-1378	5577	6583	80
H24A	-2090	6277	5514	63
H25A	-1444	6976	4651	104
H26A	-88	7116	4925	84
H27A	1134	5766	4813	69
H27B	1203	5092	5491	69
H27C	1952	5603	5377	69
H28A	1242	7334	5145	62
H28B	2044	7256	5760	62
H28C	1319	7701	6033	62
H32A	2677	8573	6738	35
H33A	2392	9851	6236	40
H34A	2558	10927	7113	41
H35A	3011	10744	8480	38
H36A	3300	9472	8987	33
H37A	4153	8383	9351	40
H37B	4547	8062	8617	40
H37C	4264	7452	9238	40
H38A	2617	8265	9426	46
H38B	2645	7321	9354	46
H38C	2001	7815	8767	46
H42A	4194	4119	7509	48
H43A	4407	2756	7467	51
H44A	5388	2170	8402	43

H45A	6177	2940	9341	44
H46A	5973	4297	9394	37
H47A	5645	5551	7477	58
H47B	5124	6323	7530	58
H47C	4746	5550	7074	58
H48A	6130	5659	9096	62
H48B	5558	5618	9749	62
H48C	5572	6391	9200	62
H52A	780	4761	8286	41
H53A	-582	4708	8041	51
H54A	-1217	3595	7419	50
H55A	-491	2534	7043	76
H56A	870	2586	7288	72
H52B	701	4286	8931	65
H53B	-654	4301	8554	68
H54B	-1219	3893	7259	58
H55B	-430	3470	6340	55
H56B	925	3454	6718	53
H52C	1114	4347	6709	40
H54C	-232	4374	6266	52
H53C	-1073	3779	7041	65
H55C	-567	3156	8259	80
H56C	779	3129	8702	61
H57A	2014	3421	9397	54
H57B	2068	4362	9315	54
H57C	2829	3829	9323	54
H58A	2109	2392	8202	68
H58B	2918	2726	8008	68
H58C	2189	2634	7298	68

X-ray experiment details of 4

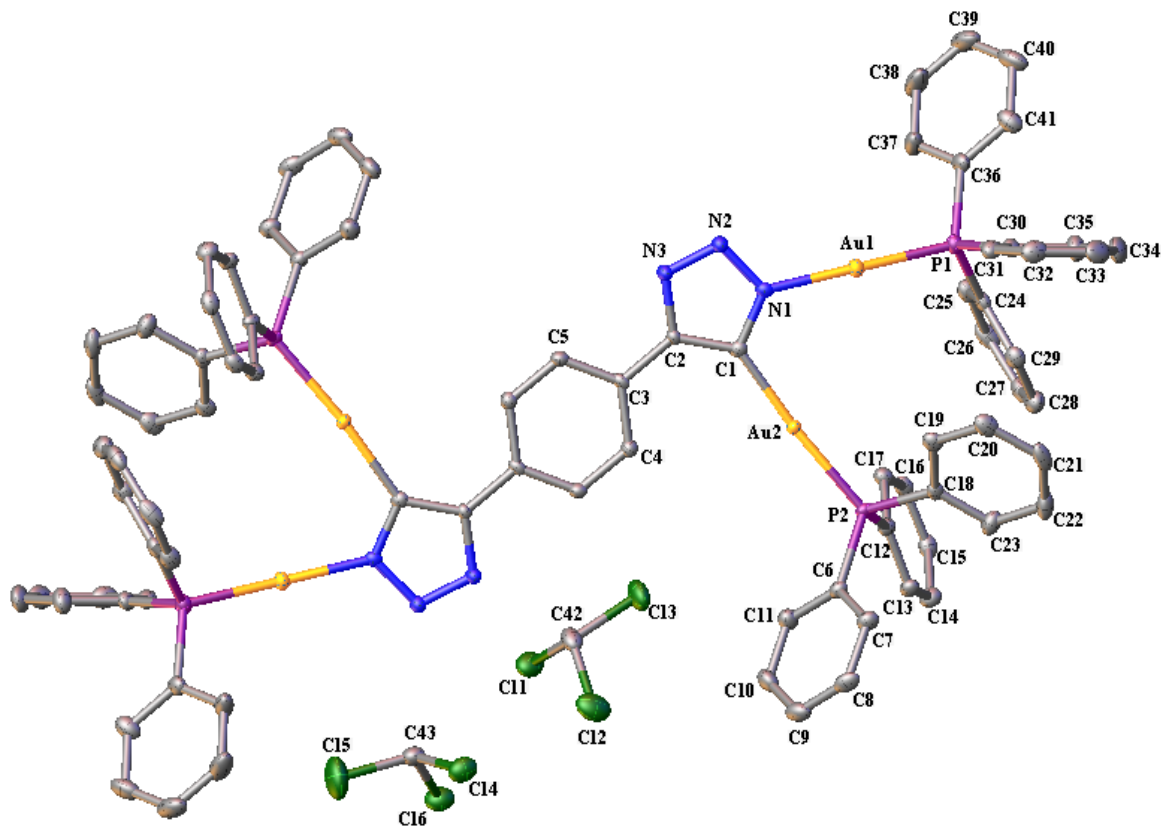


Figure S44. Solid structure (hydrogens are removed for clarity) of **4**.

The single crystals deposited from the reaction mixture are suitable for the single crystal X-ray diffraction experiment. Figure S44 depicts the solid state structure of the complex **4**.

X-Ray Intensity data were collected at 100 K on a Bruker **DUO** diffractometer using MoK α radiation ($\lambda = 0.71073 \text{ \AA}$) and an APEXII CCD area detector.

Raw data frames were read by program SAINT¹ and integrated using 3D profiling algorithms. The resulting data were reduced to produce hkl reflections and their intensities and estimated

standard deviations. The data were corrected for Lorentz and polarization effects and numerical absorption corrections were applied based on indexed and measured faces.

The structure was solved and refined in SHELXTL6.1,¹¹ using full-matrix least-squares refinement. The non-H atoms were refined with anisotropic thermal parameters and all of the H atoms were calculated in idealized positions and refined riding on their parent atoms. The asymmetric unit contains half of complex **4** and two chloroform solvent molecules. In the final cycle of refinement, 10005 reflections (of which 9177 are observed with $I > 2\sigma(I)$) were used to refine 499 parameters and the resulting R_1 , wR_2 and S (goodness of fit) were 2.85%, 7.28% and 1.058, respectively. The refinement was carried out by minimizing the wR_2 function using F^2 rather than F values. R_1 is calculated to provide a reference to the conventional R value but its function is not minimized.

SHELXTL6 (2008). Bruker-AXS, Madison, Wisconsin, USA.

Table S20. Crystal data and structure refinement for **4**.

Identification code	xy06	
Empirical formula	C86 H68 Au4 Cl12 N6 P4	
Formula weight	2522.61	
Temperature	100(2) K	
Wavelength	0.71073 Å	
Crystal system	Triclinic	
Space group	P $\bar{1}$	
Unit cell dimensions	$a = 12.4497(8)$ Å	$\alpha = 91.385(1)^\circ$.
	$b = 12.8216(8)$ Å	$\beta = 106.155(1)^\circ$.
	$c = 15.5296(10)$ Å	$\gamma = 112.428(1)^\circ$.
Volume	2177.1(2) Å ³	
Z	1	

Density (calculated)	1.924 Mg/m3
Absorption coefficient	7.208 mm-1
F(000)	1206
Crystal size	0.19 × 0.09 × 0.06 mm3
Theta range for data collection	1.38 to 27.50°.
Index ranges	-16≤h≤16, -16≤k≤16, -20≤l≤20
Reflections collected	54170
Independent reflections	10005 [R(int) = 0.0498]
Completeness to theta = 27.50°	100.00%
Absorption correction	Integration
Max. and min. transmission	0.6595 and 0.3398
Refinement method	Full-matrix least-squares on F2
Data / restraints / parameters	10005 / 0 / 499
Goodness-of-fit on F2	1.058
Final R indices [I>2sigma(I)]	R1 = 0.0285, wR2 = 0.0728 [9177]
R indices (all data)	R1 = 0.0317, wR2 = 0.0745
Largest diff. peak and hole	5.863 and -2.366 e.Å-3

$$R_1 = \sum(|F_O| - |F_C|) / \sum|F_O|$$

$$wR2 = [\sum[w(F_O^2 - F_C^2)^2] / \sum[w(F_O^2)^2]]^{1/2}$$

$$S = [\sum[w(F_O^2 - F_C^2)^2] / (n-p)]^{1/2}$$

$$w = 1/[\sigma^2(F_O^2) + (m*p)^2 + n*p], p = [\max(F_O^2, 0) + 2*F_C^2]/3, m \text{ & } n \text{ are constants.}$$

Table S21. Atomic coordinates ($\times 10^4$) and equivalent isotropic displacement parameters ($\text{\AA}^2 \times 10^3$) for **4**. U(eq) is defined as one third of the trace of the orthogonalized U_{ij} tensor.

	x	y	z	U(eq)
Au1	8748(1)	2104(1)	7934(1)	15(1)
Au2	10874(1)	3226(1)	10125(1)	11(1)
P1	6841(1)	819(1)	7716(1)	16(1)
P2	10103(1)	2975(1)	11313(1)	13(1)
N1	10541(3)	3133(3)	8170(2)	13(1)
N2	11072(3)	3407(3)	7506(2)	15(1)

N3	12272(3)	3897(3)	7889(2)	14(1)
C1	11405(4)	3454(3)	9000(3)	13(1)
C2	12518(4)	3937(3)	8808(3)	12(1)
C3	13777(4)	4454(3)	9418(3)	13(1)
C4	14044(4)	4583(3)	10363(3)	14(1)
C5	14755(2)	4877(2)	9070(2)	14(1)
C6	10986(2)	4051(2)	12308(2)	15(1)
C7	10532(2)	4786(2)	12615(2)	19(1)
C8	11254(5)	5578(4)	13398(3)	23(1)
C9	12387(5)	5635(4)	13866(3)	26(1)
C10	12850(5)	4923(4)	13558(3)	26(1)
C11	12153(4)	4140(4)	12778(3)	22(1)
C12	9934(4)	1640(4)	11752(3)	15(1)
C13	9917(4)	1508(4)	12640(3)	18(1)
C14	9704(4)	457(4)	12931(3)	22(1)
C15	9532(4)	-473(4)	12344(3)	20(1)
C16	9586(4)	-352(4)	11473(3)	18(1)
C17	9782(4)	713(4)	11177(3)	17(1)
C18	8585(4)	2974(3)	10960(3)	16(1)
C19	8251(4)	3437(4)	10172(3)	18(1)
C20	7097(4)	3455(4)	9881(3)	24(1)
C21	6278(4)	3008(4)	10361(4)	25(1)
C22	6603(4)	2554(4)	11137(4)	28(1)
C23	7765(4)	2537(4)	11446(4)	23(1)
C24	6778(4)	-12(4)	8653(3)	17(1)
C25	7111(4)	-936(4)	8674(3)	23(1)
C26	7115(4)	-1533(4)	9401(4)	26(1)
C27	6786(4)	-1230(4)	10117(4)	26(1)
C28	6476(4)	-292(4)	10112(3)	24(1)
C29	6481(4)	318(4)	9386(3)	20(1)
C30	5688(4)	1380(4)	7619(3)	18(1)
C31	5954(4)	2505(4)	7474(3)	20(1)

C32	5078(5)	2952(5)	7391(3)	26(1)
C33	3932(5)	2275(5)	7448(4)	29(1)
C34	3665(5)	1158(5)	7588(4)	32(1)
C35	4526(4)	703(5)	7675(4)	27(1)
C36	6306(4)	-218(4)	6696(3)	21(1)
C37	7140(5)	-599(5)	6521(4)	33(1)
C38	6775(6)	-1411(5)	5762(5)	44(2)
C39	5597(6)	-1813(5)	5180(4)	40(1)
C40	4768(6)	-1422(4)	5348(4)	34(1)
C41	5126(5)	-627(4)	6109(3)	26(1)
C11	12479(1)	6258(1)	6260(1)	35(1)
C12	13621(2)	4750(1)	5948(1)	44(1)
C13	14995(1)	6769(1)	7285(1)	39(1)
C42	13538(4)	5680(4)	6761(3)	27(1)
C14	11054(1)	1696(1)	5424(1)	33(1)
C15	8586(2)	1409(2)	5234(2)	61(1)
C16	10194(1)	3400(1)	4693(1)	33(1)
C43	10100(5)	2411(4)	5459(3)	25(1)

Table S22. Bond lengths (Å) for **4**.

Bond	Length (Å)	Bond	Length (Å)
Au1-N1	2.033(4)	C18-C23	1.392(6)
Au1-P1	2.2374(11)	C18-C19	1.402(6)
Au2-C1	2.023(4)	C19-C20	1.391(6)
Au2-P2	2.2822(10)	C20-C21	1.386(7)
P1-C30	1.809(5)	C21-C22	1.378(8)
P1-C24	1.826(5)	C22-C23	1.401(7)
P1-C36	1.832(5)	C24-C29	1.394(6)
P2-C18	1.814(4)	C24-C25	1.395(6)
P2-C6	1.815(3)	C25-C26	1.379(7)
P2-C12	1.817(4)	C26-C27	1.381(8)
N1-N2	1.357(5)	C27-C28	1.396(7)
N1-C1	1.362(5)	C28-C29	1.387(7)
N2-N3	1.323(5)	C30-C31	1.391(6)
N3-C2	1.368(5)	C30-C35	1.402(7)

C1-C2	1.407(6)	C31-C32	1.392(7)
C2-C3	1.464(6)	C32-C33	1.388(8)
C3-C5	1.395(5)	C33-C34	1.379(8)
C3-C4	1.402(6)	C34-C35	1.381(7)
C4-C5#1	1.392(5)	C36-C41	1.382(7)
C5-C4#1	1.392(5)	C36-C37	1.388(7)
C6-C11	1.392(5)	C37-C38	1.401(7)
C7-C8	1.397(5)	C38-C39	1.378(9)
C8-C9	1.368(8)	C39-C40	1.388(9)
C9-C10	1.389(7)	C40-C41	1.391(7)
C10-C11	1.385(7)	Cl1-C42	1.760(5)
C12-C17	1.388(6)	Cl2-C42	1.766(6)
C12-C13	1.399(6)	Cl3-C42	1.759(5)
C13-C14	1.383(6)	Cl4-C43	1.766(5)
C14-C15	1.394(7)	Cl5-C43	1.757(5)
C15-C16	1.382(7)	Cl6-C43	1.753(5)
C16-C17	1.404(6)		

Symmetry transformations used to generate equivalent atoms:

#1 -x+3,-y+1,-z+2

Table S23. Bond angles ($^{\circ}$) for 4.

Bond	Angle ($^{\circ}$)	Bond	Angle ($^{\circ}$)
N1-Au1-P1	173.81(10)	C13-C14-C15	120.0(4)
C1-Au2-P2	174.50(12)	C16-C15-C14	120.5(4)
C30-P1-C24	105.5(2)	C15-C16-C17	119.2(4)
C30-P1-C36	106.6(2)	C12-C17-C16	120.8(4)
C24-P1-C36	105.7(2)	C23-C18-C19	120.1(4)
C30-P1-Au1	116.27(15)	C23-C18-P2	122.2(4)
C24-P1-Au1	110.55(14)	C19-C18-P2	117.7(3)
C36-P1-Au1	111.51(15)	C20-C19-C18	119.5(4)
C18-P2-C6	106.44(16)	C21-C20-C19	120.3(5)
C18-P2-C12	105.9(2)	C22-C21-C20	120.4(4)
C6-P2-C12	103.83(17)	C21-C22-C23	120.2(5)
C18-P2-Au2	109.63(15)	C18-C23-C22	119.6(5)
C6-P2-Au2	115.63(9)	C29-C24-C25	119.1(4)
C12-P2-Au2	114.62(14)	C29-C24-P1	120.4(3)
N2-N1-C1	110.6(3)	C25-C24-P1	120.3(4)
N2-N1-Au1	123.8(3)	C26-C25-C24	120.3(5)

C1-N1-Au1	124.5(3)	C25-C26-C27	120.7(4)
N3-N2-N1	108.4(3)	C26-C27-C28	119.5(5)
N2-N3-C2	108.3(3)	C29-C28-C27	120.1(5)
N1-C1-C2	104.0(3)	C28-C29-C24	120.2(4)
N1-C1-Au2	119.4(3)	C31-C30-C35	119.2(4)
C2-C1-Au2	136.5(3)	C31-C30-P1	119.1(3)
N3-C2-C1	108.6(4)	C35-C30-P1	121.7(4)
N3-C2-C3	121.0(4)	C30-C31-C32	120.2(4)
C1-C2-C3	130.4(4)	C33-C32-C31	120.2(5)
C5-C3-C4	117.7(4)	C34-C33-C32	119.7(5)
C5-C3-C2	120.4(3)	C33-C34-C35	120.8(5)
C4-C3-C2	121.9(4)	C34-C35-C30	120.0(5)
C5#1-C4-C3	120.9(4)	C41-C36-C37	119.7(5)
C4#1-C5-C3	121.5(3)	C41-C36-P1	122.9(4)
C11-C6-C7	119.4(2)	C37-C36-P1	117.4(4)
C11-C6-P2	118.2(3)	C36-C37-C38	119.9(5)
C7-C6-P2	122.38(9)	C39-C38-C37	120.0(6)
C8-C7-C6	119.2(2)	C38-C39-C40	120.1(5)
C9-C8-C7	120.7(4)	C39-C40-C41	119.9(5)
C8-C9-C10	120.4(4)	C36-C41-C40	120.4(5)
C11-C10-C9	119.8(5)	Cl3-C42-Cl1	110.7(3)
C10-C11-C6	120.5(4)	Cl3-C42-Cl2	109.9(3)
C17-C12-C13	119.1(4)	Cl1-C42-Cl2	110.8(3)
C17-C12-P2	118.8(3)	Cl6-C43-Cl5	111.0(3)
C13-C12-P2	122.1(3)	Cl6-C43-Cl4	111.2(3)
C14-C13-C12	120.5(4)	Cl5-C43-Cl4	109.6(3)

Symmetry transformations used to generate equivalent atoms:

#1 -x+3,-y+1,-z+2

Table S24. Anisotropic displacement parameters ($\text{\AA}^2 \times 10^3$) for **4**. The anisotropic displacement factor exponent takes the form: $-2\pi^2 [h^2 a^*{}^2 U^{11} + \dots + 2 h k a^* b^* U^{12}]$.

	U11	U22	U33	U23	U13	U12
Au1	13(1)	14(1)	17(1)	1(1)	5(1)	4(1)
Au2	12(1)	12(1)	11(1)	1(1)	5(1)	5(1)
P1	14(1)	15(1)	19(1)	1(1)	5(1)	5(1)
P2	15(1)	13(1)	12(1)	1(1)	5(1)	6(1)
N1	16(2)	11(2)	12(2)	0(1)	3(1)	6(1)

N2	14(2)	16(2)	13(2)	2(1)	3(1)	4(1)
N3	13(2)	15(2)	12(2)	1(1)	3(1)	3(1)
C1	17(2)	10(2)	14(2)	2(1)	5(2)	6(2)
C2	11(2)	10(2)	12(2)	0(1)	3(2)	4(1)
C3	14(2)	8(2)	13(2)	0(1)	0(2)	4(2)
C4	15(2)	13(2)	15(2)	3(2)	5(2)	6(2)
C5	17(2)	15(2)	11(2)	1(2)	3(2)	7(2)
C6	19(2)	13(2)	15(2)	2(2)	8(2)	6(2)
C7	25(2)	16(2)	19(2)	1(2)	8(2)	9(2)
C8	38(3)	13(2)	22(2)	1(2)	15(2)	10(2)
C9	34(3)	18(2)	18(2)	-1(2)	7(2)	2(2)
C10	20(2)	24(2)	24(2)	0(2)	1(2)	2(2)
C11	21(2)	22(2)	23(2)	-1(2)	6(2)	8(2)
C12	16(2)	18(2)	15(2)	2(2)	5(2)	9(2)
C13	21(2)	16(2)	16(2)	-1(2)	7(2)	6(2)
C14	26(2)	22(2)	19(2)	6(2)	8(2)	10(2)
C15	17(2)	16(2)	28(2)	7(2)	6(2)	8(2)
C16	18(2)	13(2)	21(2)	-1(2)	2(2)	8(2)
C17	18(2)	18(2)	16(2)	1(2)	3(2)	8(2)
C18	15(2)	13(2)	19(2)	-1(2)	5(2)	6(2)
C19	21(2)	13(2)	19(2)	-2(2)	4(2)	8(2)
C20	26(2)	20(2)	26(2)	-2(2)	2(2)	15(2)
C21	14(2)	17(2)	41(3)	-7(2)	3(2)	8(2)
C22	19(2)	21(2)	46(3)	1(2)	16(2)	6(2)
C23	25(2)	20(2)	29(3)	6(2)	15(2)	10(2)
C24	12(2)	13(2)	21(2)	2(2)	2(2)	2(2)
C25	21(2)	20(2)	28(2)	-1(2)	5(2)	10(2)
C26	23(2)	14(2)	36(3)	1(2)	-3(2)	10(2)
C27	17(2)	20(2)	29(3)	8(2)	0(2)	2(2)
C28	23(2)	23(2)	24(2)	5(2)	9(2)	5(2)
C29	20(2)	13(2)	24(2)	1(2)	5(2)	5(2)
C30	15(2)	22(2)	17(2)	1(2)	2(2)	9(2)

C31	20(2)	26(2)	16(2)	5(2)	4(2)	12(2)
C32	34(3)	30(3)	23(2)	5(2)	7(2)	22(2)
C33	26(3)	43(3)	25(2)	2(2)	2(2)	25(2)
C34	16(2)	45(3)	34(3)	4(2)	6(2)	12(2)
C35	19(2)	30(3)	31(3)	8(2)	7(2)	9(2)
C36	19(2)	17(2)	19(2)	0(2)	7(2)	0(2)
C37	22(2)	35(3)	34(3)	-13(2)	13(2)	0(2)
C38	40(3)	37(3)	48(4)	-16(3)	28(3)	0(3)
C39	51(4)	30(3)	25(3)	-7(2)	16(3)	-1(3)
C40	39(3)	23(2)	22(3)	-2(2)	-3(2)	3(2)
C41	27(2)	19(2)	25(2)	3(2)	0(2)	8(2)
Cl1	36(1)	47(1)	27(1)	10(1)	7(1)	25(1)
Cl2	48(1)	46(1)	37(1)	2(1)	-1(1)	30(1)
Cl3	24(1)	37(1)	40(1)	10(1)	6(1)	-1(1)
C42	21(2)	30(3)	23(2)	11(2)	3(2)	7(2)
Cl4	43(1)	35(1)	30(1)	6(1)	13(1)	24(1)
Cl5	32(1)	56(1)	85(1)	14(1)	21(1)	4(1)
Cl6	44(1)	33(1)	25(1)	7(1)	9(1)	21(1)
C43	28(2)	29(2)	17(2)	1(2)	6(2)	12(2)

Table S25. Hydrogen coordinates ($\times 10^4$) and isotropic displacement parameters ($\text{\AA}^2 \times 10^3$) for **4**.

	x	y	z	U(eq)
H4A	13397	4297	10620	17
H5A	14599	4794	8432	17
H7A	9743	4746	12295	23
H8A	10955	6082	13607	28
H9A	12861	6166	14404	31
H10A	13641	4971	13881	31
H11A	12474	3661	12562	27
H13A	10052	2144	13046	22
H14A	9674	369	13531	26
H15A	9377	-1196	12544	24

H16A	9493	-981	11080	21
H17A	9809	799	10577	21
H19A	8808	3736	9839	22
H20A	6868	3775	9351	28
H21A	5487	3015	10153	30
H22A	6038	2252	11464	33
H23A	7992	2229	11984	27
H25A	7336	-1155	8185	28
H26A	7345	-2159	9409	31
H27A	6771	-1656	10608	31
H28A	6262	-71	10606	29
H29A	6281	963	9389	24
H31A	6737	2969	7432	24
H32A	5266	3722	7295	32
H33A	3333	2580	7390	35
H34A	2879	695	7625	39
H35A	4332	-67	7773	33
H37A	7958	-309	6916	40
H38A	7340	-1684	5649	53
H39A	5352	-2360	4662	48
H40A	3957	-1696	4944	41
H41A	4556	-363	6225	31
H42A	13259	5233	7235	32
H43A	10378	2833	6084	30

8. Photophysical study of complex 1 and 8

UV-Visible absorption spectra were recorded on a Shimadzu UV-1800 Spectrophotometer. Corrected steady-state fluorescence spectra were acquired on a Photon Technology International (PTI) spectrophotometer. All fluorescence measurements were performed using a 1 cm square quartz cuvette.

Absorption and emission spectra of complex 1

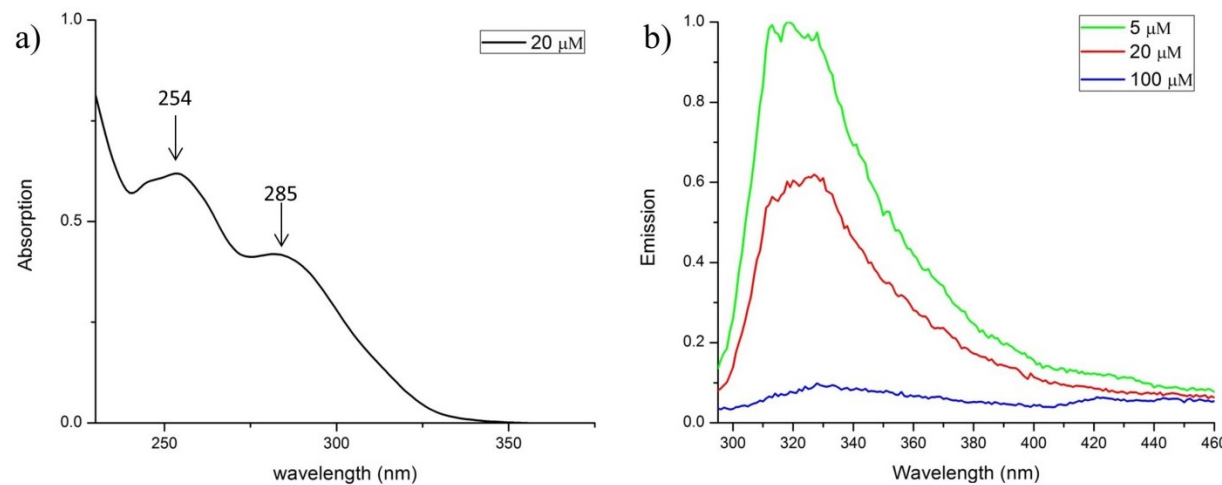


Figure S45. a) The UV-vis absorption spectrum of complex **1** (20 μM). b) The emission spectra of complex **1** (excited at 285 nm). All experiments are performed in dichloromethane at 298 K. The UV-vis absorption and emission spectra of complex **1** in dichloromethane at 298 K are depicted in Figure S45. In the absorption spectrum (Figure S45a), there are two absorption bands at 254 and 285 nm. Exciting DCM solutions of **1** at 285 nm provides one broad emission band at 324 nm (Figure S45b). The intensity of the emission is concentration dependent. As the concentration of **1** increases, the emission intensity decrease due to the intermolecular quenching.

Absorption and emission spectra of complex 9.

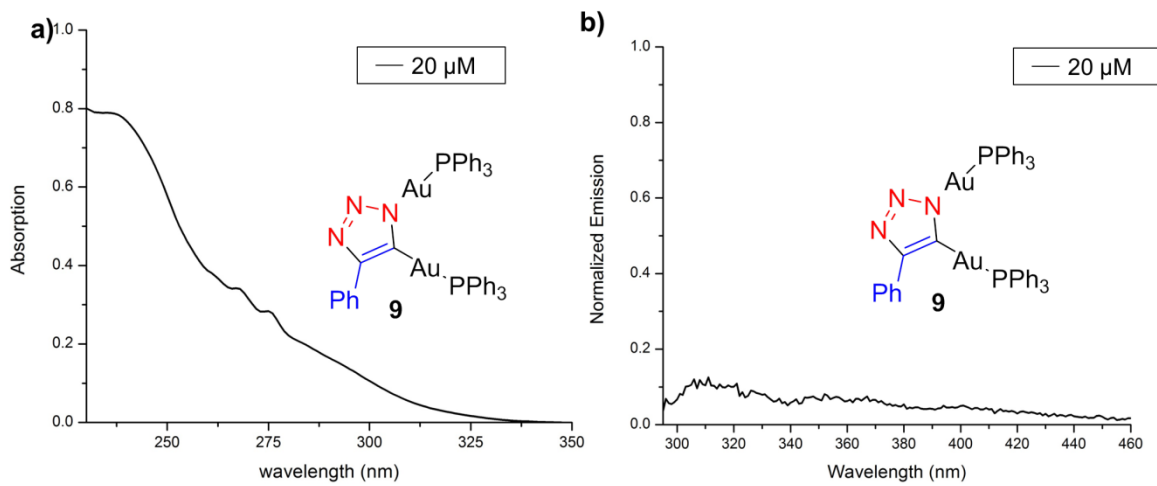


Figure S46 a) The UV-vis absorption spectrum of complex **9** (20 μM). b) The emission spectra of complex **9** (excited at 285 nm). All experiments are performed in dichloromethane at 298 K.

Absorption and emission spectra of oligomeric **8**.

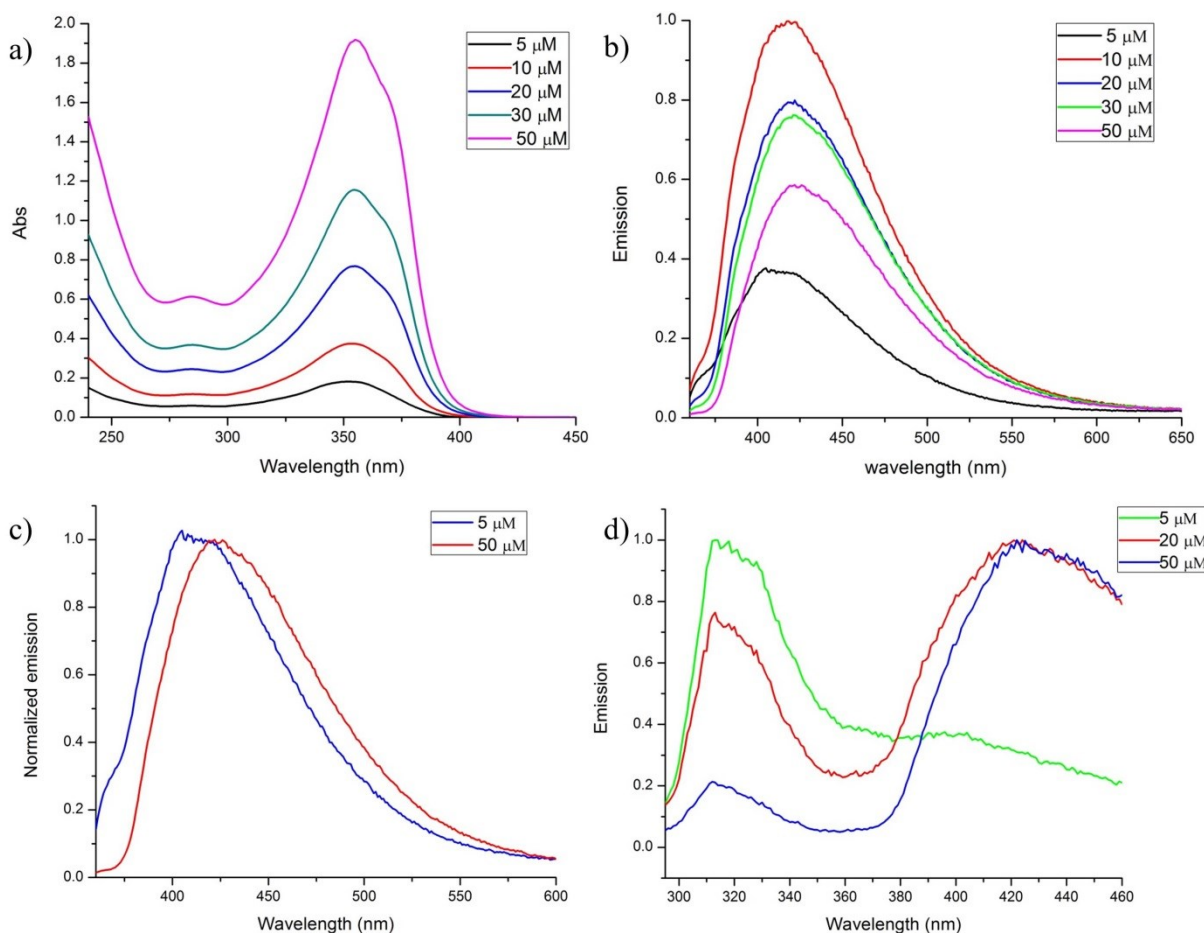


Figure S47. a) The UV-vis absorption spectra of complex **8** (5-50 μM). b) The emission spectra of complex **8** (excited at 353 nm). c) Normalized emission spectra of complex **8** with concentrations as 5 μM and 50 μM (excited at 353 nm). d) Emission spectra of complex **8** (excited at 285 nm). All the experiments are performed in dichloromethane at 298 K.

The UV-vis absorption and emission spectra of complex **8** in dichloromethane at 298K are depicted in Figure S47. In the absorption spectra (Figure S47a), there are two major absorption bands at 285 and 353 nm. In both absorption spectra of **1** and **8**, the absorption band at 285 nm is observed which is related to the Au₄ cluster core. The absorption band at 353 nm can be assigned to the fluorene organic linker. In the emission spectra excited at 353 nm (Figure S47b), there is only one major emission band at 425 nm. Interestingly, as the concentration of the DCM solution

of **8** increases; the emission band significantly shifts towards the lower energy. Specifically, comparing the emission band of a 50 μM sample with a 5 μM sample, there is an 18 nm red shift (Figure S47c) which indicates in 50 μM sample **8** has a higher degree of oligomerization. Finally, exciting a DCM solution of **8** at 285 nm (Figure S47d) results in an emission band at 320 nm, which is almost identical to the emission spectra of complex **1** (Figure S45b) and indicates that both **1** and **8** have the Au_4 cluster core.

9. Reference

1. Koster, S. D. Ph.D. Dissertation, Ruhr-University Bochum, **2011**.
2. Partyka, D. V.; Updegraff, J. B.; Zeller, M.; Hunter, A. D.; Gray, T. G. *Organometallics* **2007**, *26*, 183-186
3. Coates, G. E.; Parkin, C., *J. Chem. Soc.* **1962**, 3220-3226.
4. Deeming, A. J.; Donovan-Mtunzi, S.; Hardcastle, K., *J. Chem. Soc., Dalton Trans.* **1986**, *3*, 543-545.
5. Wong, W.-Y.; Choi, K.-H.; Lu, G.-L.; Shi, J.-X.; Lai, P.-Y.; Chan, S.-M.; Lin, Z., *Organometallics* **2001**, *20*, 5446-5454.
6. Hurst, S. K.; Cifuentes, M. P.; McDonagh, A. M.; Humphrey, M. G.; Samoc, M.; Luther-Davies, B.; Asselberghs, I.; Persoons, A., *J. Organomet. Chem.* **2002**, *642*, 259-267.
7. (a) Gierer, A.; Wirtz, K., *Z. Naturforschung A* **1953**, *8*, 532-538. (b) Chen, H. C.; Chen, S. H., *J. Phys. Chem.* **1984**, *88*, 5118-5121.
8. (a) Einstein, A., *Ann. der Phys.* **1905**, *322*, 549-560. (b) Sharma, M.; Yashonath, S., *J. Phys. Chem. B* **2006**, *110* (34), 17207-17211.h
9. (a) Evans, R.; Deng, Z.; Rogerson, A. K.; McLachlan, A. S.; Richards, J. J.; Nilsson, M.; Morris, G. A., *Angew. Chem. Int. Ed.* **2013**, *52*, 3199-3202. (b) Immelspach, A.; Finze, M.; Raub, S., *Angew. Chem. Int. Ed.* **2011**, *50*, 2628-2631. (c) Zuccaccia, D.; Macchioni, A., *Organometallics* **2005**, *24*, 3476-3486. (d) Dixon, J. A.; Schiessler, R. W., *J. Phys. Chem.* **1954**, *58*, 430-432.
10. Gallego, M. L.; Guijarro, A.; Castillo, O.; Parella, T.; Mas-Balleste, R.; Zamora, F., *CrystEngComm* **2010**, *12*, 2332-2334.
11. SHELXTL6 (2008). Bruker-AXS, Madison, Wisconsin, USA.